RESEARCH REPORT

VTT-R-08949-13

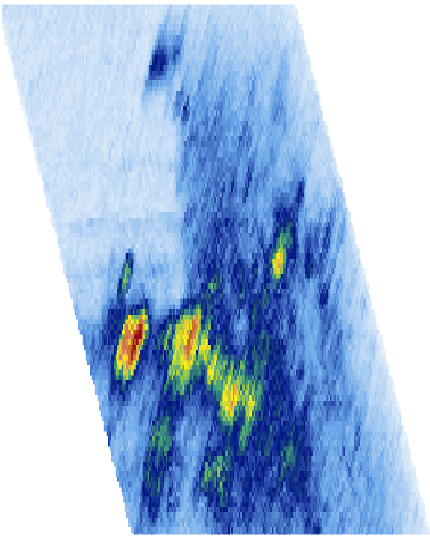

Non-destructive examination of BWR and Alloy 52 NGW mock-ups

Author: Esa Leskelä

Confidentiality: Public

Report's title	
Non-destructive examination of BWR and Alloy 52 NGW mock-ups	
Customer, contact person, address SINI - Structural integrity of Ni-base alloy welds project	**Order reference**
Project name Structural Integrity of Ni-base Alloy welds	**Project number/Short name** 71232/SINI
Author(s) Esa Leskelä	**Pages** 73
Keywords phased array, ultrasonic testing, PAUT, dissimilar metal weld, DMW, Alloy 182, Alloy 52, narrow gap weld	**Report identification code** VTT-R-08949-13

Summary

This work report summarizes the non-destructive examinations on BWR and Alloy 52 NGW dissimilar metal weld mock-ups. The goal of this study was to evaluate the weld quality of BWR and Alloy 52 NGW dissimilar metal weld (DMW) mock-ups with non-destructive examination (NDE) methods. The focus was on the use of commercial qualified phased array ultrasonic testing (PAUT) procedure for the detection of both inner surface breaking and embedded flaws. The type of the expected flaws was manufacturing flaws like lack of fusion, cracks, pores, etc.

Because ultrasonic testing is less sensitive to some manufacturing flaw types such as pores and inclusions, the testing was accompanied with radiographic examination. In addition, the both surfaces of BWR weld were examined with visual and liquid penetrant testing.

The phased array inspection of the DMW mock-ups showed the well-known challenge of the inspection of such structures. Several embedded flaws in the BWR mock up and one embedded flaw in the Alloy 52 NGW mock-up were detected. Both metallurgical and geometrical indications were also detected. Even though those indications were easily discriminated from flaw indications, they can mask shallow flaws and thus reduce the reliability of the inspection.

The study also served as an implementation of the commercial qualified PAUT procedure as a preparation for PARENT round robin testing of DMWs.

Confidentiality	Public

Espoo, 17.12.2013

Written by	Reviewed by	Accepted by
Esa Leskelä Senior Scientist	Ari Koskinen Team Leader	Pentti Kauppinen Technology Manager

VTT's contact address

VTT Technical Research Centre of Finland, Kemistintie 3, P.O.Box 1000, 02044 VTT

Distribution (customer and VTT)

SINI Project, VTT Kirjaamo

Preface

This work report describes the results obtained from the inspection of BWR and Alloy 52 NGW dissimilar metal weld (DMW) mock-ups. The work was carried out during 2011–2013 at VTT. This research work is a part of the NDE task in SINI - Structural integrity of Ni-base alloy welds research project funded by VTT, Aalto University and Industrial Consortium.

Espoo, 17.12.2013

Author

Contents

Acronyms and abbreviations

AS	axial probe with small footprint
ASME	American Society of Mechanical Engineering
AX	axial
BWR	boiling water reactor
CIRCD	circumferential downstream
CIRCU	circumferential upstream
CL	circumferential probe with large footprint
CS	carbon steel
DMW	dissimilar metal weld
FSH	full screen height
HAZ	heat-affected zone
ID	inner diameter
ISI	in-service inspection
LW	longitudinal wave
MCDU	Motor Control Drive Unit
NDE	non-destructive evaluation/examination
NDT	non-destructive testing
NGW	narrow gap weld
NPP	nuclear power plant
OD	outer diameter
PA	phased array
PARENT	Program to Assess the Reliability of Emerging Nondestructive Techniques
PAUT	phased array ultrasonic testing
PSI	pre-service inspection
PT	penetrant testing
SCC	stress-corrosion cracking
SNR	signal-to-noise ratio
SS	stainless steel
SW	shear wave
TR	transmission-receiver
TRL	transmission-receiver longitudinal
TRS	transmission-receiver shear
UT	ultrasonic testing
VC	volume-corrected
VT	visual testing
WCL	weld centre line

1. Introduction

The main challenges of ultrasonic inspection of dissimilar metal welds (DMWs) are the boundaries, different material types and the anisotropic weld metal affecting to the propagation of the ultrasonic waves. The ultrasonic waves suffer from strong attenuation, velocity variation, beam skewing and distortion in austenitic material. The challenging metallurgical interfaces and microstructural variations often cause misinterpretation of ultrasonic data and strong noise can mask shallow flaws. Geometrical access limitations and discontinuities may cause incomplete coverage of the volume to be inspected [1].

The impact of the microstructure to ultrasonic testing of DMWs can be reduced by using lower frequency (1.5 MHz) dual (TR) probes and longitudinal wave (LW) together with shear wave (SW). The use of TR probes reduces the near-surface dead zone and eliminates "ghost echoes" caused by internal reflections in wedge. TR probes also have better sensitivity and signal-to-noise ratio (SNR) due to convolution of T and R beams which reduces ultrasonic noise [2]. The use of longitudinal wave improves inspection capability in austenitic steel structures. The use of shear waves can reduce the size of the smallest detectable flaw because shear wave length is approximately half of the wave length of longitudinal waves.

This report summarizes the non-destructive examinations on BWR and Alloy 52 NGW dissimilar metal weld mock-ups. The focus is on phased array ultrasonic testing.

2. Goal

The goal of this study was to evaluate the weld quality of BWR and Alloy 52 NGW DMW mock-ups by NDE methods. The focus was on the use of commercial qualified PAUT procedure in detection of both inner surface (weld root side) breaking and embedded flaws. The type of the possible flaws was manufacturing flaws like lack of fusion, cracks, pores etc. The study also served as an implementation of the commercial qualified PAUT procedure as a preparation for PARENT round robin testing of DMW specimens.

3. Specimens

3.1 BWR mock-up

A schematic picture of the BWR mock-up is shown in Figure 1. The root side of the weld was milled, Figure 3. Unlike shown in Figure 1, the weld toe was not completely removed (Figure 2) and the stainless steel (SS) safe end and the carbon steel (CS) nozzle together with buttering were of different thicknesses – 41 mm and 51 mm respectively.

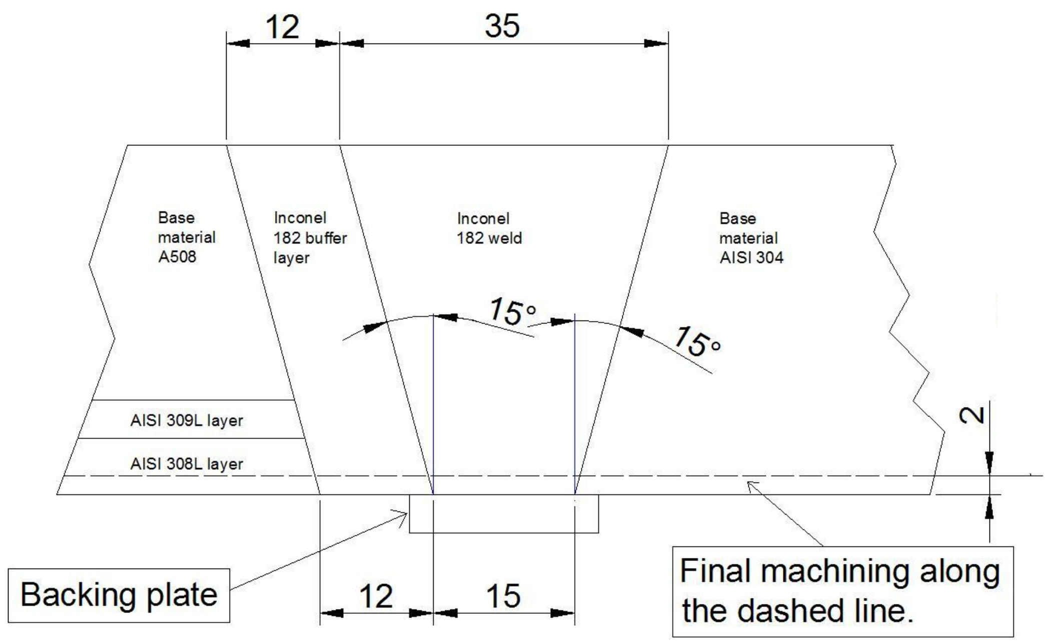

Figure 1. Schematic picture of the BWR mock-up weld.

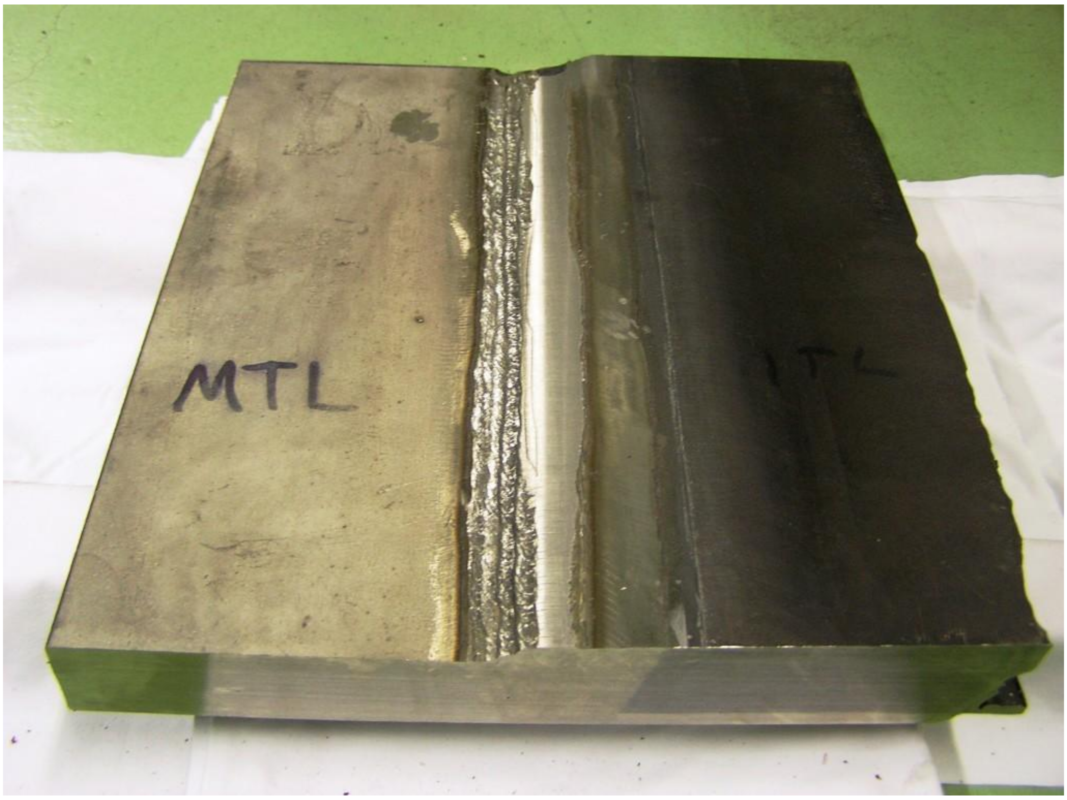

Figure 2. The BWR mock-up.

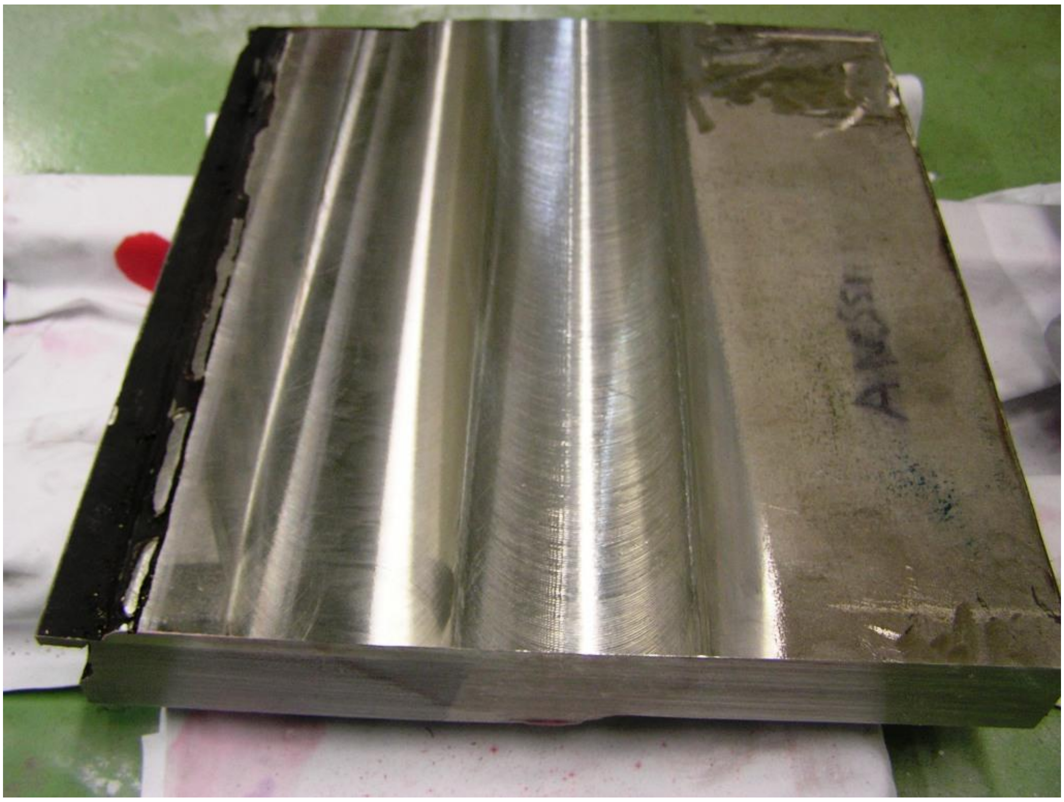

Figure 3. The root side of the BWR mock-up.

The weld profile of the BWR mock-up shown in Figure 4 was measured using profile gauge.

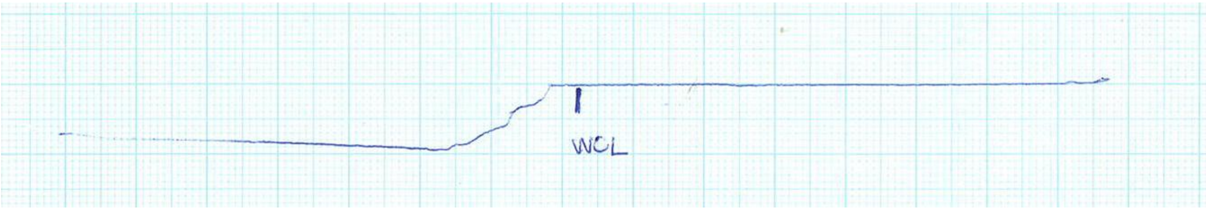

Figure 4. The weld profile of the BWR mock-up.

3.2 Alloy 52 NGW mock-up

A schematic picture of the dissimilar metal Alloy 52 narrow gap weld (NGW) mock-up is shown in Figure 5. Unlike the drawing, the surfaces of the mock-up were not machined after welding. On the top surface there was a counter bore on the CS side.

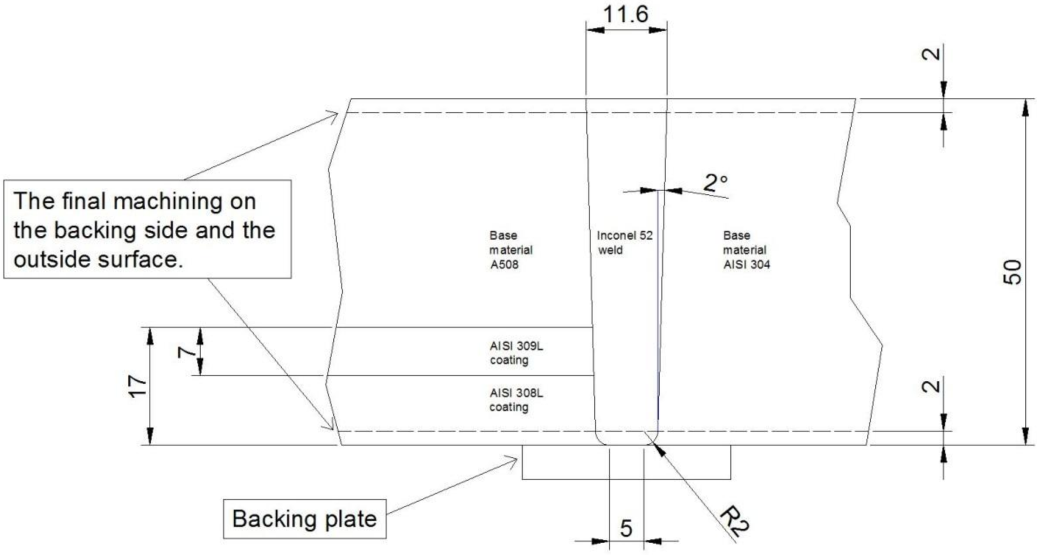

Figure 5. Schematic picture of the Alloy 52 NGW mock-up.

4. Limitations

The PAUT procedure used is developed for in-service inspection (ISI) of piping welds conducted from the outer surface. However, in this case the procedure was applied for inspection after manufacturing (pre-service inspection, PSI).

The volume to be examined using PAUT followed the requirements of ASME Code Section XI and was limited to the inner third of the material volume and heat affected zone (HAZ) for a distance of 6.35 mm beyond the extend of the weld cap. The volume to be examined is shown in Figure 6.

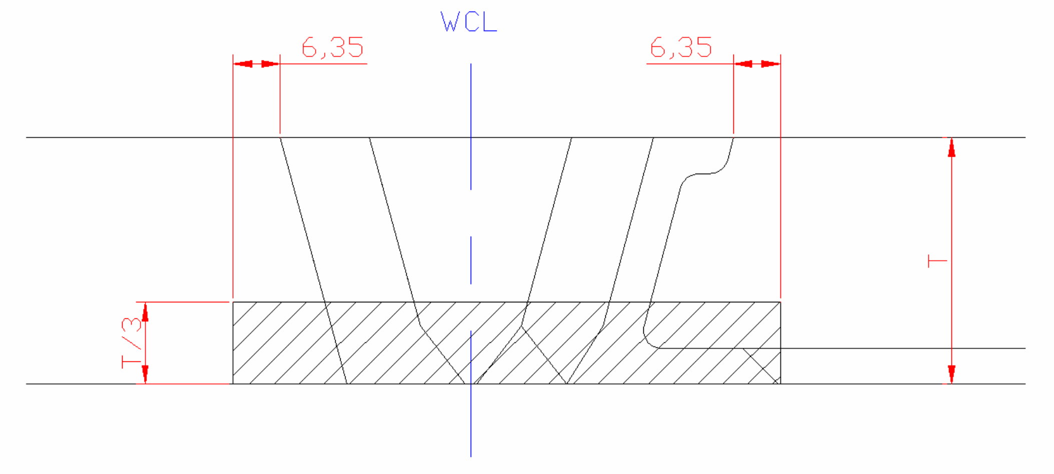

Figure 6. Volume to be examined according to ASME XI [3]

The procedure provides additional coverage of the complete weld volume, butter material and base material for a distance of 6.35 mm from each weld toe or butter interface in order to identify, characterize and size indications originating from the inner surface but extending to mid-wall or higher. The volume to be interrogated according to the procedure [4] is shown in Figure 7.

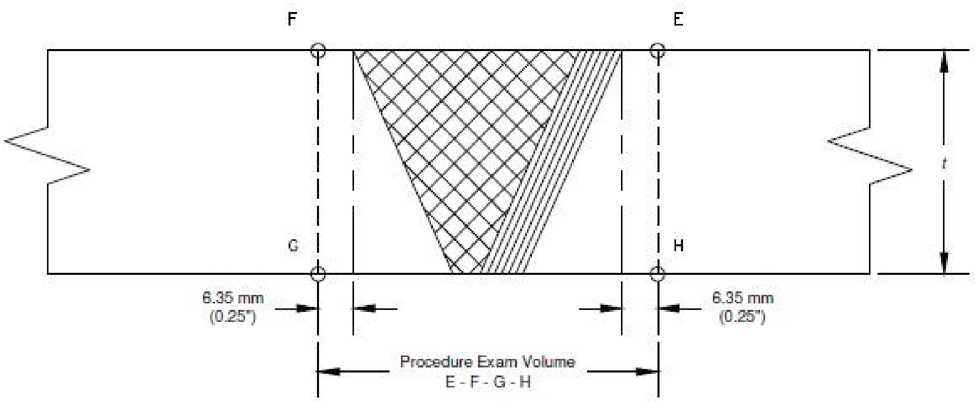

Figure 7. Volume to be interrogated according to the procedure [4].

Only circumferential flaws of the BWR mock-up were examined because no axial flaws were expected to occur and there was not a proper flat wedge for axial flaw inspection available at the examination time. The access was limited remarkably due to the shape of the weld so that the data from one scan line in PA examination was completely missed; see Figure 8 and Figure 9.

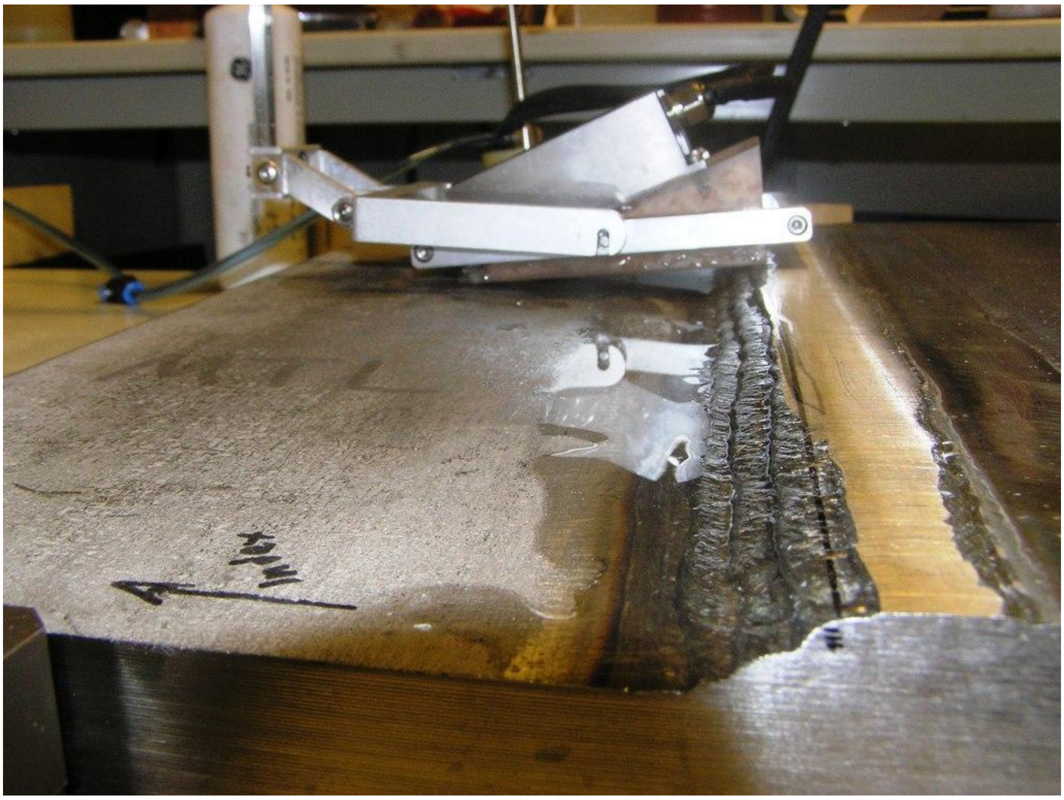

Figure 8. The access limitation in phased array testing of the BWR mock-up due to the change in the wall thickness.

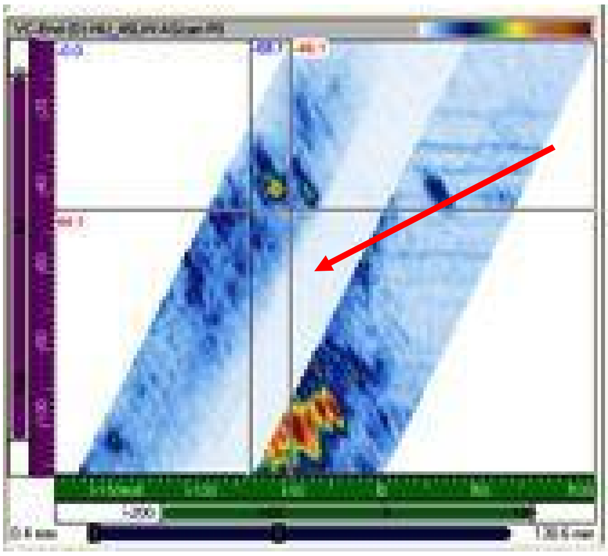

Figure 9. D-scan where an example of the adverse effect of the access limitation to the phased array data can be seen. Data from one scan line pointed with an arrow is completely missing due to a loss of contact.

There was approximately a 30 mm long area in the other end of the BWR mock-up with no interest, Figure 10. The examination of that area was skipped.

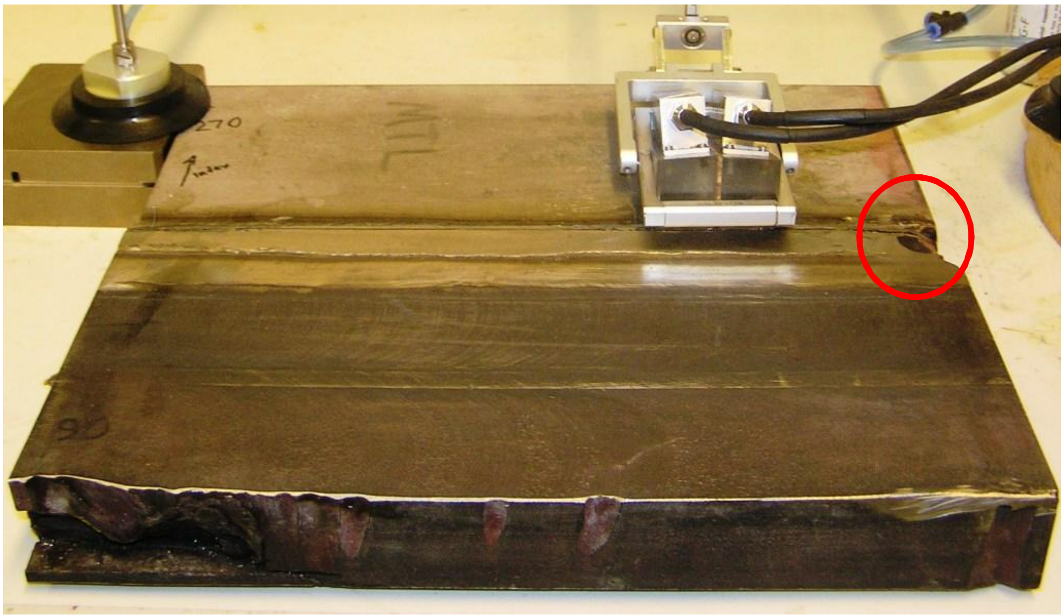

Figure 10. Area with no interest in the BWR mock-up circled.

During the examination of the Alloy 52 NGW mock-up, a proper flat wedge for axial flaw examination was available. The shape of the mock-up – a counter bore on the SS side and the concave top of the weld – caused remarkable access limitations for both circumferential and axial flaw examination, Figure 11 and Figure 12. The welding had also caused some deformation on the scanning surface near weld making the acoustic coupling insufficient. These factors lowered the coverage and reliability of the inspection.

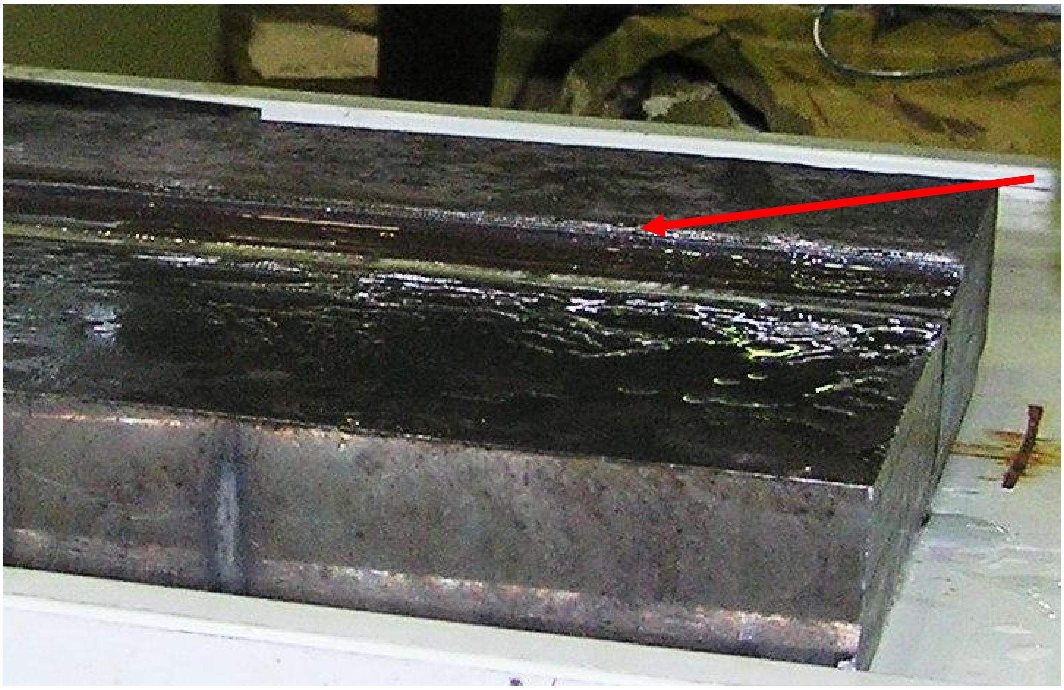

Figure 11. The counter bore pointed with red arrow on the scanning surface of the Alloy 52 NGW mock-up. In addition, the top of the weld was concave and weld root not machined.

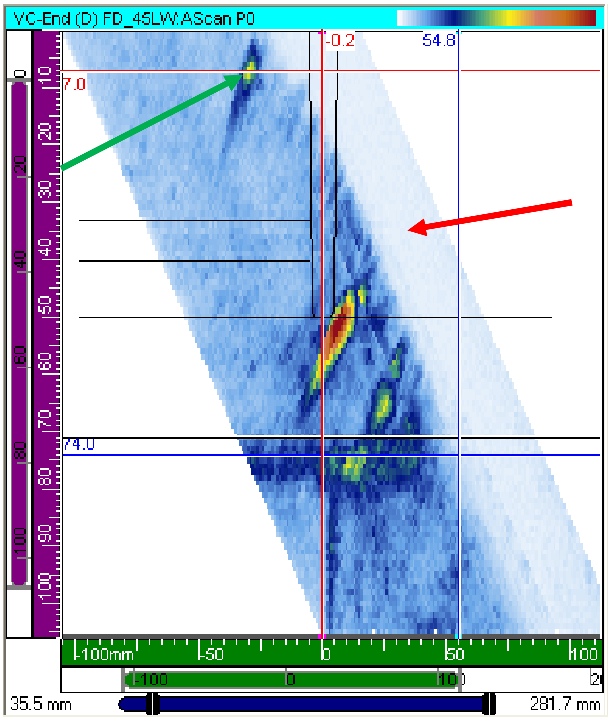

Figure 12. D-scan where an example of the adverse effect of the access limitation to the ultrasonic data can be seen. Data from one scan line pointed with red arrow is missing due to insufficient coupling. The geometrical indication from the corner of the counter bore is pointed with green arrow.

5. Methods

An advanced ultrasonic phased array procedure for the detection of possible inner and inner surface breaking fabrication flaws was assessed. Because ultrasonic testing is less sensitive to some fabrication flaws such as pores and inclusions, the testing was accompanied with radiographic examination. In addition, the both surfaces of the BWR weld were examined with visual (VT) and liquid penetrant testing (PT). For the Alloy 52 NGW mock-up, no VT or PT was performed due to the unfinished surfaces.

5.1 Personnel

The personnel conducting inspections and data analysis was qualified according to EN 473.

5.2 Visual testing

Visual testing was executed with naked eye according to EN ISO 17637 [5] and the acceptance level was B according to EN ISO 5817 [6].

5.3 Liquid penetrant testing

The liquid penetrant testing was performed according to EN 571-1 [7] and the acceptance level was 2X according to EN ISO 23277 [8].

5.4 Phased array ultrasonic testing

5.4.1 Phased array procedure

The phased array ultrasonic inspection of the BWR mock-up was conducted by applying a procedure established by Zetec [3]. For the examination of the Alloy 52 NGW mock-up a revised version [4] of the procedure was used. The procedures mentioned are implementation of EPRI-developed phased array technology for application to the examination of dissimilar metal welds associated with nuclear power plants. They are applicable for the encoded phased array ultrasonic examination of wrought full penetration dissimilar metal piping butt welds, conducted from the external (OD) surface using the contact method. This includes DM piping systems susceptible to stress corrosion cracking (SCC) [3, 4].

The procedures are applicable to the volumetric examination of the above mentioned welds and the adjacent base materials for the following flaw types:

- Far-surface breaking planar flaws parallel to the weld (circumferential flaws)
- Far-surface breaking planar flaws transverse to the weld (axial flaws).

The techniques described in the procedures address the detection, length sizing and through-wall sizing of discontinuities within the examination volume described in Chapter 4 of this report.

5.4.2 Ultrasonic equipment and scanner

The inspection according to the procedure [3] is aimed to be carried out using OmniScan alone as a data acquisition unit. Deviating from that, the inspection of the BWR mock-up was carried out using OmniScan with UltraVision Software Control. The revised version [4] of the procedure used during the inspection of the Alloy 52 NGW mock-up allows using UltraVision Software Control in data acquisition.

Scanning was performed using SPIDER motorized scanner manufactured by Phoenix ISL together with MCDU2 motor controller unit manufactured by Olympus driven by UltraVision software. The inspection system is shown in Figure 13. The data analysis was performed using UltraVision software.

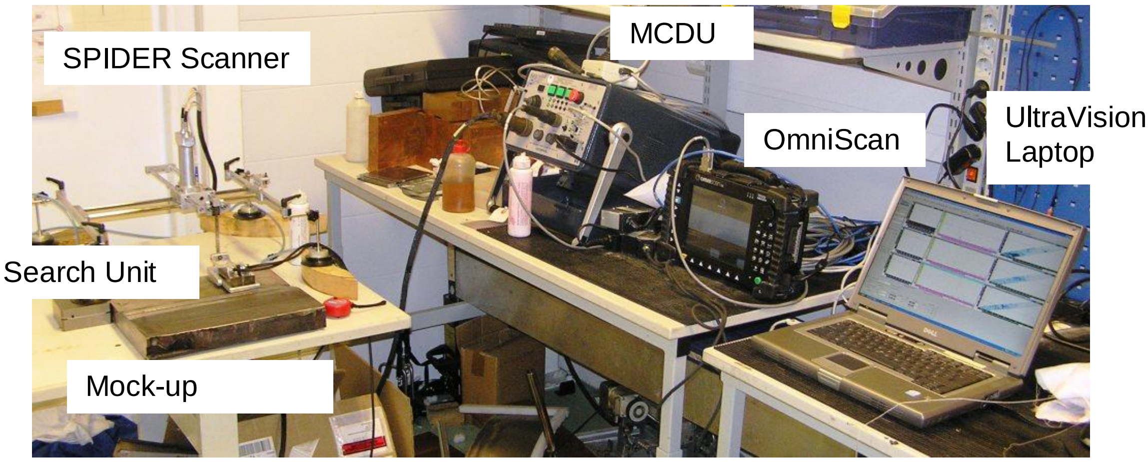

Figure 13. The phased array inspection system.

5.4.3 Ultrasonic phased array probe and wedge details

The procedure uses dual two-dimensional (2D) array configuration. The essential parameters of the probes are listed in Table 1.

Table 1. Essential variables of the phased array probes [3].

Type	CL	AS
Reference	1.5M32X2E64-15	1.5M5X3E17.5-9
Manufacturer	Imasonic	Imasonic
Frequency	1.5 MHz	1.5 MHz
Total aperture	64.0 x 15.0 mm	17.35 x 8.85 mm
Elements on primary axis	32	5
Elements on secondary axis	2	3
Element size on primary axis	1.8 mm	3.35 mm
Element size on secondary axis	7.3 mm	2.85 mm
Primary axis pitch	2.0 mm	3.50 mm
Secondary axis pitch	7.5 mm	3.00 mm

The Rexolite wedges allow the formation of several beam angles simultaneously. Wedges are cut two-dimensionally. The one dimension, wedge angle, controls the refracted angle and the other dimension, roof angle, affects the beam focusing or skewing capabilities.

The wedge used in the inspection of the BWR mock-up deviated from the one described in the procedure [4] because it was not reasonable to develop a specific wedge for this single purpose taking into account the schedule of the task. The procedure is developed for the piping weld inspection and the mock-up studied here was flat. The only flat wedges available were designed for somewhat thicker material out of the coverage range of the procedure. That led the focal depth of the ultrasonic sound beam being not optimized for the material depth studied here.

To find out the optimal focal depth, beam simulations for different focal law groups were performed using Zetec's Advanced PA Calculator software. The optimal focal depth depends on the roof angle of the TR wedge. The simulation results are presented in Figure 14. Simulations show that the –6 dB focal zone of the 45 and 60 degree LW together with 60 degree SW focal laws cover the inspection volume well. The –6 dB focal zone of the 45 degree SW focal law is mainly in the deeper location than the volume to be inspected.

TRL 45

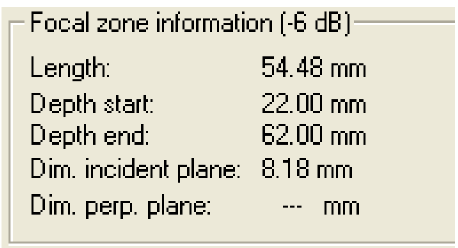

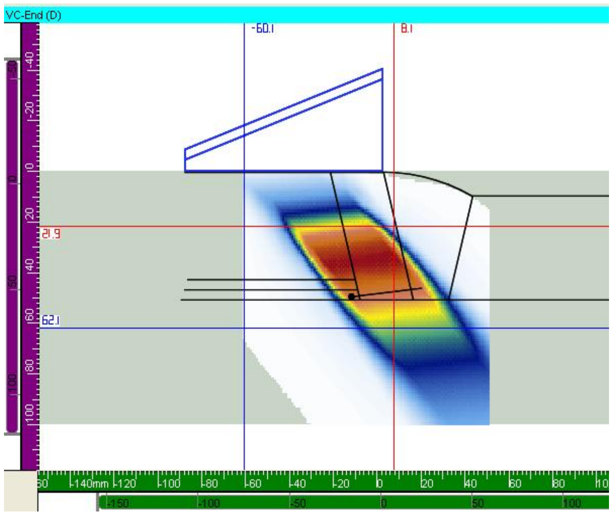

TRL 60

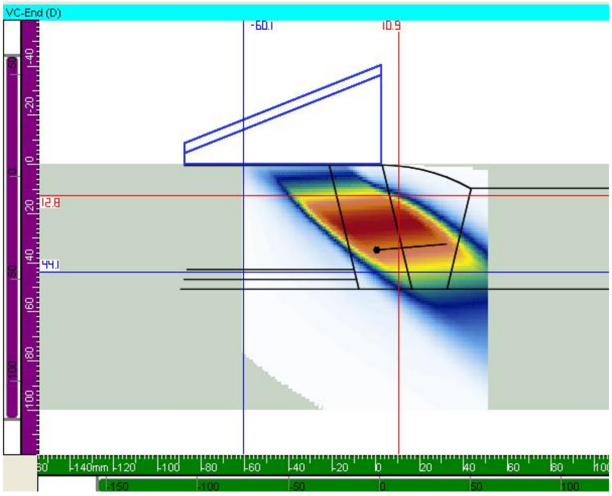

Focal zone information (-6 dB)

Length:	58.69 mm
Depth start:	13.00 mm
Depth end:	44.00 mm
Dim. incident plane:	10.86 mm
Dim. perp. plane:	--- mm

TRL 70

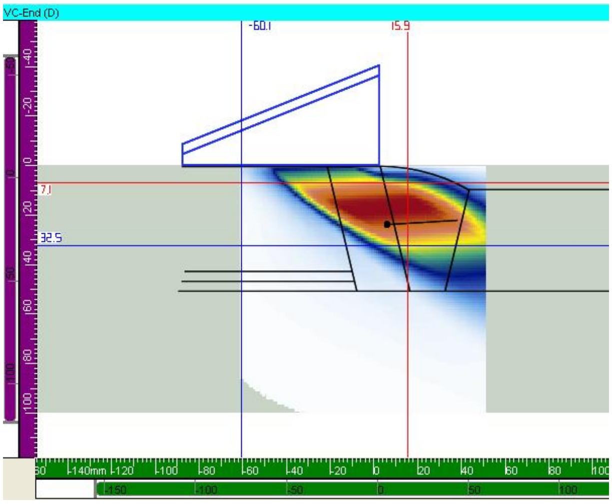

Focal zone information (-6 dB)

Length:	64.84 mm
Depth start:	7.00 mm
Depth end:	33.00 mm
Dim. incident plane:	15.73 mm
Dim. perp. plane:	--- mm

TRS 45

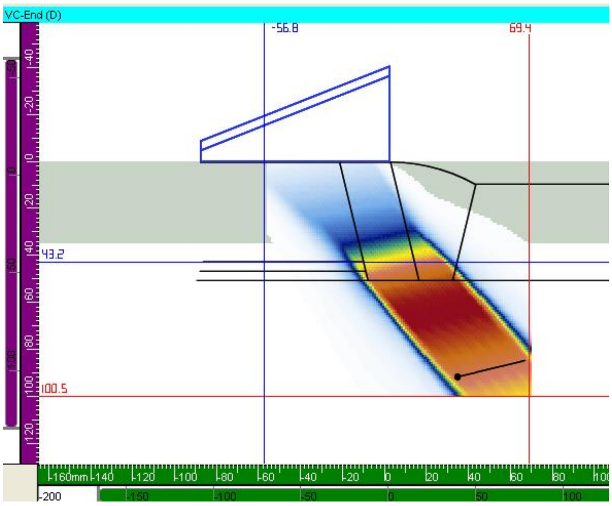

Focal zone information (-6 dB)

Length:	81.98 mm
Depth start:	43.00 mm
Depth end:	100.00 mm
Dim. incident plane:	7.41 mm
Dim. perp. plane:	--- mm

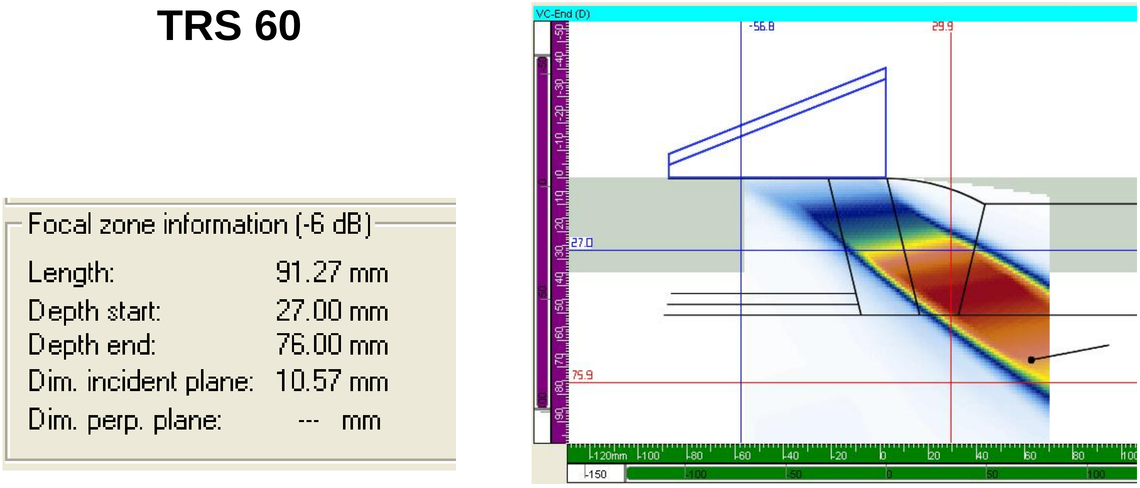

Figure 14. The simulation results for longitudinal and shear wave focal law groups.

When inspecting the Alloy 52 NGW mock-up, wedges described in the procedure [4] were available. The cut of the wedge for the CL probes was optimized for the thickness of 30 but still covering the material thickness of 46 mm. For the axial flaw examination, only a wedge for longitudinal wave mode was available.

The search unit is an assembly of two array probes mounted on wedges joined together with an acoustical barrier to allow for transmit-receive (TR) operation. The essential variables of the search units are shown in Table 2.

Table 2. Essential variables of the search units.

Flaw type	Configuration, wave mode	Probe type	Probe position, skew	Contour	Assembly model	Manuf.	Wedge angle	Roof angle
CIRC	T/R, Long., Shear	CL	Nozzle, 90° Pipe, 270°	Flat		Dekra	19.5°	4.0°
CIRC	T/R, Long., Shear	CL	Nozzle, 90° Pipe, 270°	Flat	10040617	Zetec	22.3°	7.0°
AXIAL	T/R Long.	AS	Weld, 0° Weld, 180°	Flat	10042608	Zetec	15.0°	0°

5.4.4 Phased array focal laws

Phased array focal law is a group of parameters applied simultaneously by the OmniScan and UltraVision system during pulse transmission and reception to create a desired beam in the material. Combining several focal laws creates a focal law group which define the ultrasonic techniques used in this study. The focal law groups were created using the Zetec Advanced PA Calculator. The focal law groups are shown in Table 3. The focal law input parameters are shown in Table 4.

Table 3. Phased array focal law groups [4].

Flaw type	Configuration, wave mode	Focal law group	Focal law type	Refracted angles	Beam skew angle
CIRC	T/R, Long.	CIRCD TRL 90 CIRCU TRL 270	Linear	45°, 60°, 70°	0°
CIRC	T/R, Shear	CIRCD TRS 90 CIRCU TRS 270	Linear	45°, 60°	0°
AXIAL	T/R, Long.	AX TRL 0 AX TRL 180	Azimuthal	25°, 35°, 45°, 55°	-25° to 25°, resolution 2.5°

Table 4. Focal law input parameters [4].

	Circumferential flaws	Axial flaws
Probe type	**CL**	**AS**
Primary aperture	10	Full aperture
Resolution	1	N/A
Pulser stop	23	N/A
Improved resolution	Yes	N/A
Array type	1-D linear array	2-D matrix array
Scan type	Linear	Azimuthal
Focusing type	Auto	Half path
Focusing position	N/A	Plate thickness ± 6 mm
L-wave sound velocity in CS	5890 m/s	
S-wave sound velocity in CS	3230 m/s	
L-wave sound velocity in SS	5770 m/s	
S-wave sound velocity in SS	3150 m/s	
Pipe radius	Flat (parallelepiped)	

5.4.5 Mounting of phased array transducers

The transmitter (T) and receiver (R) probes are mounted according to Figure 15 and Figure 16.

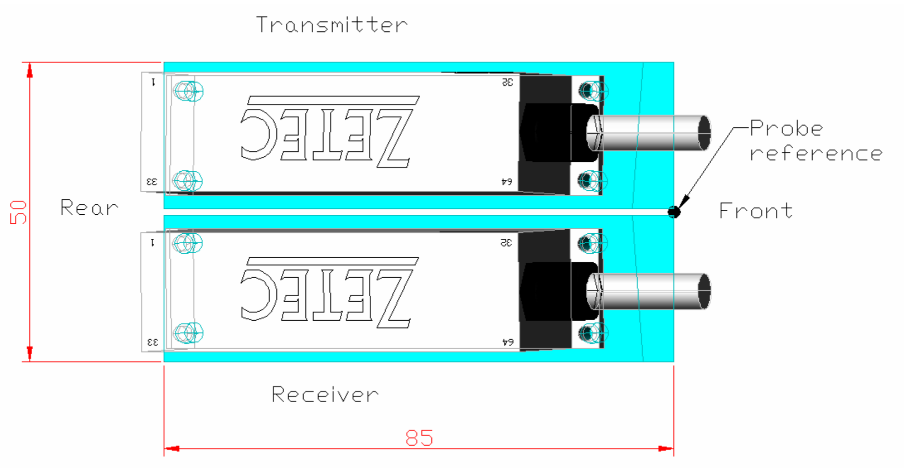

Figure 15. Mounting of the CL probes to the wedge [3].

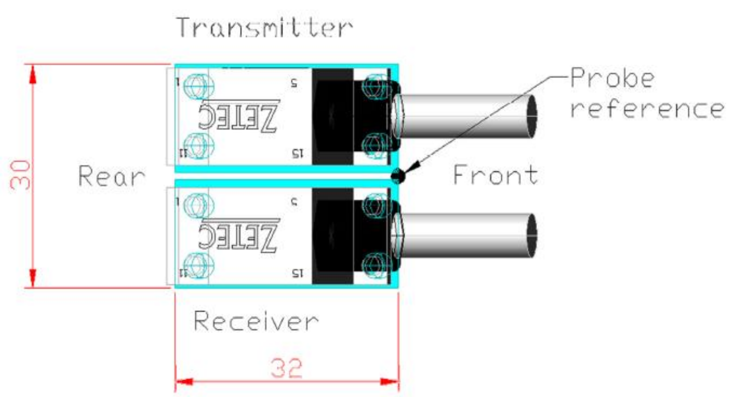

Figure 16. Mounting of the AS probes to the wedge [4].

5.4.6 Cabling and connections

The cabling and the connections of the inspection system are shown in Figure 17.

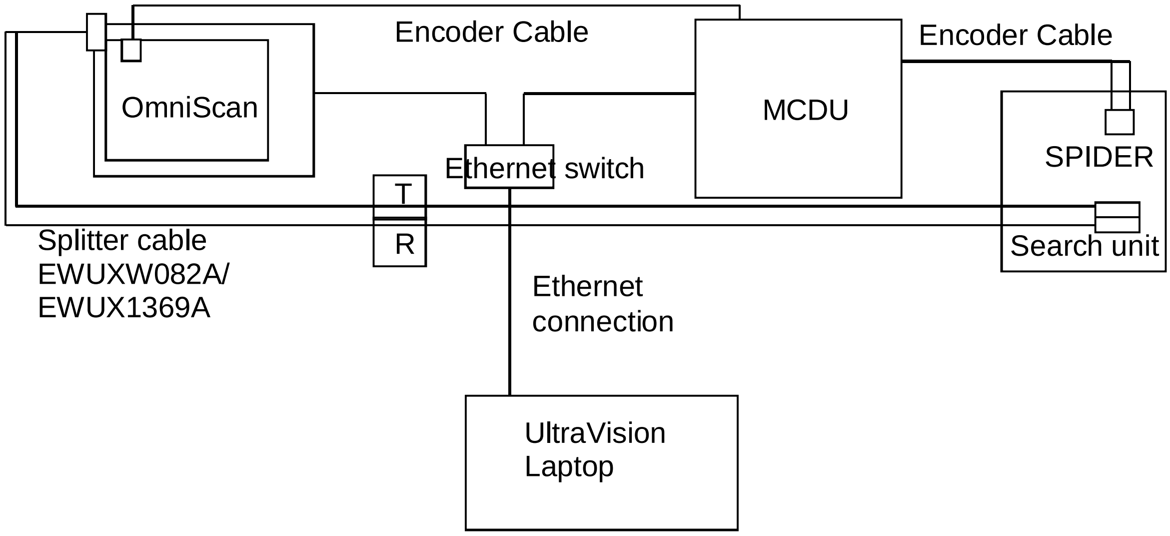

Figure 17. Cabling and connections diagram.

5.4.7 Ultrasonic couplant

The mixture of water and ultrasonic gel was used to create an acoustic coupling between the wedge and the specimen. Glycerine was used as a couplant between the probes and the wedges.

5.4.8 Calibration and reference blocks

An austenitic V2 block (Figure 18) was used for system delay setting. The austenitic reference block MEUXE24A (Figure 18) for circumferential flaws and MEUXE25A for axial flaws (Figure 19) containing side drilled holes were used for calibration verification.

Figure 18. Reference block MEUXE024A and V2 block.

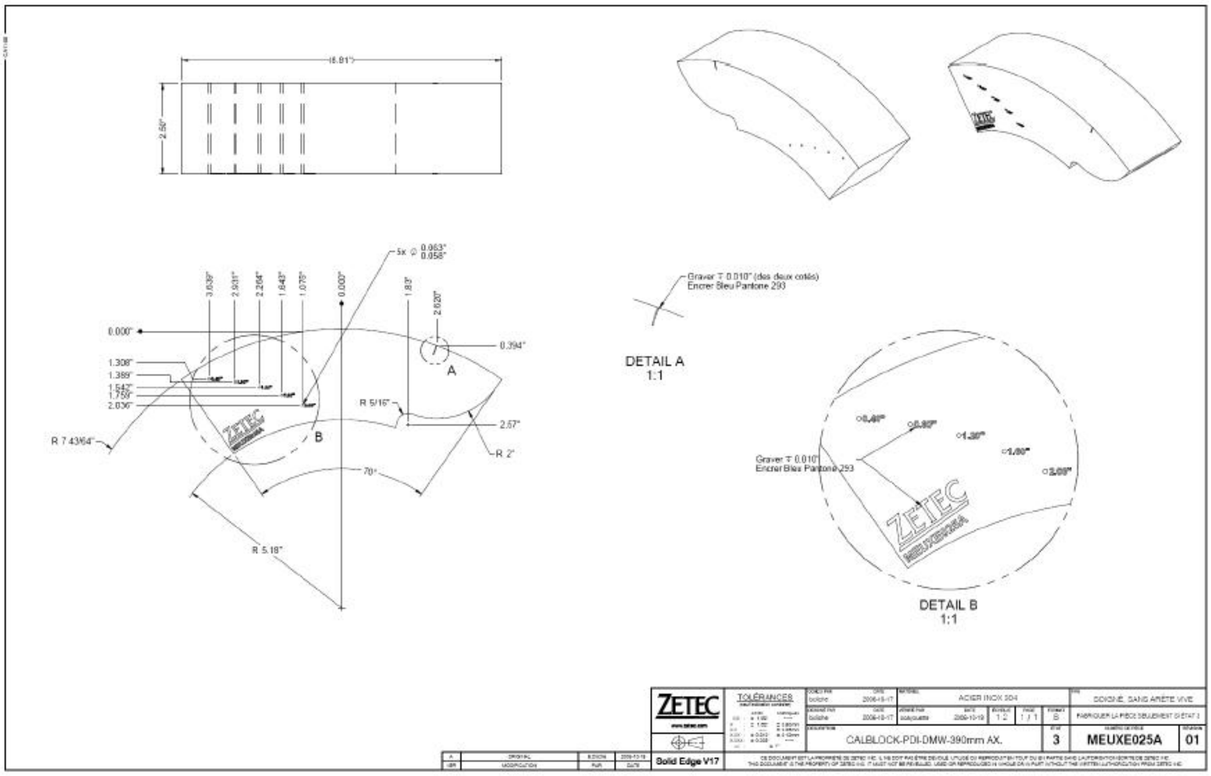

Figure 19. Reference block MEUXE025A [3].

5.4.9 Calibration

The system delay setting for different setups was performed using the V2 block by maximizing the 45 degree echo from the 50 mm curve before the inspections. Calibration verification was performed after all inspection periods.

5.4.10 Inspection sensitivity setting

The sensitivity of the ultrasonic beam was set so that the average noise level of the 45 degrees focal law in the weld root area was about 10 to 15 % of the full screen height (FSH).

5.4.11 Reference system

The reference system is shown in Figure 20 [4]. As a deviation, the scanning of the BWR mock-up was performed in the opposite direction.

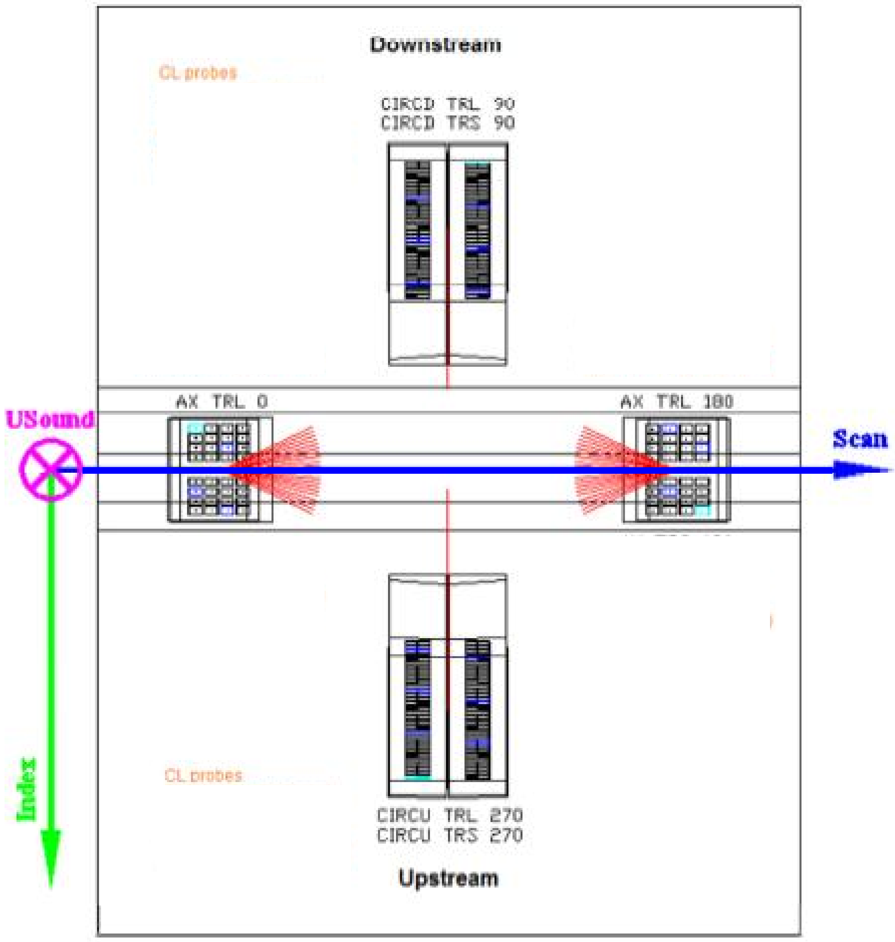

Figure 20. The reference system used in the inspections [5].

5.4.12 Scan plans

The scan plans were made according to the procedures [3, 4]. The procedures include an Excel worksheet for calculation of the scanning index (y axis) resolution based on the given test block parameters so that the requirements presented in Figure 21, Figure 22 and Figure 23 are fulfilled. The scan plans are shown in Figure 24, Figure 25 and Figure 26. The resolution in the scanning direction (x axis) was 2 mm. Scanning of the circumferential flaws was divided in two parts in x direction due to a limited axis length of the scanning device. The overlap between the two scans was 25 mm.

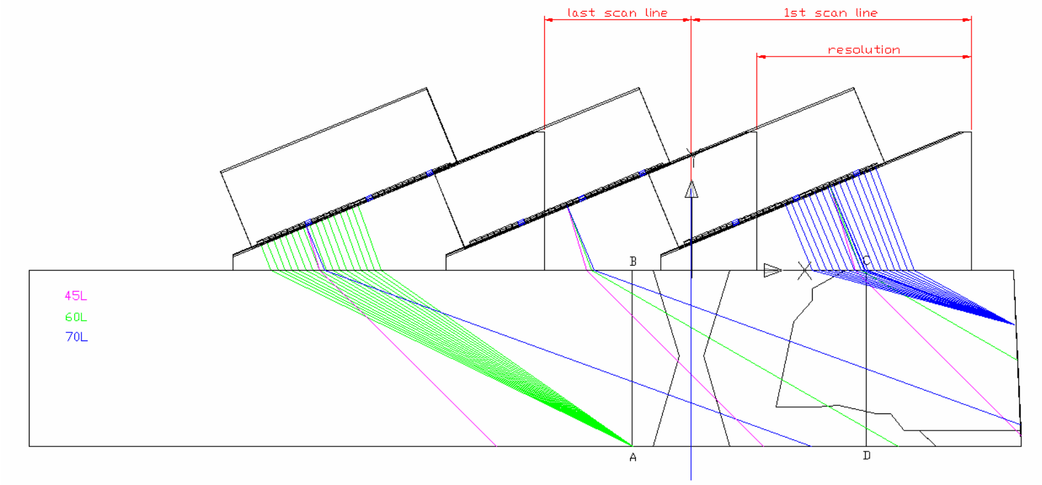

Figure 21. Index positions for circumferential flaw examinations with longitudinal waves [3].

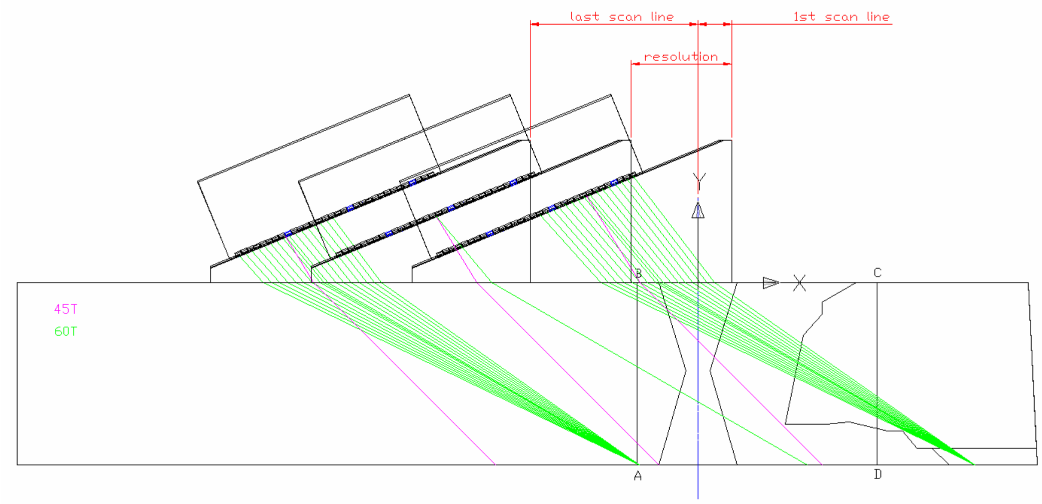

Figure 22. Index positions for circumferential flaw examinations with shear waves [3].

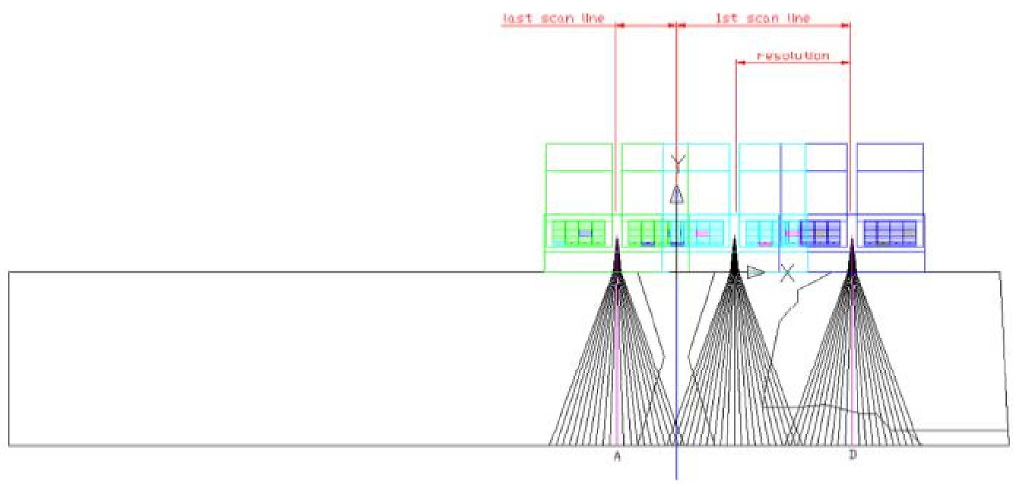

Figure 23. Index positions for axial flaw examination [4].

SCAN PLAN

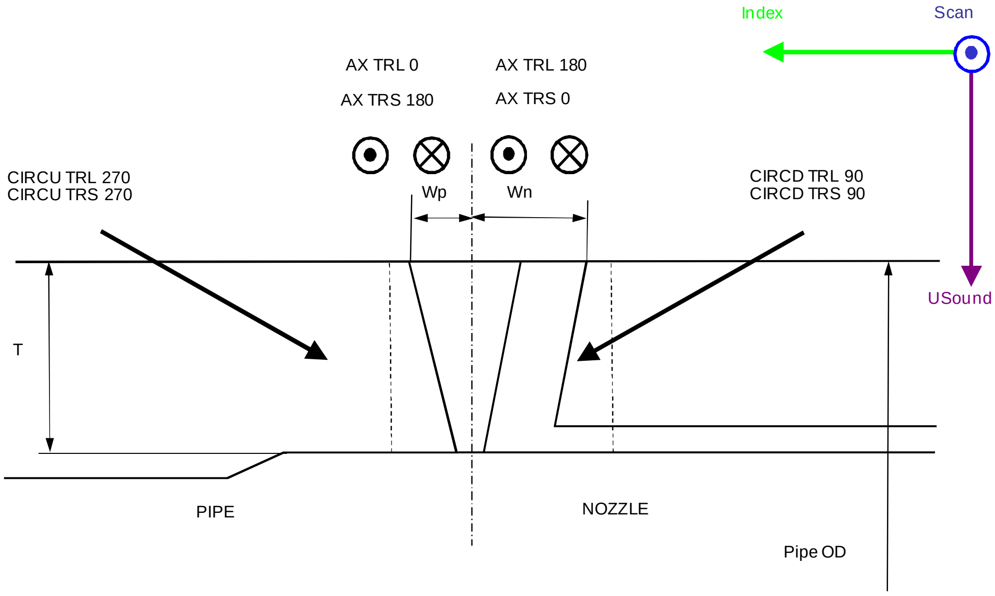

Procedure :	*151811_Zetec_OmniScanPA_03_revA*	***Pipe Thickness T :***	*51,0*	mm
Plant / Unit :	*VTT Lab*	***Pipe OD :***	*10000,0*	mm
Weld Id. :	*SINI*	***Weld Extent Pipe Side Wp :***	*18,0*	mm
Dual Side Access :	*Full Access*	***Weld Extent Nozzle Side Wn :***	*43,0*	mm
Complete Pipe:	*Plate*	***Access Limitation Pipe Side Lp :***	*200,0*	mm
		Access Limitation Nozzle Side Ln :	*200,0*	mm
		Weld Length:	*350,0*	mm

SCANNING SEQUENCES CIRCUMFERENTIAL FLAWS

Focal law group	Probe Type	MinTB	MaxTB	Scan			Index			# Lines	Done ?
				Start	Stop	Resol.	Start	Stop	Resol.		
		(mm)	(mm)	(mm)	(mm)	(mm)	(mm)	(mm)	(mm)		(OK / NA)
CIRCD TRL 90	CL	127,5	159,4	25,0	325,0	2,0	-78,8	46,1	31,2	5	
CIRCU TRL 270	CL	127,5	159,4	25,0	325,0	2,0	-71,1	53,8	31,2	5	
CIRCD TRS 90	CL	127,5	159,4	25,0	325,0	2,0	-84,8	-32,3	26,3	3	
CIRCU TRS 270	CL	127,5	159,4	25,0	325,0	2,0	7,3	59,8	26,3	3	

Figure 24. Scan plan for the phased array inspection of the BWR mock-up.

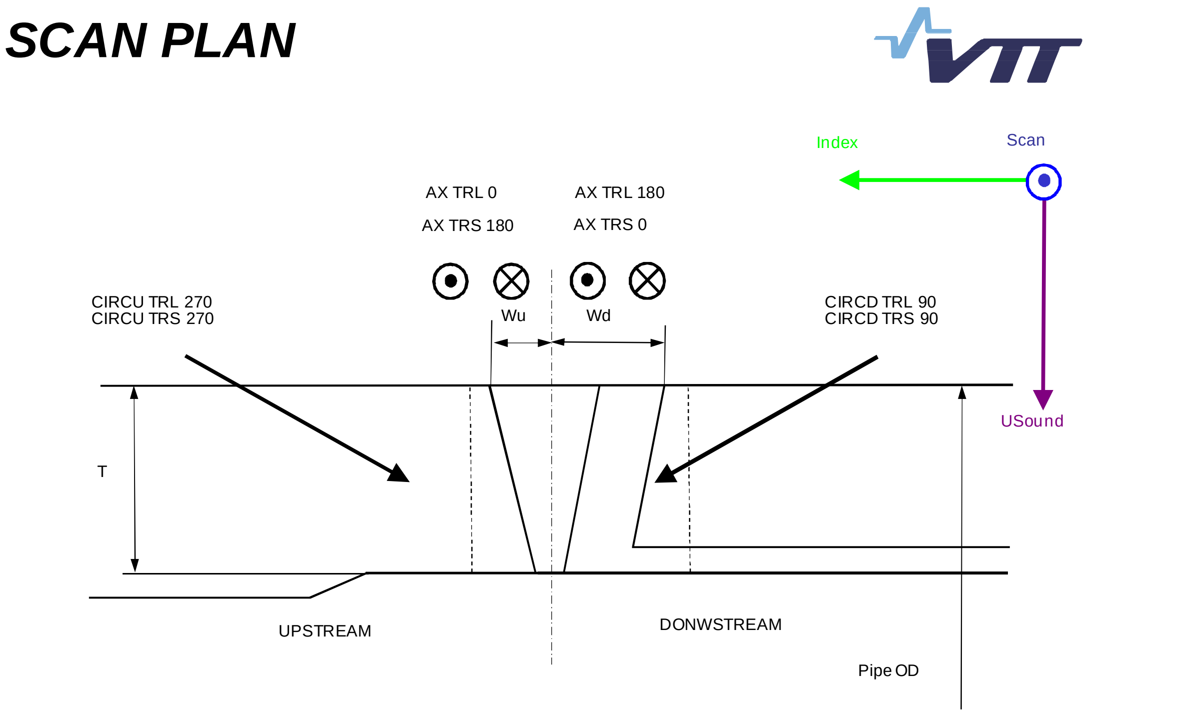

Procedure :	*C3467_ZETEC_OmniScanPA_03_revE*	**Pipe Thickness T :**	*50,0*	mm
Plant / Unit :	*VTT NDE Laboratory*	**Pipe OD :**	*1019,0*	mm
Weld Id. :	*SINI NG Weld 1*	**Weld Extent Upstream Side Wu :**	*6,0*	mm
Dual Side Access :	*Yes*	**Weld Extent Downstream Side Wd :**	*6,0*	mm
Complete Pipe:	*no*	**Access Limitation Up Side Lu :**	*150,0*	mm
Add. Exam. volume:	*6,4* mm	**Access Limitation Down Side Ld :**	*130,0*	mm
		Weld Length:	*340,0*	mm

SCANNING SEQUENCES CIRCUMFERENTIAL FLAWS

Focal law group	Probe Type	MinTB	MaxTB	Scan			Index			# Lines	Done ?
				Start	End	Resol.	Start	End	Resol.		
		(mm)	(mm)	(mm)	(mm)	(mm)	(mm)	(mm)	(mm)		(OK / NA)
CIRCD TRL 90	CL	125,0	156,3	25,0	315,0	2,0	-40,1	34,1	24,7	4	
CIRCU TRL 270	CL	125,0	156,3	25,0	315,0	2,0	-34,1	40,1	24,7	4	
CIRCD TRS 90	CL	125,0	156,3	25,0	315,0	2,0	-45,0	4,7	24,9	3	
CIRCU TRS 270	CL	125,0	156,3	25,0	315,0	2,0	-4,7	46,1	25,4	3	

Figure 25. Scan plan for the circumferential flaw inspection of the Alloy 52 NGW mock-up.

SCAN PLAN

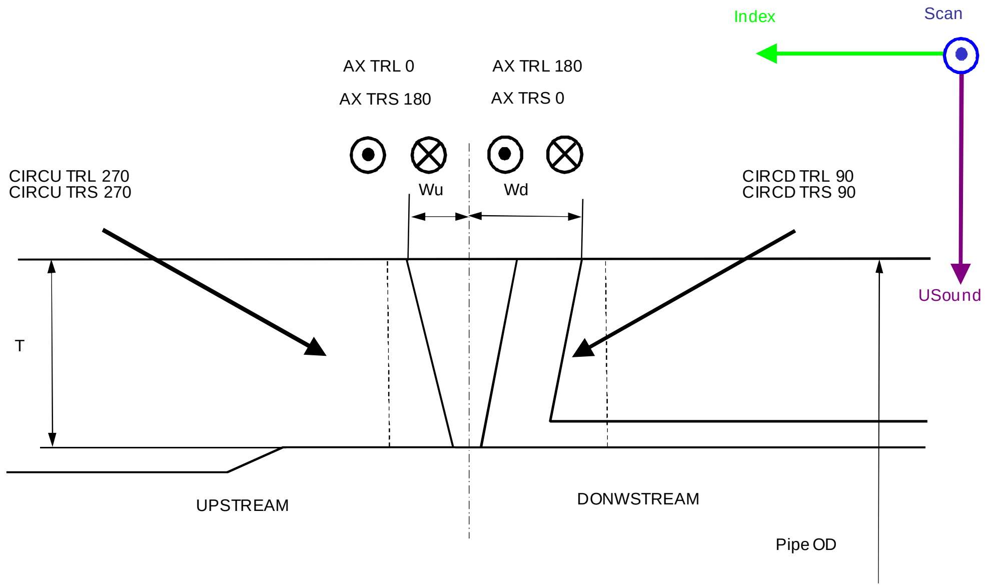

Procedure :	*C3467_ZETEC_OmniScanPA_03_revE*	*Pipe Thickness T :*	*50,0* mm
Plant / Unit :	*VTT NDE Laboratory*	*Pipe OD :*	*1019,0* mm
Weld Id. :	*SINI NG Weld 1*	*Weld Extent Upstream Side Wu :*	*6,0* mm
Dual Side Access :	*Yes*	*Weld Extent Downstream Side Wd :*	*6,0* mm
Complete Pipe:	*no*	*Access Limitation Up Side Lu :*	*150,0* mm
Add. Exam. volume:	*6,4* mm	*Access Limitation Down Side Ld :*	*30,0* mm
		Weld Length:	*340,0* mm

SCANNING SEQUENCES CIRCUMFERENTIAL FLAWS

Focal law group	*Probe Type*	*MinTB*	*MaxTB*	*Scan*			*Index*			*# Lines*	
				Start	*End*	*Resol.*	*Start*	*End*	*Resol.*		
		(mm)	(mm)	(mm)	(mm)	(mm)	(mm)	(mm)	(mm)		
AX TRL 0	*AL*	*215,5*	*269,3*	*44,0*	*340,0*	*2,0*	*-8,0*	*12,4*	*5,1*	*5*	
AX TRL 180	*AL*	*215,5*	*269,3*	*0,0*	*296,0*	*2,0*	*-8,0*	*12,4*	*5,1*	*5*	

Figure 26. Scan plan for the axial flaw inspection of the Alloy 52 NGW mock-up.

5.4.13 Scanning speed

The scanning speed was below 25 mm so that the complete collection of A-scans was ensured.

5.4.14 Merging of the data groups

The focal law groups were merged so that the data from each angle could be analysed separately.

5.4.15 Pre-analysis data verification

Before data analysis, pre-analysis data quality verification for the raw data was performed according to the procedure. The ultrasonic data fulfilled the requirements stated in the procedure [3, 4].

5.4.16 Indications to be reported [3, 4]

Typically, the following indications will be evaluated and reported:

- Localized high amplitude indications
- Indications showing a through-wall character
- Indications which are offset from normal geometry, such as the weld centre line, root, counter bore areas and metallurgical interfaces
- Indications that display unique response as compared to benchmark responses.

5.4.17 Discrimination of indications

The discrimination of indications into geometrical, metallurgical and flaw indications was performed according to the procedures [3, 4]

5.4.18 Circumferential flaw length sizing [3, 4]

The flaw length was determined in circumferential (Scan axis) position by locating the start and end points of the flaw according to the full amplitude drop method.

5.5 Radiographic examination

For the BWR mock-up, both conventional film and digital radiography were applied. For the Alloy 52 NGW mock up, only film radiography was applied. The radiographic examination was performed for the full weld volume including the HAZ. The radiographic examination of the BWR mock-up was performed using Betatron 7.5 MeV accelerator. The radiographic examination of the Alloy 52 NGW mock-up was performed using Seifert 275 kV X-ray equipment.

6. Results

6.1 Results of the inspection of the BWR mock-up

6.1.1 Visual Testing

Low surface flaws (Figure 27) and a flaw in the interface of the cladding and ferrite base material (Figure 28) were detected in the visual testing of the BWR mock-up.

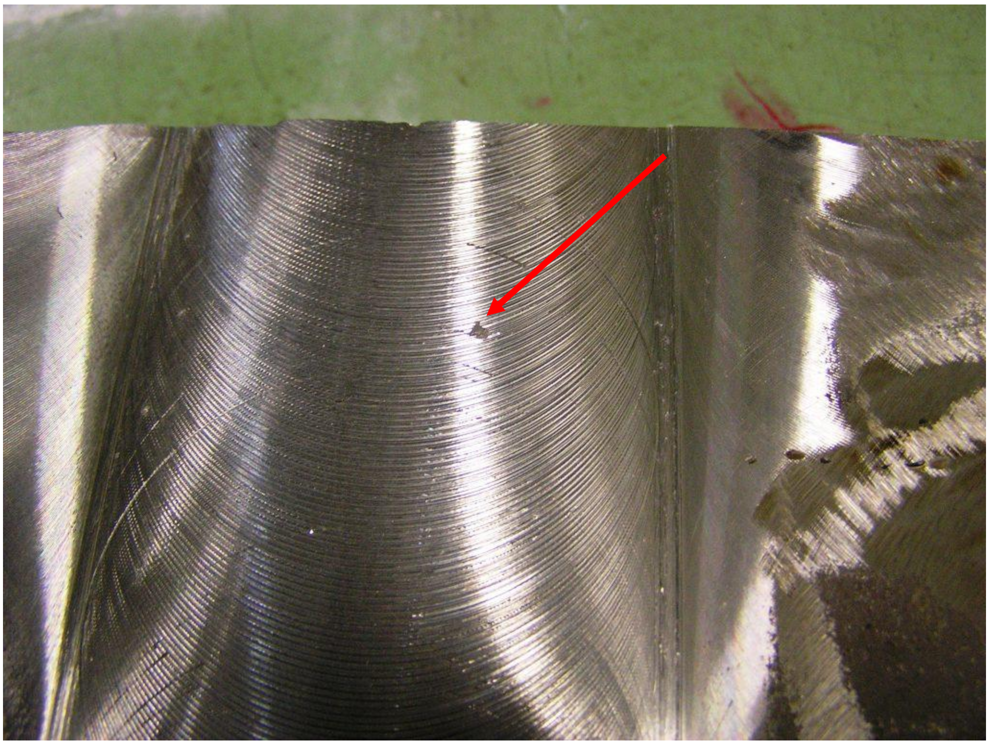

Figure 27. An example of a low surface flaw in the BWR mock-up pointed with an arrow.

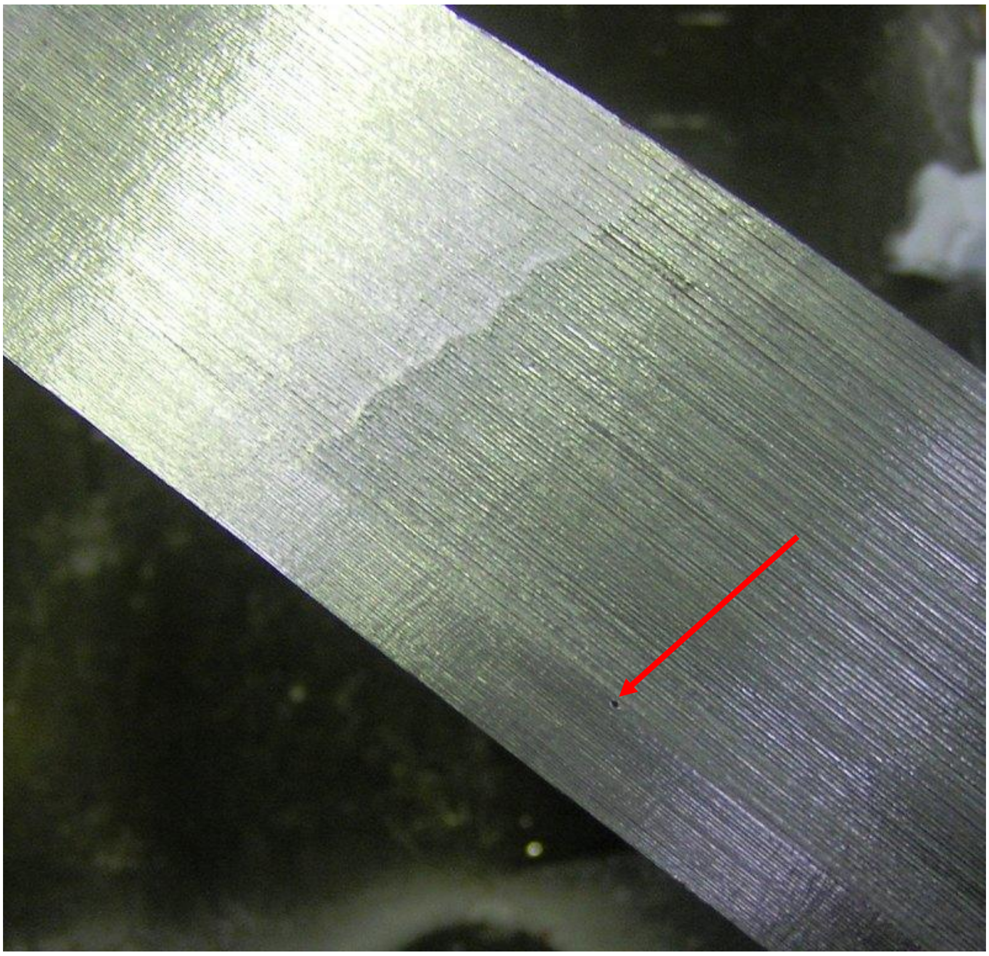

Figure 28. A small flaw at the interface of the cladding and ferrite base material in the BWR mock-up pointed with an arrow.

6.1.2 Liquid penetrant testing

Low surface flaws and a flaw at the interface of the cladding and ferrite base material were detected in the liquid penetrant testing of the BWR mock-up, Figure 29.

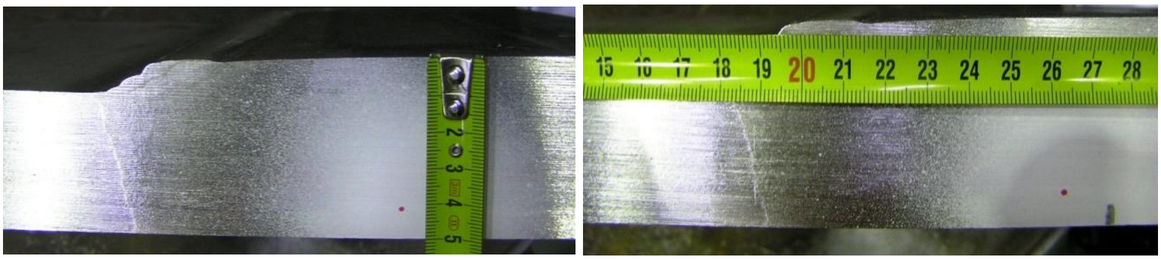

Figure 29. A small flaw at the interface of the cladding and ferrite base material in the BWR mock-up.

6.1.3 Radiographic examination

No flaws were detected in the radiographic examination of the BWR mock-up.

6.1.4 Phased array ultrasonic inspection

The results of phased array ultrasonic inspection of the BWR mock-up are reported in Table 5. The table contains flaw ID, the focal law groups which detected the flaws, the start and end points of the flaws in scanning (longitudinal) direction, the flaw location in index direction, flaw length and the flaw location in depth direction. The flaw height sizing was not performed because no flaw tip signals were detected and all the flaws were embedded. The phased array inspection and flaw data are presented in Appendix 1.

Table 5. BWR mock-up flaw table.

FLAW TABLE

Procedure : 151811_ZETEC_OmniScanPA_03_revA — **Weld Id :** BWR mock-up
Plant / Unit : VTT NDE Research Hall — **Diameter :** Plate mm
Thickness : 51,0 mm

Flaw #	Detection	Scan1	Scan2	Index1	Index2	OD Length	Height	Depth (Comments)
	(Focal law group)	(mm)	(mm)	(mm)	(mm)	(mm)	(mm)	
1	HD_45LW	8	48	-73	-62	40,0	NA	D = 41 (Carbon steel/cladding)
1	HD_60LW	12	26	-64	-63	14,0	NA	D = 40
1	HD_45SW	4	54	-79	-64	50,0	NA	D = 42
1	HD_60SW	0	50	-70	-65	50,0	NA	D = 41
1	HU_45LW	0	131	-68	-46	131,0	NA	D = 39
2	HD_60LW	12	134	19	35	122,0	NA	D = 28
2	HD_70LW	10	64	26	39	54,0	NA	D = 20
3	HD_60LW	56	86	-41	-25	30,0	NA	D = 27
4	HD_60LW	208	224	-30	-30	16,0	NA	D = 23
5	HD_45LW	268	356	-77	-41	88,0	NA	D = 12
5	HD_60LW	264	360	-75	-40	96,0	NA	D = 11
5	HD_70LW	264	290	-50	-31	26,0	NA	D = 11
5	HU_45LW	281	348	-56	-42	67,0	NA	D = 10
5	HU_60LW	269	348	-56	-39	79,0	NA	D = 10
5	HU_70LW	271	348	-56	-42	77,0	NA	D = 10

There were three flaws (1, 2 and 5) altogether in the BWR mock-up which were detected with at least two focal law groups. Flaws 1 and 5 were confirmed with at least one detection from both sides. Both flaws 3 and 4 were detected with only one focal law group. All the flaws were embedded.

Flaw 1 had a high SNR with 45° LW from both sides and with 45° SW from CS side and it could be separated from the metallurgical indication from the boundary. Flaw 1 was not detected with higher angles from the SS side due to the missed scan lines. The 70° LW focal laws from CS side and SW focal laws from SS side do not cover the flaw 1 location.

Flaw 2 was detected only with 60° and 70° LW from CS side. The indication is localized and the amplitude response is comparable with both angles. That supports the interpretation that the indication is a flaw indication, probably a lack of fusion, rather than just a metallurgical indication from the boundary between weld and parent material.

Flaws 2 and 3 have a very low SNR and were only detected with 60° LW focal law group from CS side. Still the indications have clear start and end points and are isolated from the continuous metallurgical indications at the deeper location. The indications are most probably non-planar due to the low SNR.

Flaw 5 was detected and could be isolated from the continuous metallurgical indication with all LW focal law groups from both the CS and SS side and with all SW focal law groups from the CS side.

The weld metal caused high scattering of the ultrasound. The acoustical interface of the cladding/CS boundary caused a strong metallurgical indication at varying amplitudes intermittently along the scanning length. It was clear that this metallurgical indication was not connected to the ID surface. Such indications were detected from the CS side with all longitudinal and shear wave angles. The boundary between weld joint/parent material caused indications when scanned from the SS side of the weld.

6.2 Results of the inspection of the Alloy 52 NGW mock-up

6.2.1 Visual testing

Visual testing of the Alloy 52 NGW mock-up showed no surface flaw indications. The surface condition was as welded.

6.2.2 Radiographic examination

No flaws were detected in the radiographic examination of the Alloy 52 NGW mock-up.

6.2.3 Phased array ultrasonic inspection

The results of phased array ultrasonic inspection of the BWR mock-up are reported in Table 6. The table contains flaw ID, the focal law groups which detected the flaw, the start and end points of the flaw in scanning (longitudinal) direction, the flaw location in index direction, flaw length and the flaw location in depth direction. The flaw height sizing was not performed because no flaw tip signals were detected and the flaw was embedded. The phased array inspection and flaw data are presented in Appendix 2.

Table 6. Alloy 52 NGW mock-up flaw table.

FLAW TABLE

Procedure :	Zetec_OmniScanPA_03_rev A.	***Weld Id :***	Alloy 52 mock-up		
Plant / Unit :	VTT NDE Research Hall	***Diameter :***	plate	mm	
		Thickness :	51,0	mm	

Flaw #	Detection (Focal law group)	Scan1 (mm)	Scan2 (mm)	Index1 (mm)	Index2 (mm)	OD Length (mm)	Height (mm)	Depth (mm)
1	FD_45LW	10	34	-2	4	24,0	NA	D = 20
1	FD_60LW	10	34	2	10	24,0	NA	D = 13
1	FD_70LW	10	34	0	0	24,0	NA	D = 9
1	FD_45SW	10	40	4	4	30,0	NA	D = 24
1	FD_60SW	10	48	-4	7	38,0	NA	D = 20

There was one flaw detected in the Alloy 52 NGW mock-up. Flaw 1 was detected only from the CS side of the weld and the detection was made with all focal law groups. The flaw was an embedded circumferential flaw with defined start and end points. No axial flaws were detected.

The weld metal caused high scattering of the ultrasound both in circumferential and axial scanning. The acoustical interface of the cladding/CS and weld metal/parent material boundaries caused strong metallurgical indications at varying amplitudes intermittently along the scanning length. It was clear that these metallurgical indications were not ID surface connected.

The counter bore on the mock-up surface caused a continuous geometrical indication with 45°, 60°, 70° LW and 60° SW focal law groups when scanned from the CS side. The weld root reinforcement caused a continuous geometrical indication with 45° LW and SW focal law groups when scanned from CS side and with 45° and 60° LW and SW focal law groups when scanned from the SS side.

The concave weld toe filled with coupling medium caused continuous mode converted indication at the depth of ~10–30 mm in all axial scans.

7. Validation of results

The phased array ultrasonic testing procedure used in this study was developed for ISI of the inner third of the weld and HAZ. However, the procedure provides additional coverage of the complete weld volume, butter material and base material for a distance of 6.35 mm from each weld toe or butter interface from the inner surface extending to mid-wall or higher. Due to that, the procedure is usable also for PSI. However, the full examination coverage requires an access over the weld (machined, even surface) which was not the situation with both of the mock-ups. Flaw 5 in the BWR mock-up showed that the PAUT procedure can detect flaws even in the depth of <10 mm from the OD surface.

According to many sources, the theoretical size of the smallest detectable flaw is half of the wavelength. According to the equation (1), the wavelength λ is

$$\lambda = \frac{c}{f} \qquad (1)$$

where c = sound velocity (mm/s)
f = frequency (MHz)

With longitudinal wave, c = 5770000 mm/s. The frequency used is 1.5 MHz, so λ = 3.8 mm. Theoretically, the smallest detectable flaw is therefore 3.8/2 ≈ **2 mm.**

With transverse wave, c = 3150000 mm/s. The frequency used is 1.5 MHz, so λ = 2.1 mm. Theoretically, the smallest detectable flaw is therefore 2.1/2 ≈ **1 mm.**

During the preparation of autoclave tests, hot cracking was detected in the Alloy 52 NGW mock-up. However, cracking was so low and tight that it hardly could be detected with ultrasonic technique when taking into account the challenges for ultrasonic inspection due to material properties. Also the strong geometrical indication from the weld root reinforcement has likely masked those indications. Even if the weld root was machined still a metallurgical indication from the weld root would have been expectable.

If the weld root of the Alloy 52 NGW mock-up would have been inspected using liquid penetrant testing, surface opening cracking would have been possible to detect if the cracking was not too tight. If the weld root cap was removed, conditions would have been more beneficial for the detection of hot cracking.

Radiographic examination is less sensitive with material thicknesses around 50 mm. The detection of small planar flaws may be impossible especially if they are not oriented parallel to the radiation beam.

8. Conclusions

The phased array inspection of the DMW mock-ups showed the well-known challenge of the inspection of such structures. Strong metallurgical indications were detected in both of the mock-ups. Also, geometrical issues were limiting the performance of the inspection. Several embedded flaws in the BWR mock-up and one embedded flaw in the Alloy 52 NGW mock-up were detected. The mock-up geometry also caused indications. Even though the metallurgical and geometrical indications were easily discriminated from flaw indications, they can mask shallow flaws and thus reduce the reliability of the inspection.

A flaw located at the depth of ~10 mm from the OD in the BWR mock-up proved that the PAUT procedure can detect flaw signals even in the depth of <10 mm from the OD surface which reduces the risk of under sizing deep flaws.

Small flaws connected to the weld root are very hard or impossible to discriminate due to the geometrical and/or metallurgical indications. Thus the removal of the weld root reinforcement is crucial for enhancing the reliability of ID surface connected flaw inspection.

The use of reference flaws such as side-drilled holes in realistic reference block would have helped assessing the ability of the inspection system to detect flaws as well as understanding the complex indications obtained.

9. Summary

BWR and Alloy 52 NGW dissimilar metal weld (DMW) mock-ups were non-destructively examined. The focus was on phased array ultrasonic testing using a commercial qualified phased array ultrasonic procedure developed for the inspection of DMWs. By this study, the commercial qualified PAUT procedure was implemented as a preparation for PARENT round robin testing of DMWs.

Inspection was accompanied with radiographic examination. In addition, the both surfaces of BWR weld were examined with visual and liquid penetrant testing.

The phased array inspection of the DMW mock-ups showed the well-known challenge of the inspection of such structures. Several embedded flaws in the BWR mock up and one embedded flaw in the Alloy 52 NGW mock-up were detected. Both metallurgical and geometrical indications were also detected. Even though those indications were easily discriminated from flaw indications, they can mask shallow flaws and reduce the reliability of the inspection.

References

1. Diaz et al. An Evaluation of Ultrasonic Phased Array Testing for Reactor Piping System Components Containing Dissimilar Metal Welds. Technical Letter Report. JCN N6398, Task 2A. PNNL-19018. Pacific Northwest National Laboratory, Richland, Washington, USA. November 2009.

2. Zetec Inc. Introduction to Phased Array Ultrasonic Technology Applications. Course at VTT Technical Research Centre of Finland in 2006.

3. Procedure for Encoded, Manually Driven, Phased Array Ultrasonic Examination of Dissimilar Metal Piping Welds with OmniScan PA (Document 151811_Zetec_OmniScanPA_03_revA.doc). Zetec Inc. Canada 2007.

4. Procedure for Encoded, Manually Driven, Phased Array Ultrasonic Examination of Dissimilar Metal Piping Welds (Document C3467_Zetec_OmniScanPA_03_revA.docx Revision A). Zetec Inc. Canada 2011.

5. EN ISO 17637:2011. Non-destructive testing of welds. Visual testing of fusion-welded joints. European Committee for Standardization.

6. EN ISO 5817:2006. Welding. Fusion-welded joints in steel, nickel, titanium and their alloys (beam welding excluded). Quality levels for imperfections. European Committee for Standardization.

7. EN 571-1:1997. Non-destructive testing. Penetrant testing. Part 1: General principles. European Committee for Standardization.

8. EN ISO 23277:2010. Non-destructive testing of welds. Penetrant testing of welds. Acceptance levels. European Committee for Standardization.

APPENDIX 1. The BWR mock-up phased array testing data

1.1 CIRCD TRL 90 scan 0–290 mm

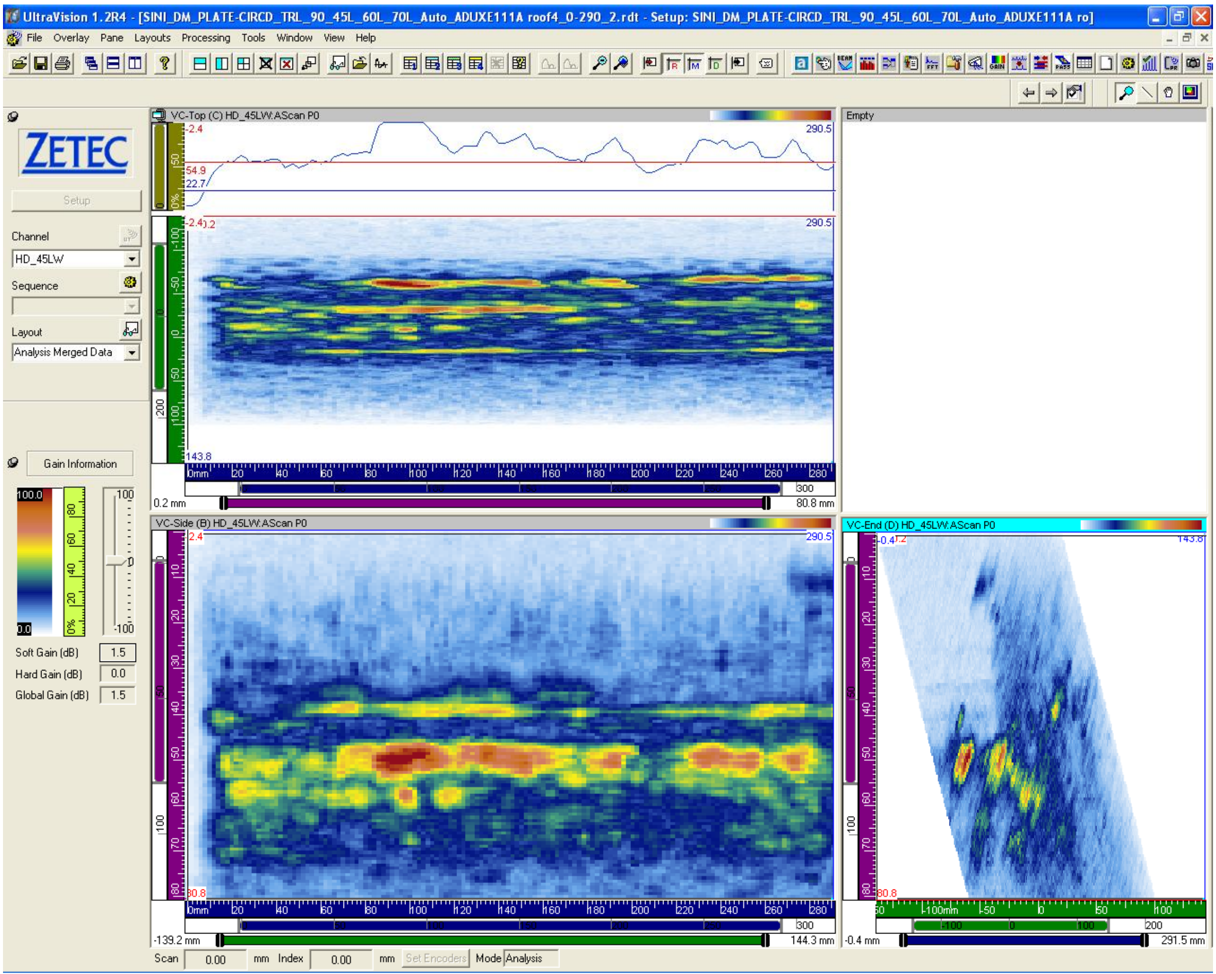

Figure 1.1. BWR mock-up data at 45° longitudinal wave from CS side. Strong metallurgical indication in the acoustical interface of the cladding-CS boundary at varying amplitudes along the scanning length.

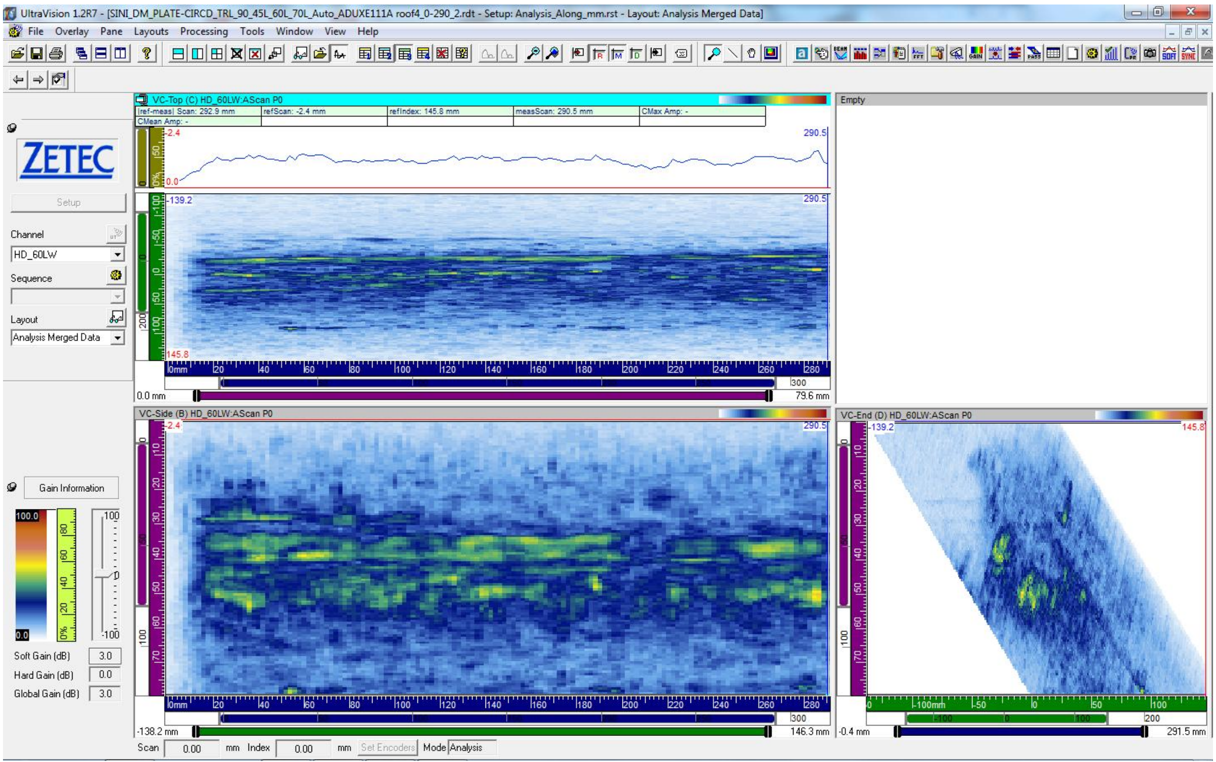

Figure 1.2. BWR mock-up data at 60° longitudinal wave from CS side. Strong metallurgical indication in the acoustical interface of the cladding-CS boundary at varying amplitudes i along the scanning length.

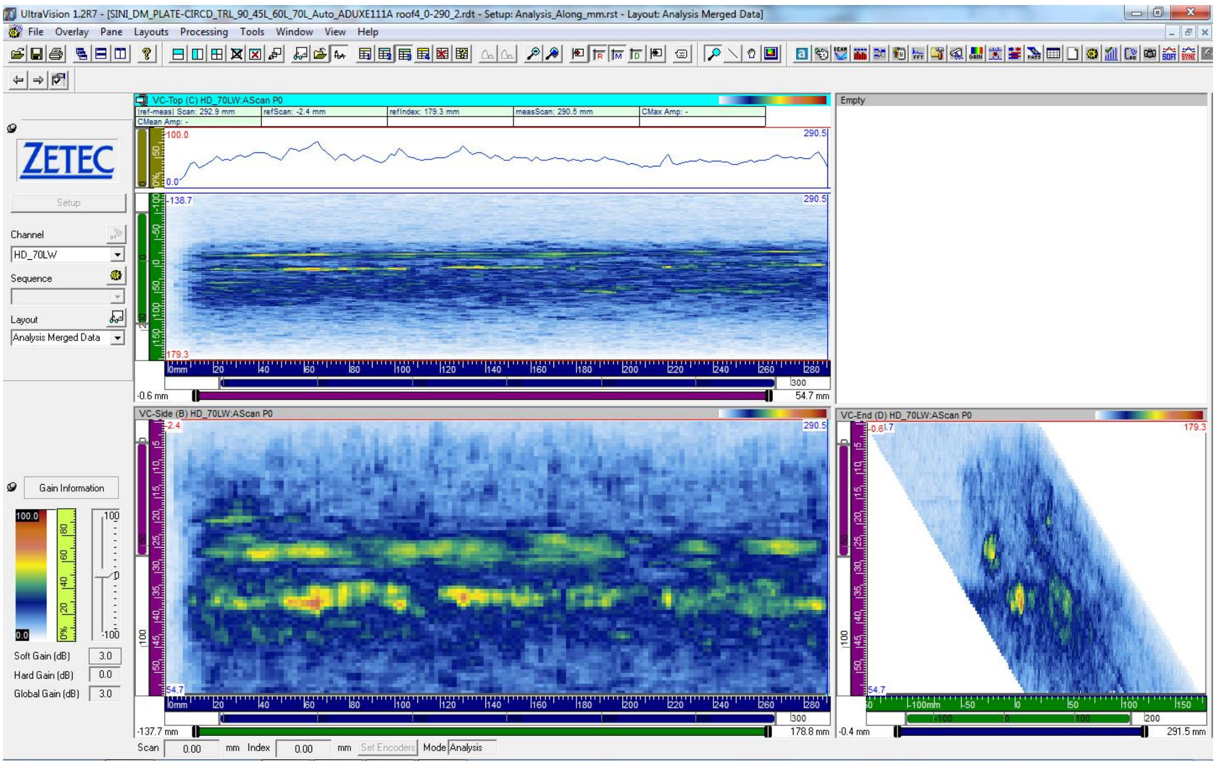

Figure 1.3. BWR mock-up data at 70° longitudinal wave from CS side. Strong metallurgical indication in the acoustical interface of the cladding-CS boundary at varying amplitudes along the scanning length.

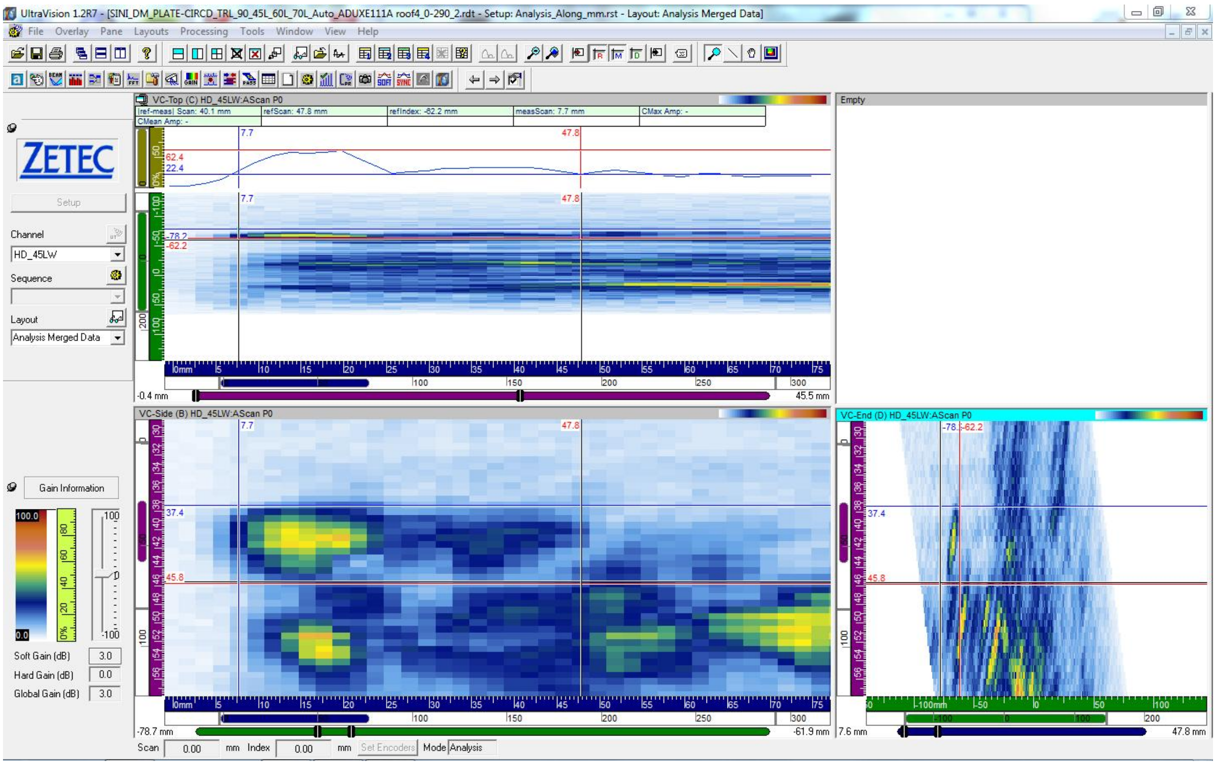

Figure 1.4. Flaw 1 at 45° longitudinal wave from CS side. Good signal-to-noise ratio (SNR) with clear start and end points.

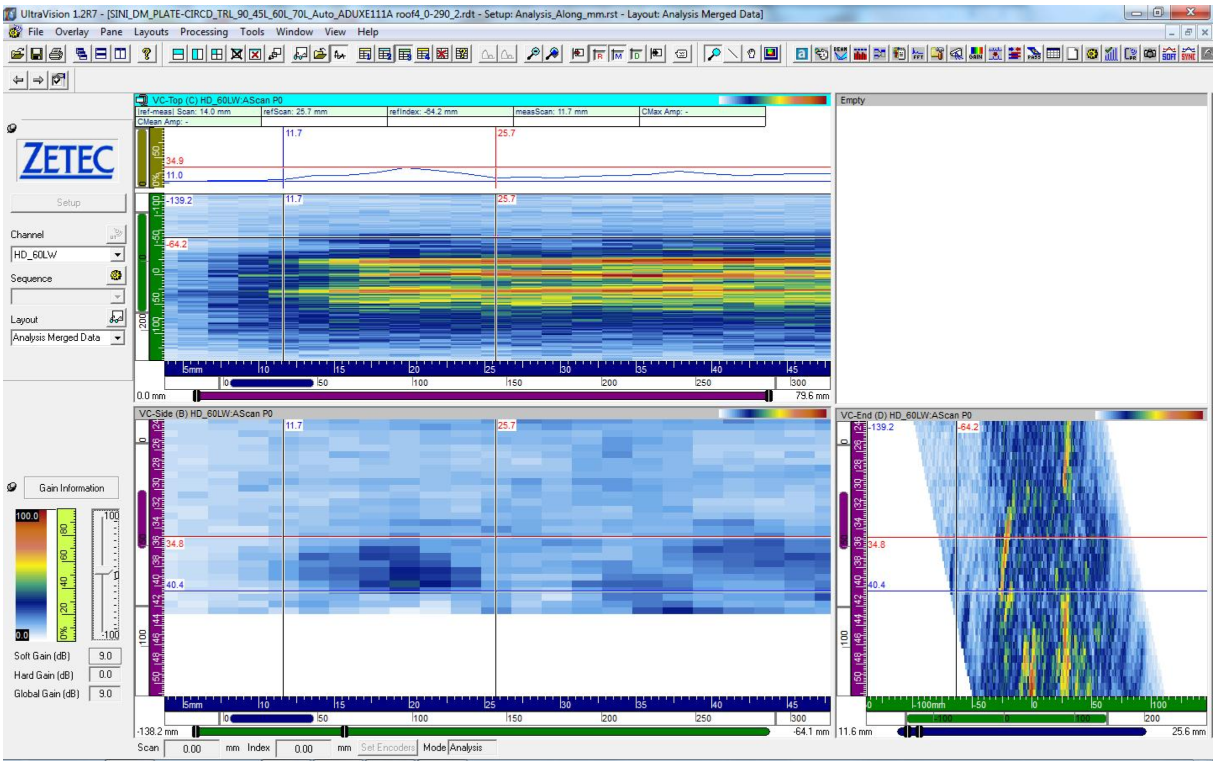

Figure 1.5. Flaw 1 at 60° longitudinal wave from CS side (only partly visible).

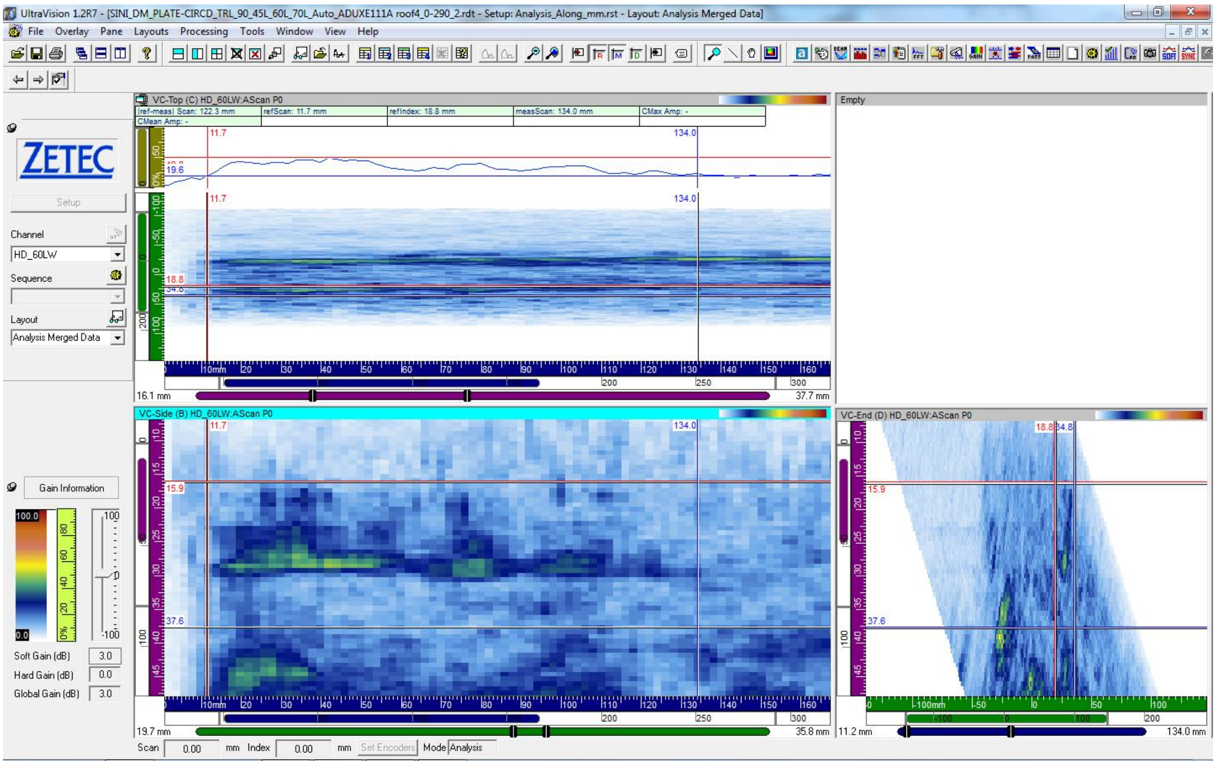

Figure 1.6. Flaw 2 at 60° longitudinal wave from CS side.

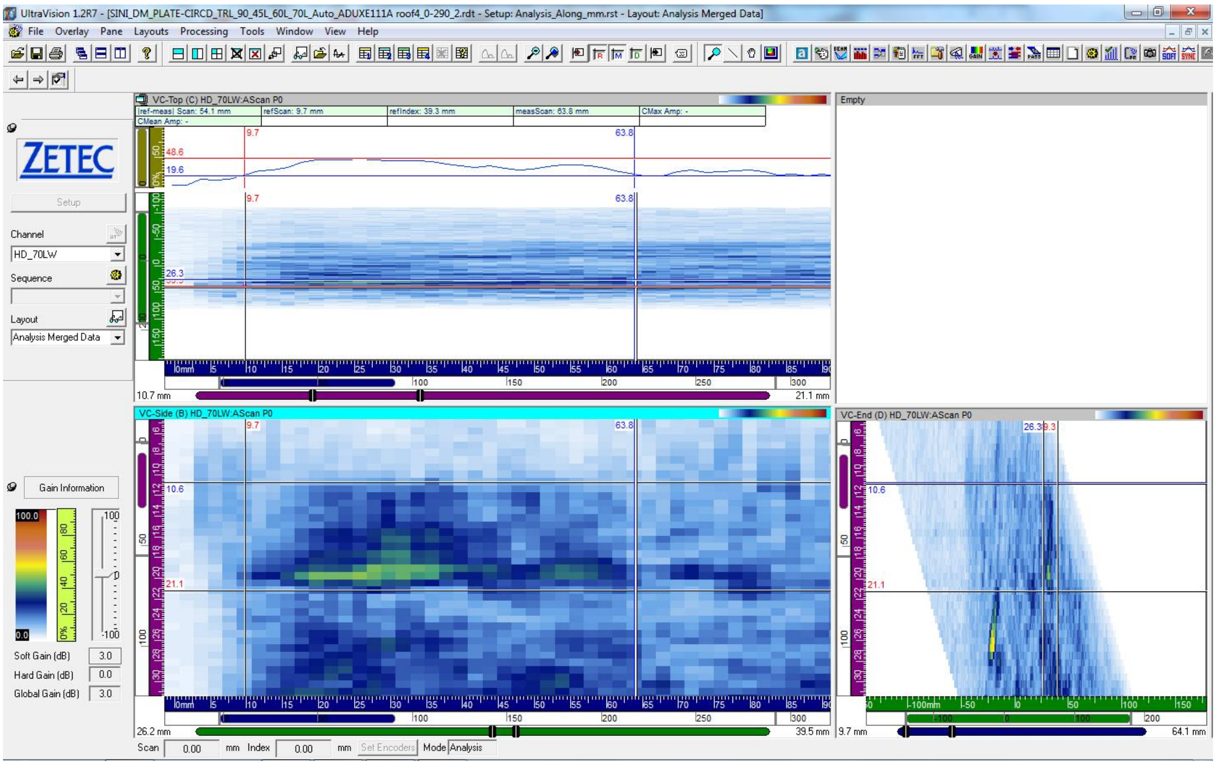

Figure 1.7. Flaw 2 at 70° longitudinal wave from CS side.

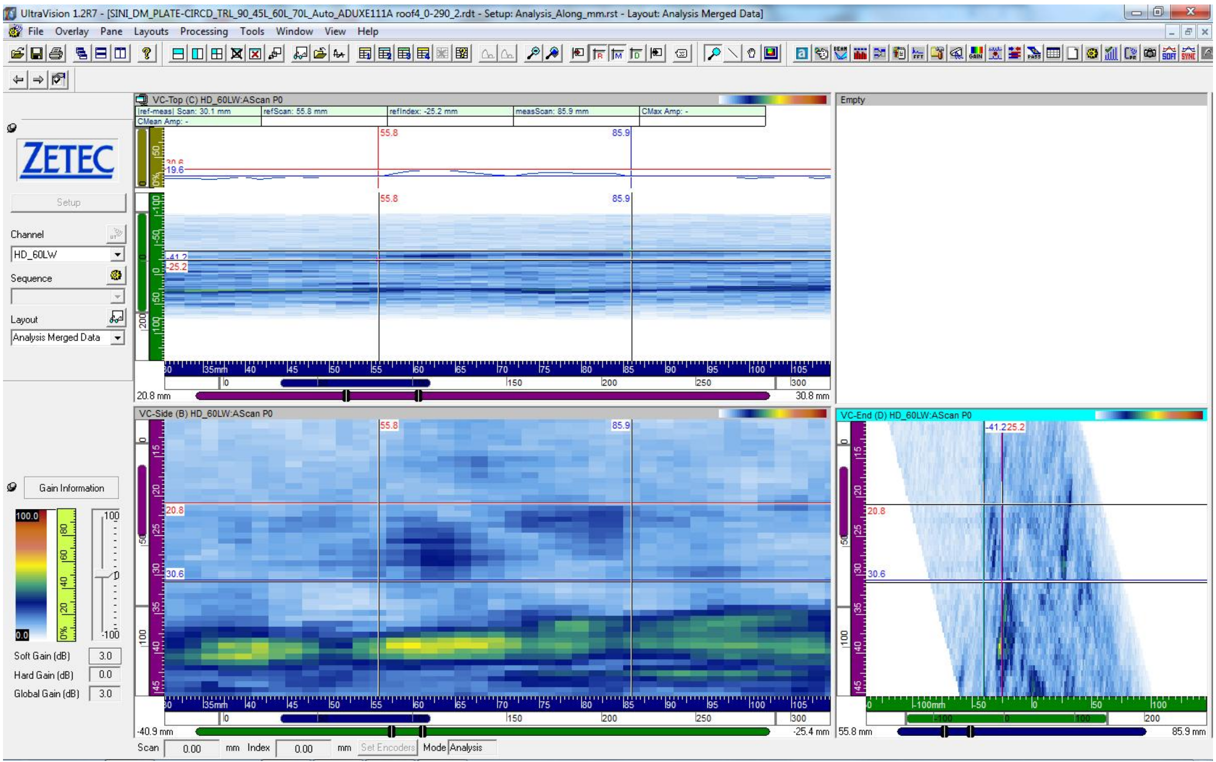

Figure 1.8. Flaw 3 at 60° longitudinal wave from CS side. Low SNR.

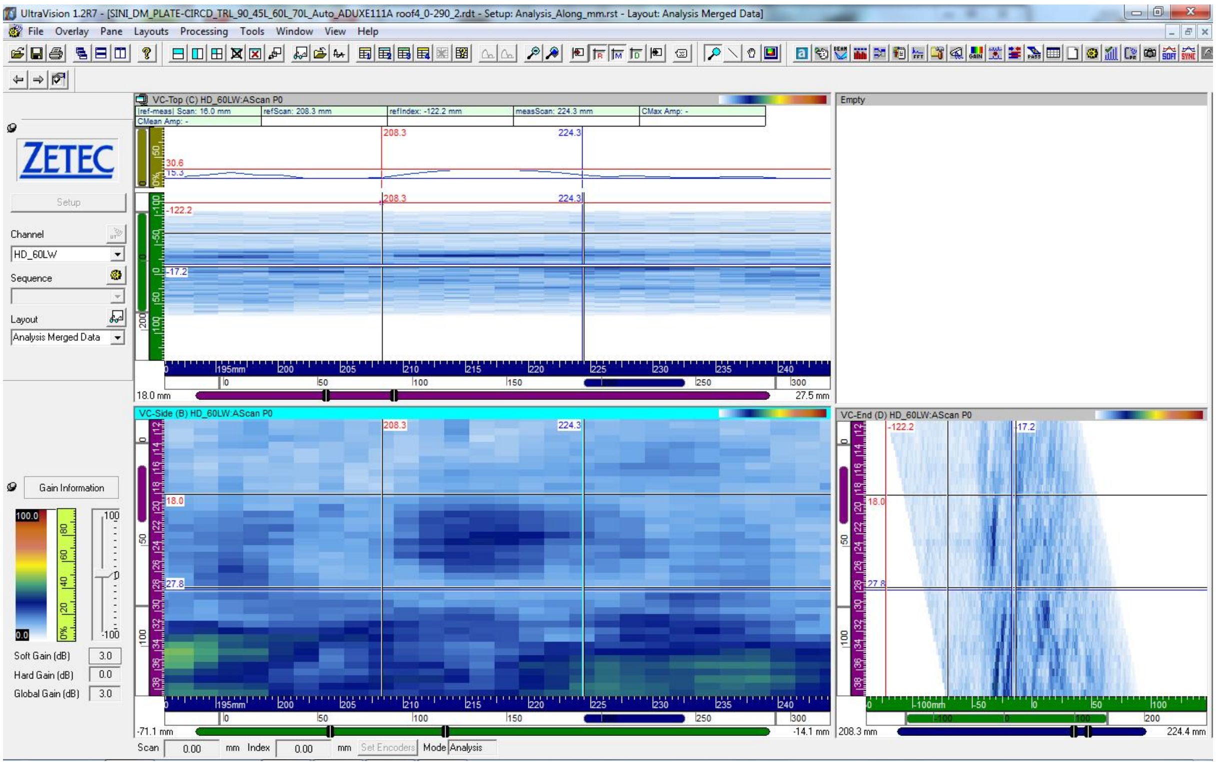

Figure 1.9. Flaw 4 at 60° longitudinal wave from CS side. Low SNR.

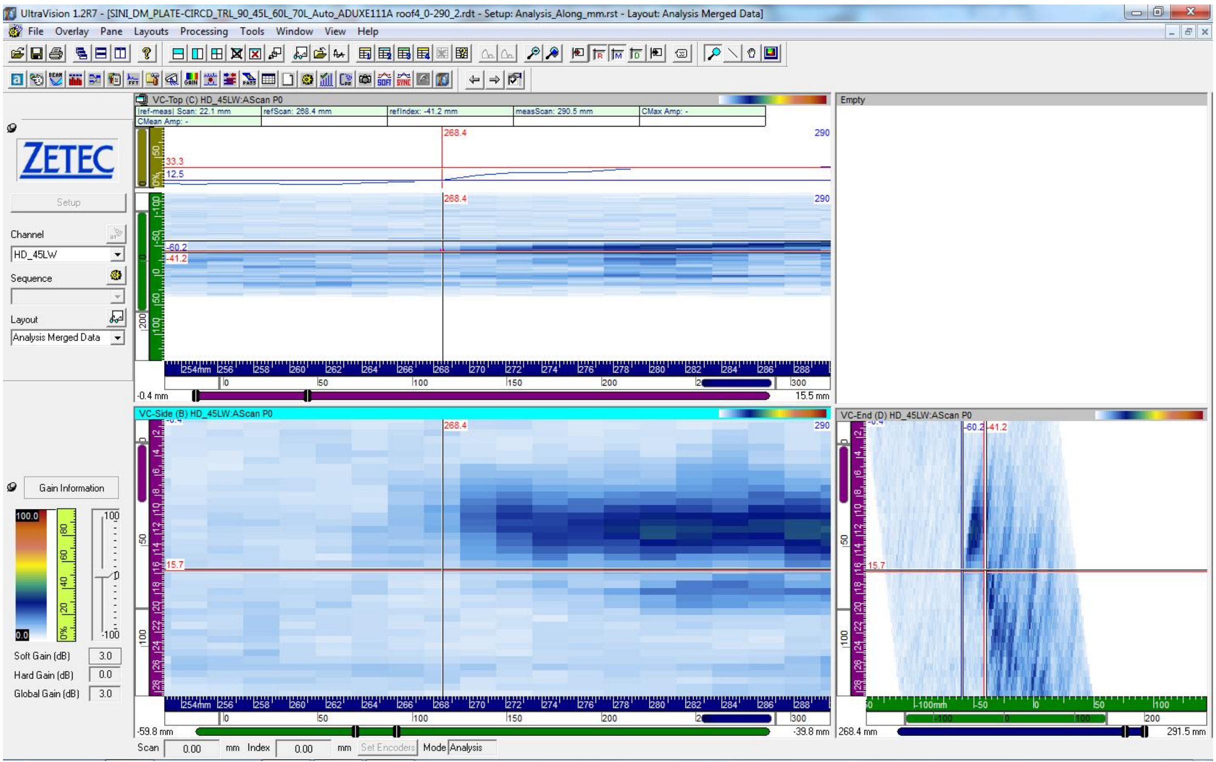

Figure 1.10. Flaw 5 at 45° longitudinal wave from CS side.

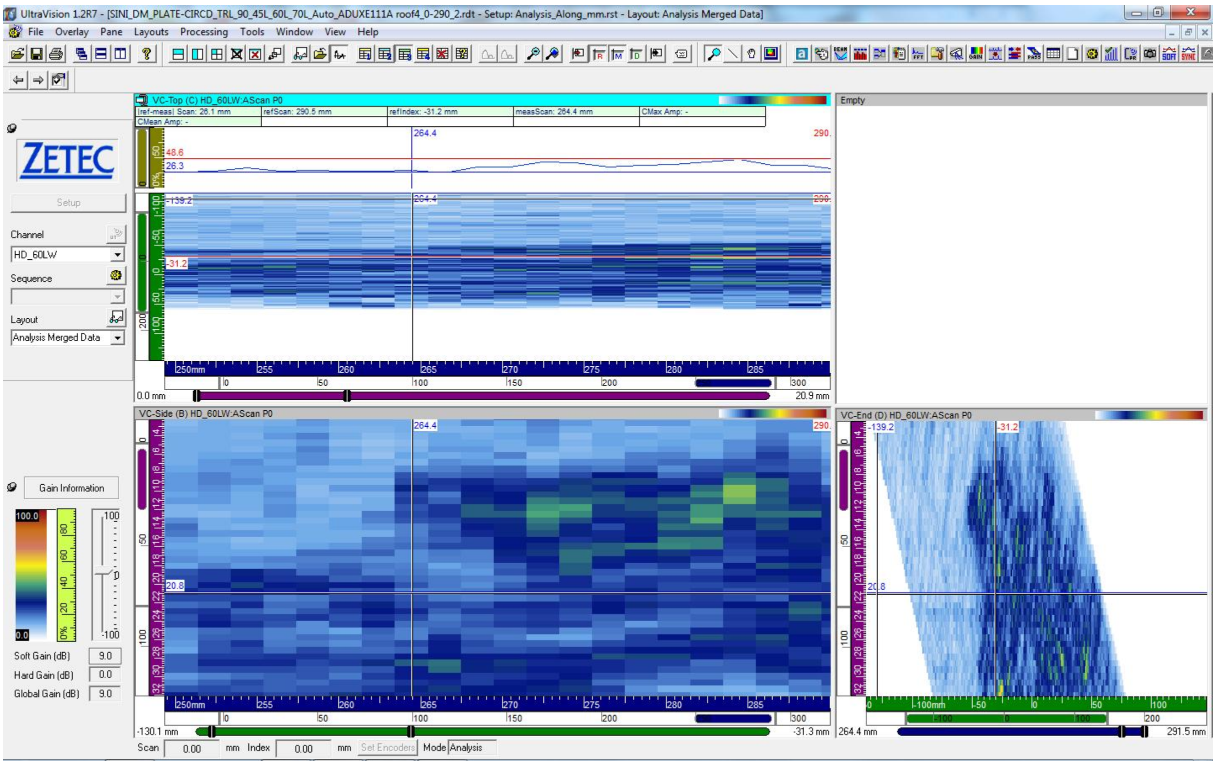

Figure 1.11. Flaw 5 at 60° longitudinal wave from CS side.

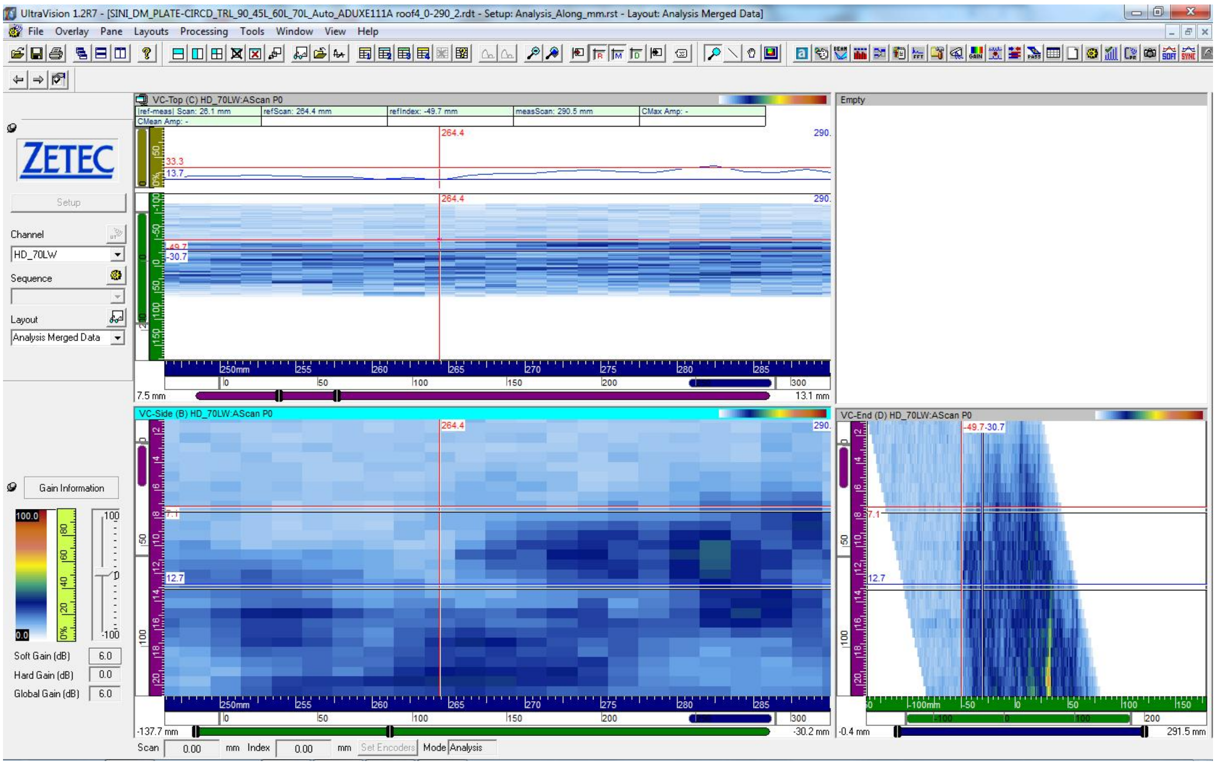

Figure 1.12. Flaw 5 at 70° longitudinal wave from CS side.

1.2 CIRCD TRL 90 scan 265–360 mm

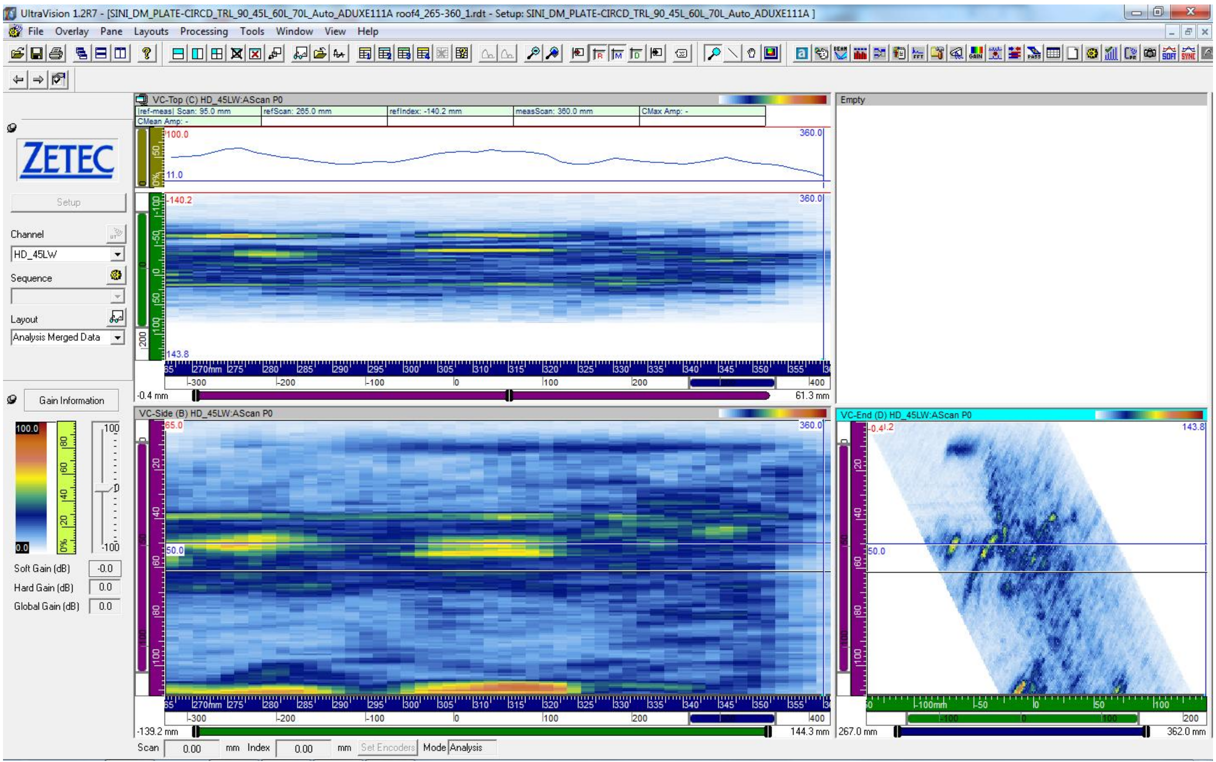

Figure 1.13. BWR mock-up data at 45° longitudinal wave from CS side. Strong metallurgical indication in the acoustical interface of the cladding-CS boundary at varying amplitudes along the scanning length.

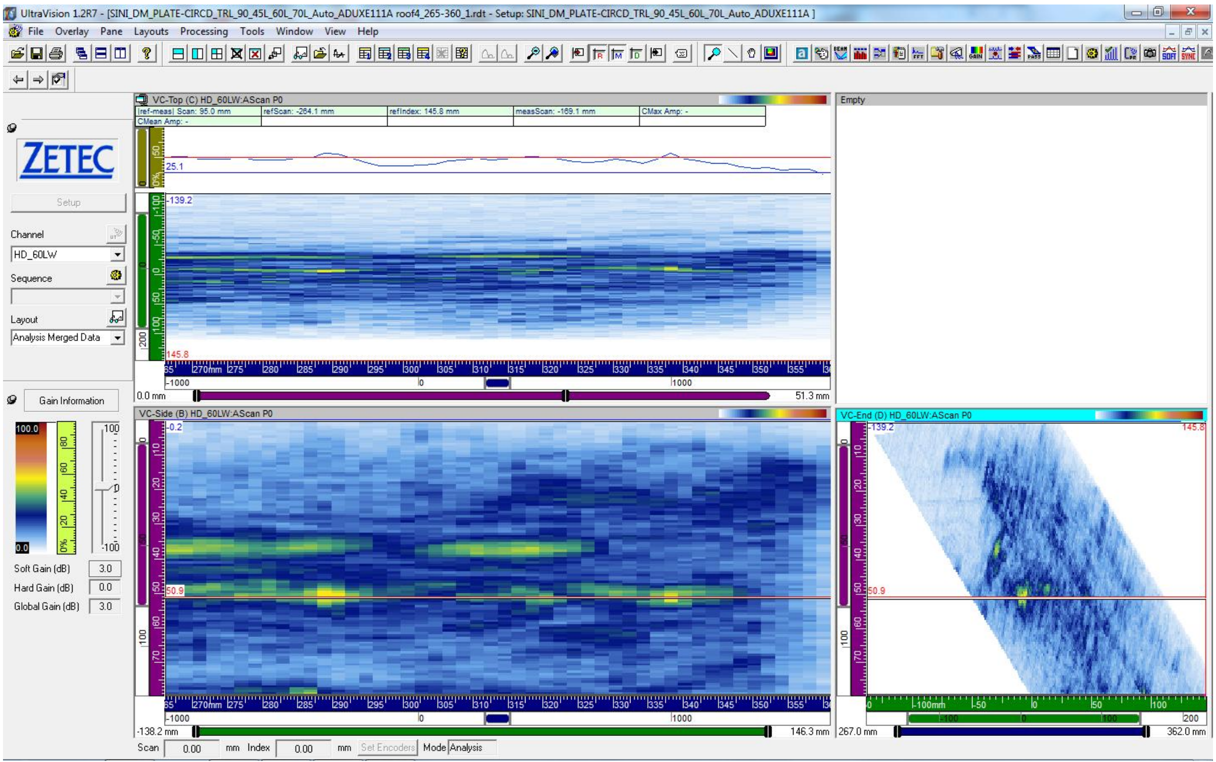

Figure 1.14. BWR mock-up data at 60° longitudinal wave from CS side. Strong metallurgical indication in the acoustical interface of the cladding-CS boundary at varying amplitudes along the scanning length.

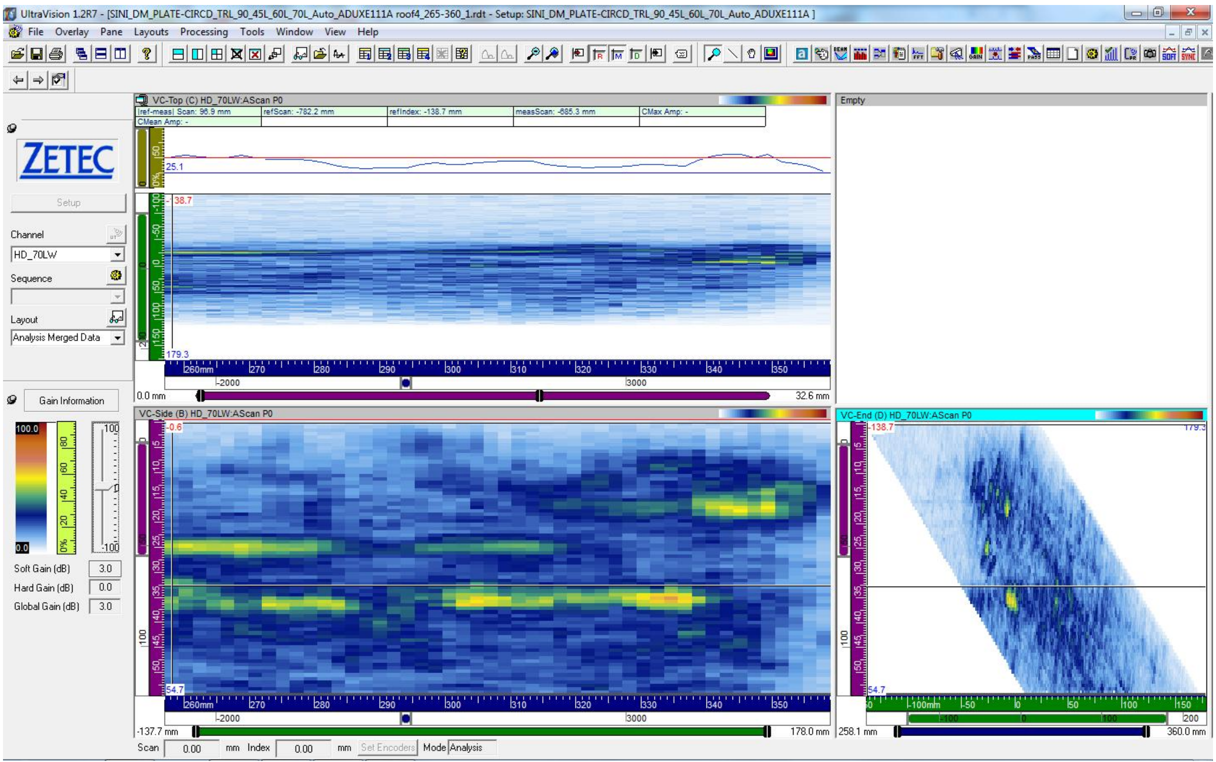

Figure 1.15. BWR mock-up data at 70° longitudinal wave from CS side. Strong metallurgical indication in the acoustical interface of the cladding-CS boundary at varying amplitudes along the scanning length.

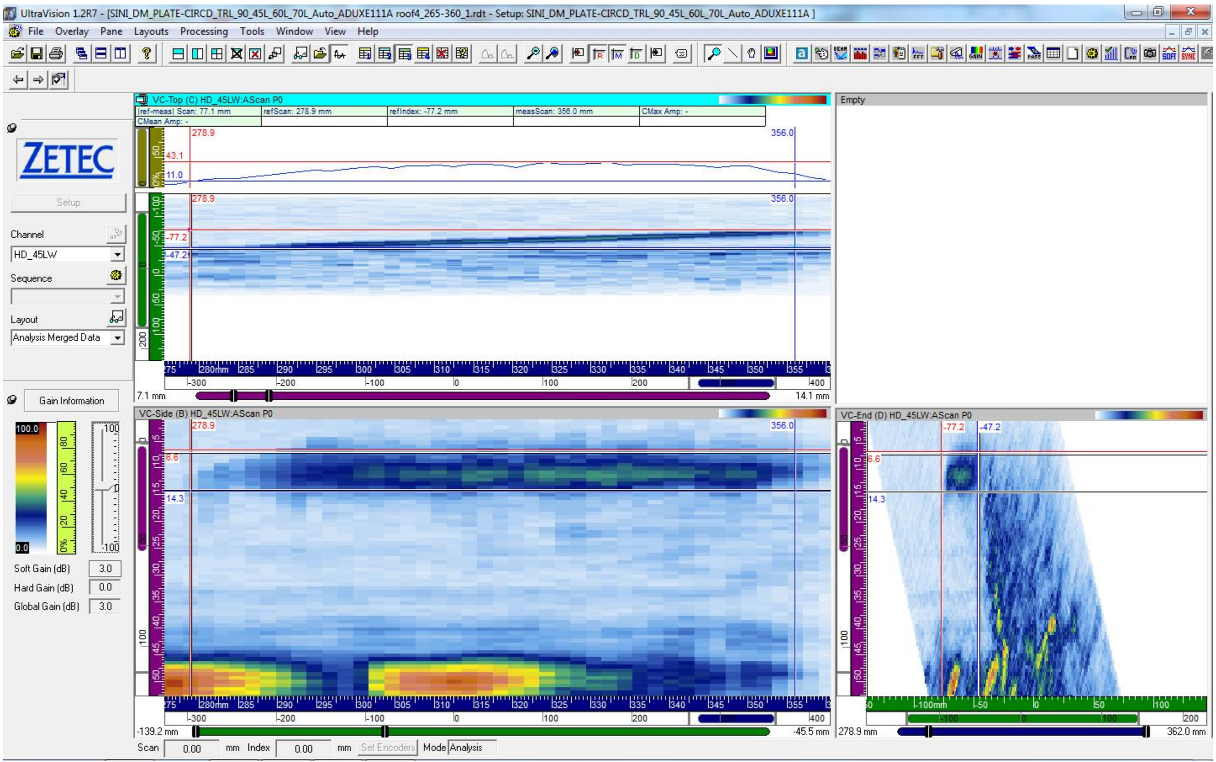

Figure 1.16. Flaw 5 at 45° longitudinal wave from CS side. Good SNR with clear start and end points. Isolated from the noise signals from the weld material

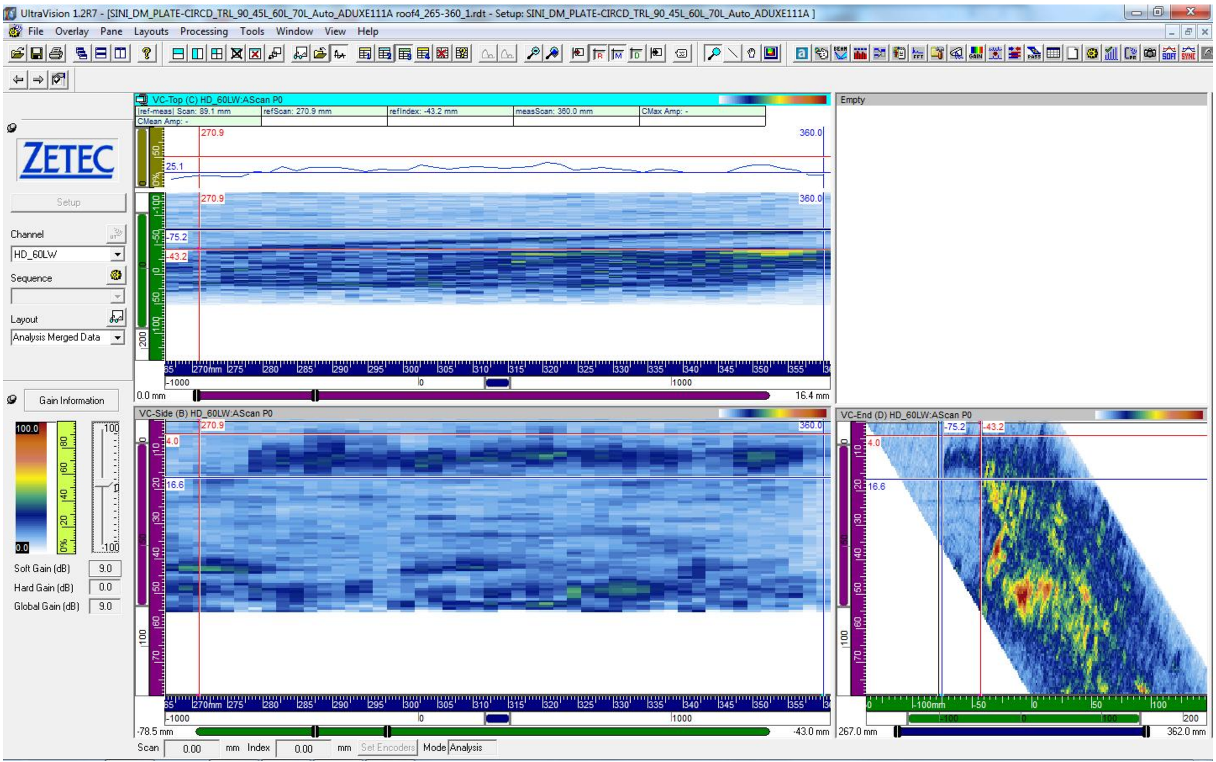

Figure 1.17. Flaw 5 at 60° longitudinal wave from CS side. Clear start and end points and isolated from the noise signals from the weld material

1.3 CIRCD TRS 90 scan 0–290 mm

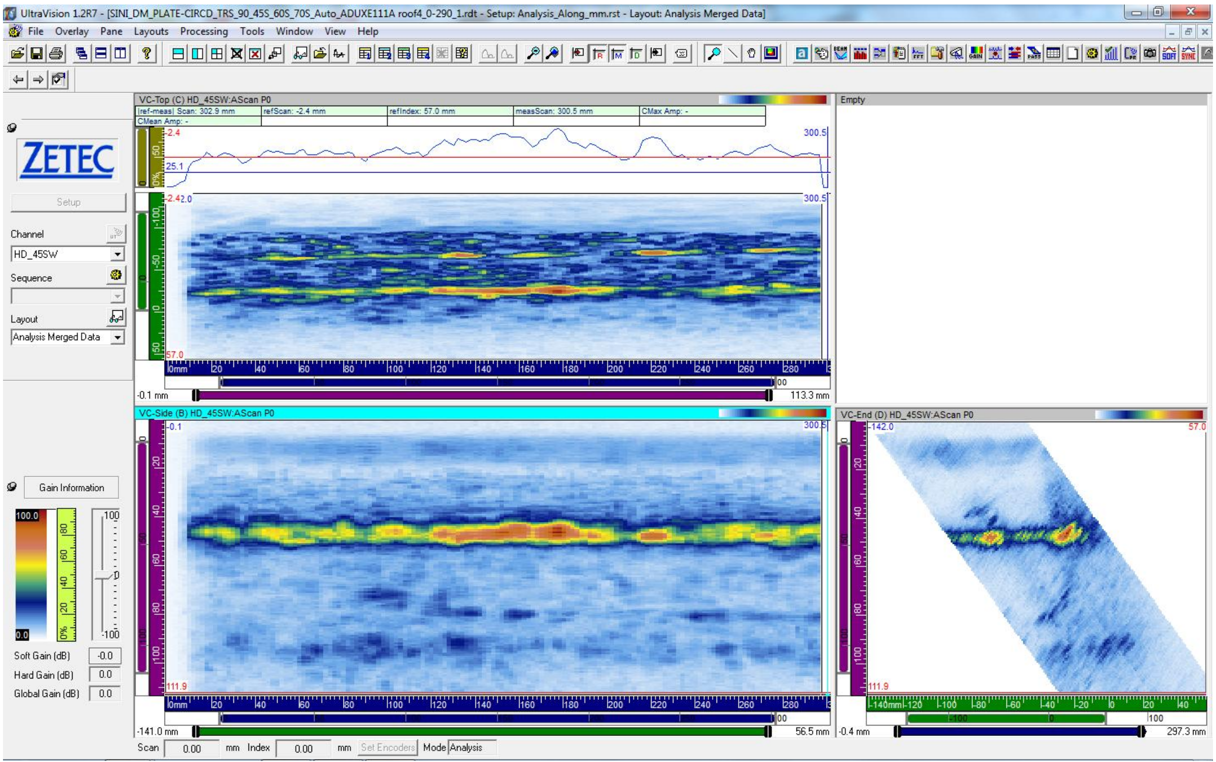

Figure 1.18. BWR mock-up data at 45° shear wave from CS side. Strong continuous metallurgical indication in the acoustical interface of the cladding-CS boundary at varying amplitudes along the scanning length.

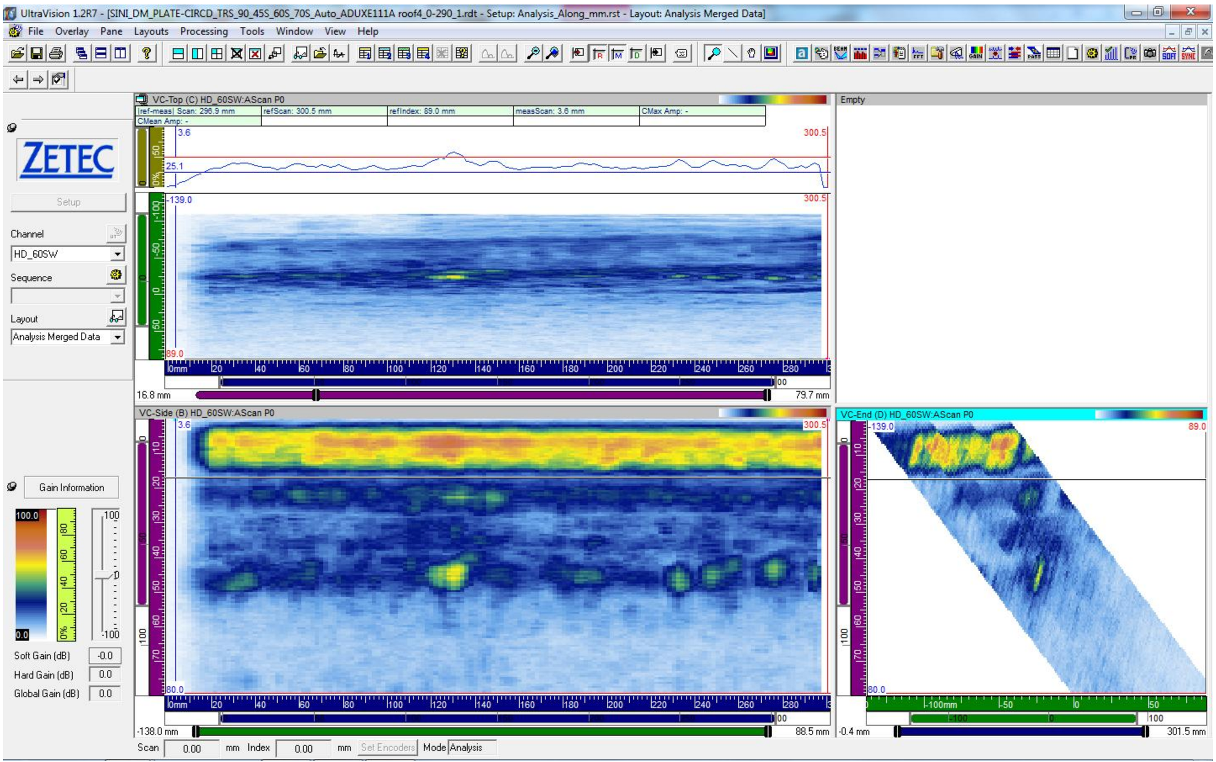

Figure 1.19. BWR mock-up data at 60° shear wave from CS side. Metallurgical indication in the acoustical interface of the cladding-CS boundary at varying amplitudes intermittently along the scanning length.

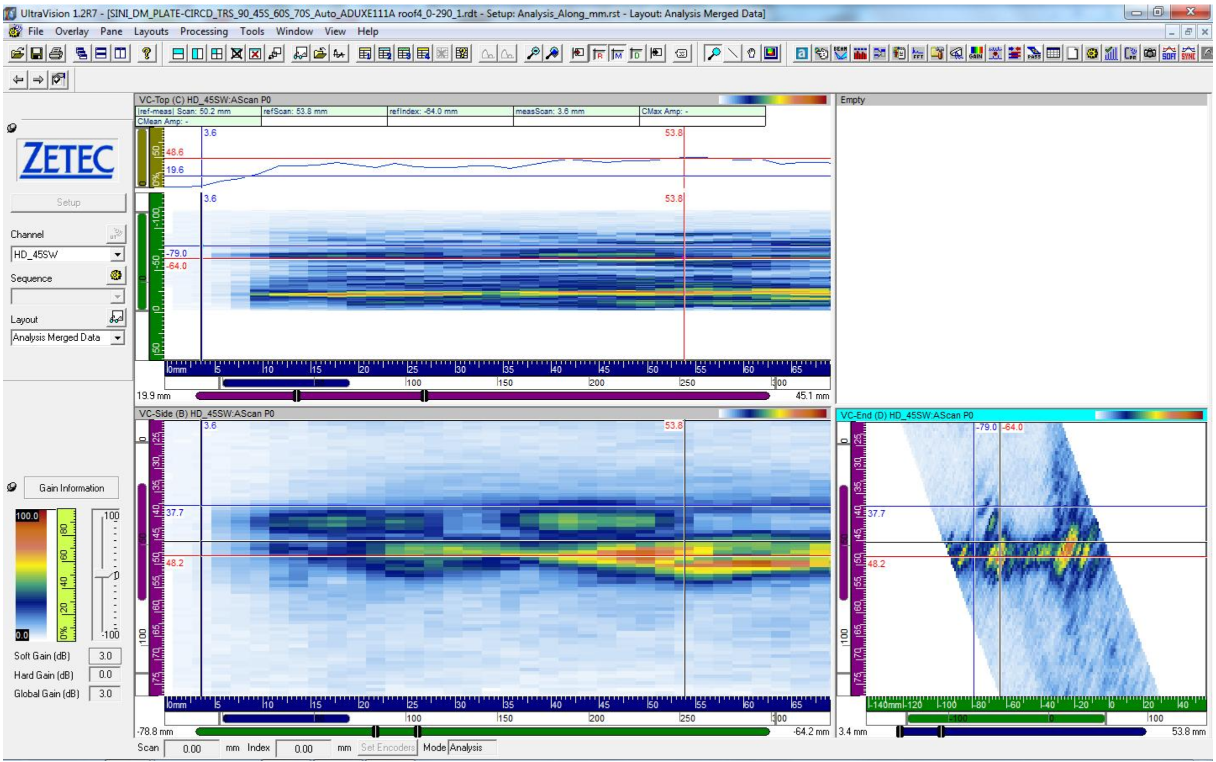

Figure 1.20. Flaw 1 at 45° shear wave from CS side. Good SNR with two amplitude peaks isolated from the metallurgical indication.

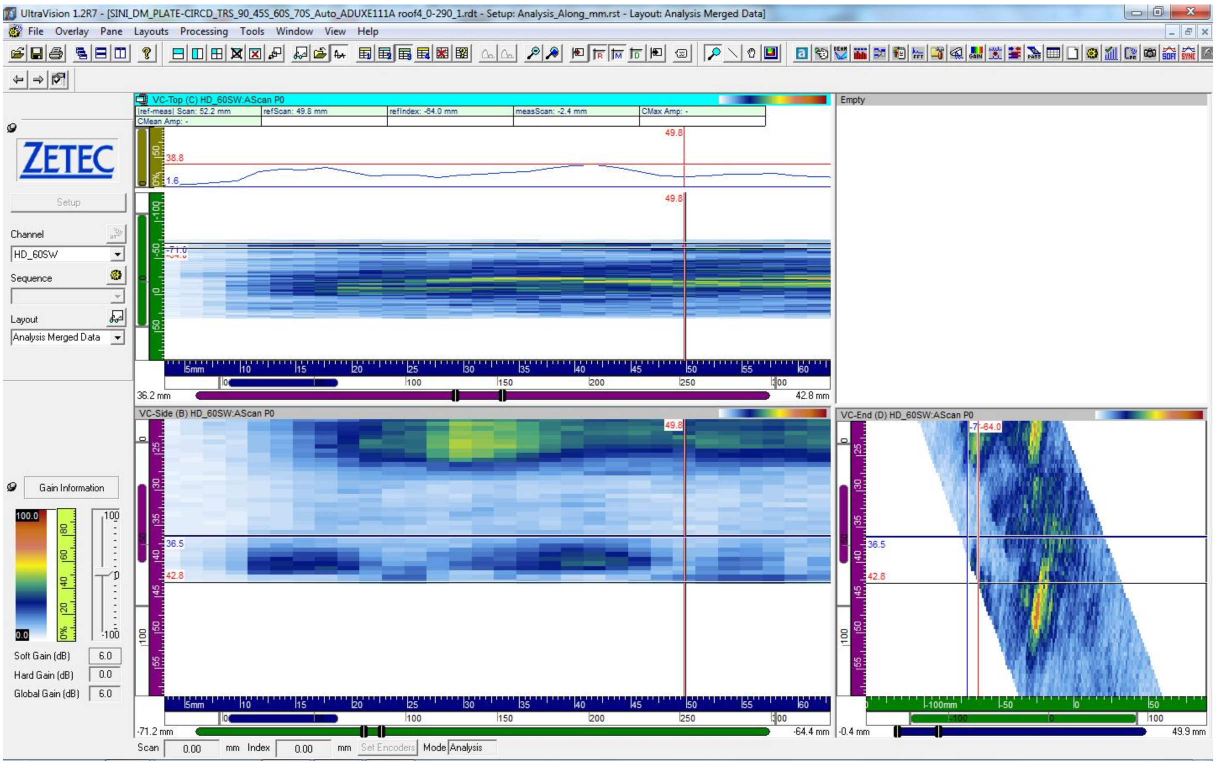

Figure 1.21. Flaw 1 at 60° shear wave from CS side.

1.4 CIRCD TRS 90 scan 265–360 mm

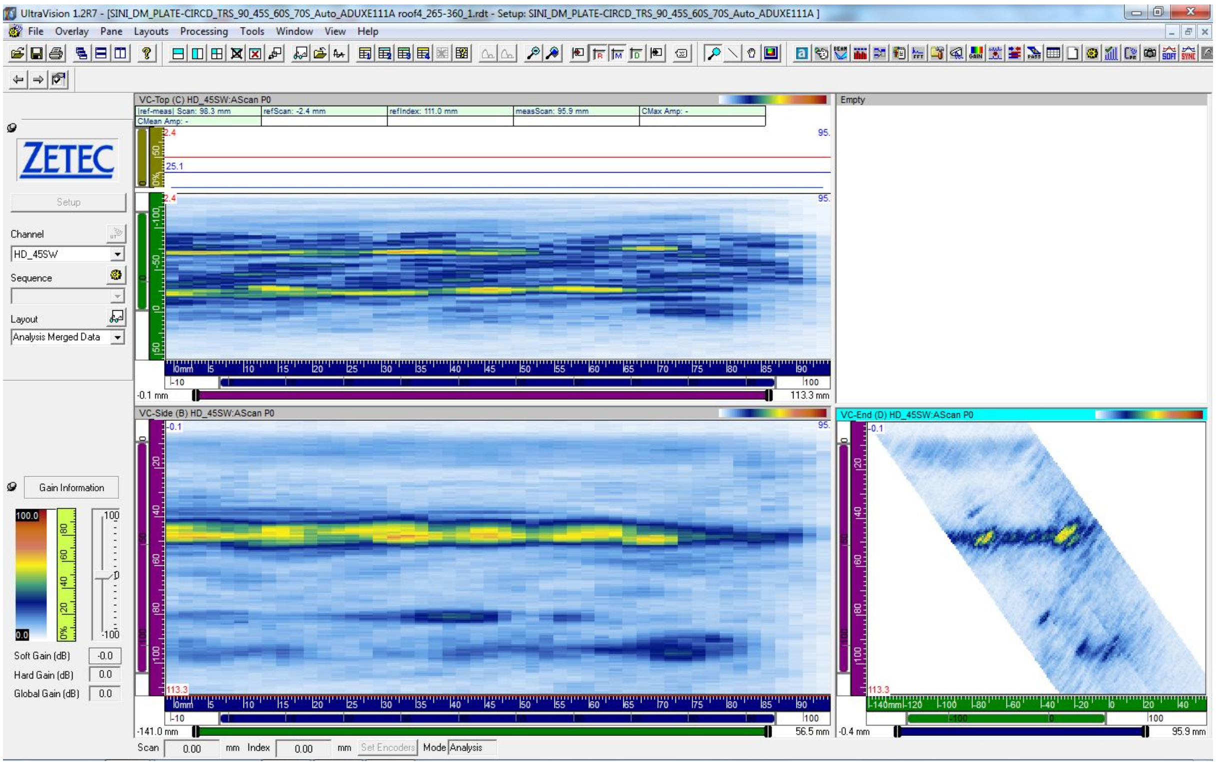

Figure 1.22. BWR mock-up data at 45° shear wave from CS side. Strong continuous metallurgical indication in the acoustical interface of the cladding-CS boundary at varying amplitudes along the scanning length.

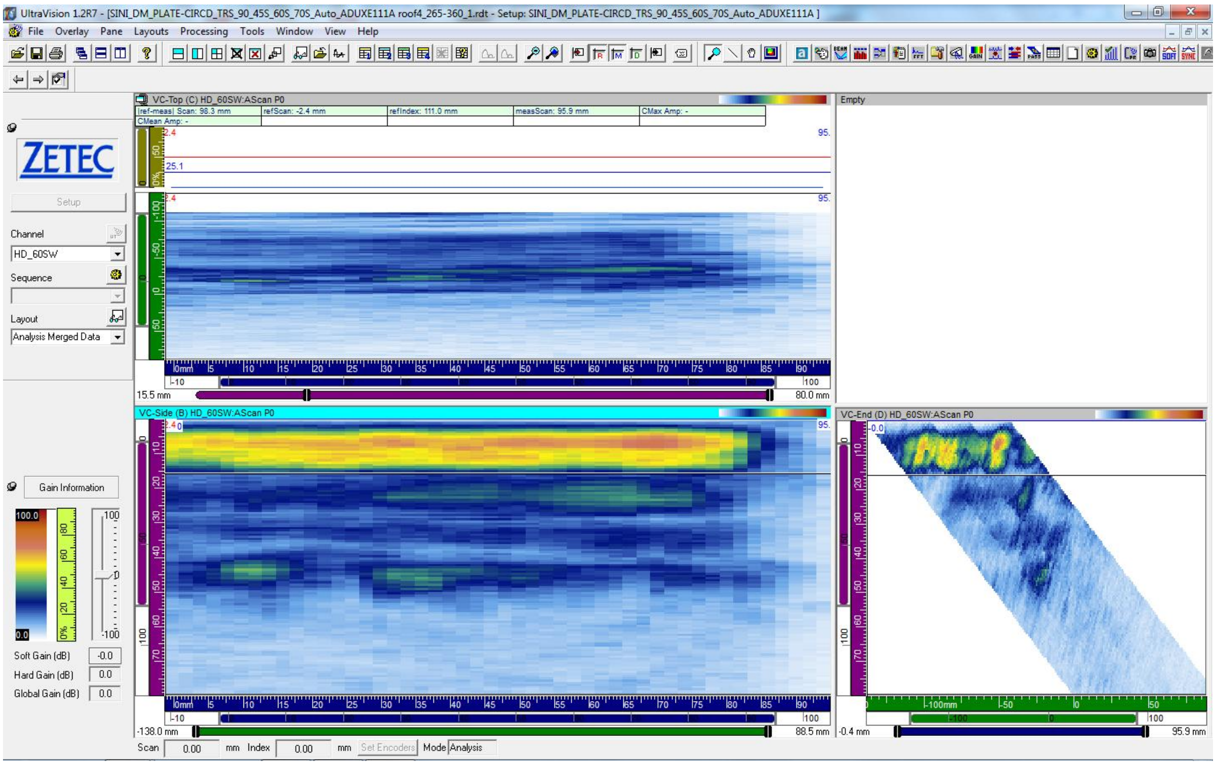

Figure 1.23. BWR mock-up data at 60° shear wave from CS side. Metallurgical indication in the acoustical interface of the cladding-CS boundary at varying amplitudes intermittently along the scanning length.

1.5 CIRCU TRL 270 Scan 0–290 mm

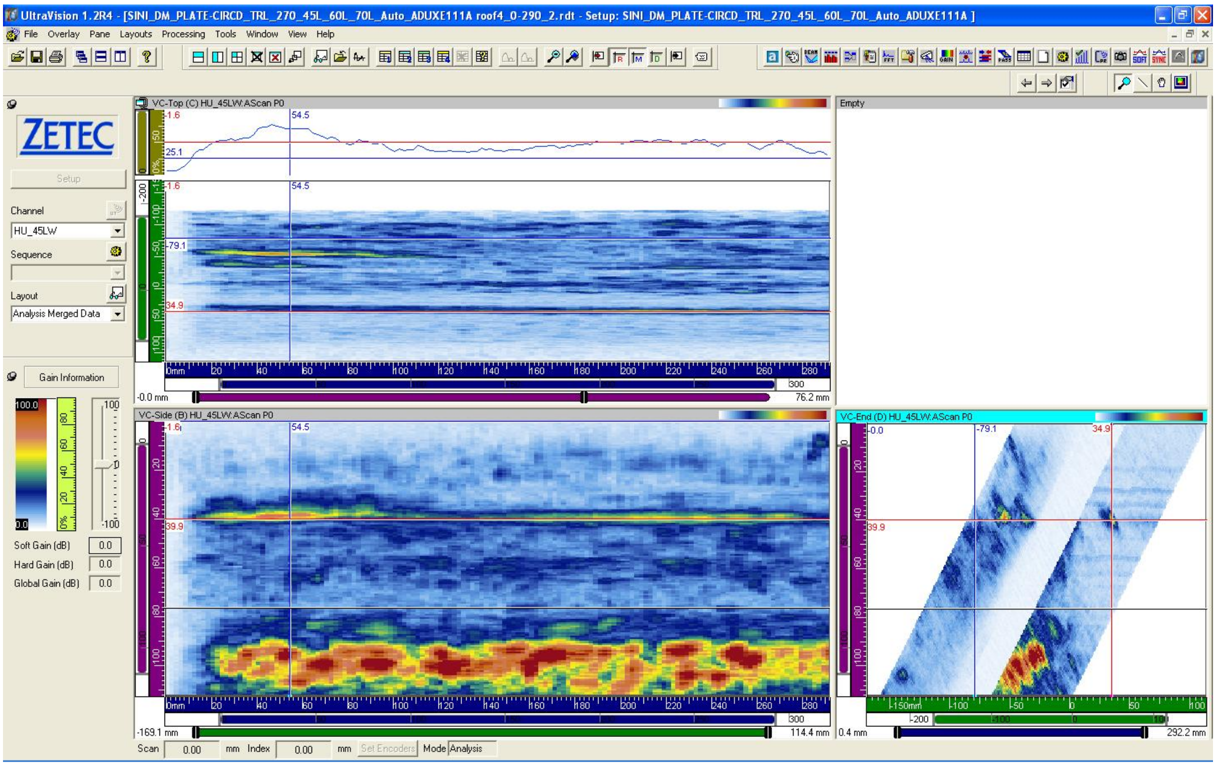

Figure 1.24. BWR mock-up data at 45° longitudinal wave from SS side. Indications from the weld joint/parent material boundary are seen in the depth of 40 mm. The weld volume coverage is missed due to the shape of the mock-up. Note that the back wall is now at the depth of 41 mm at the weld and on 51 mm at the far side (CS side).

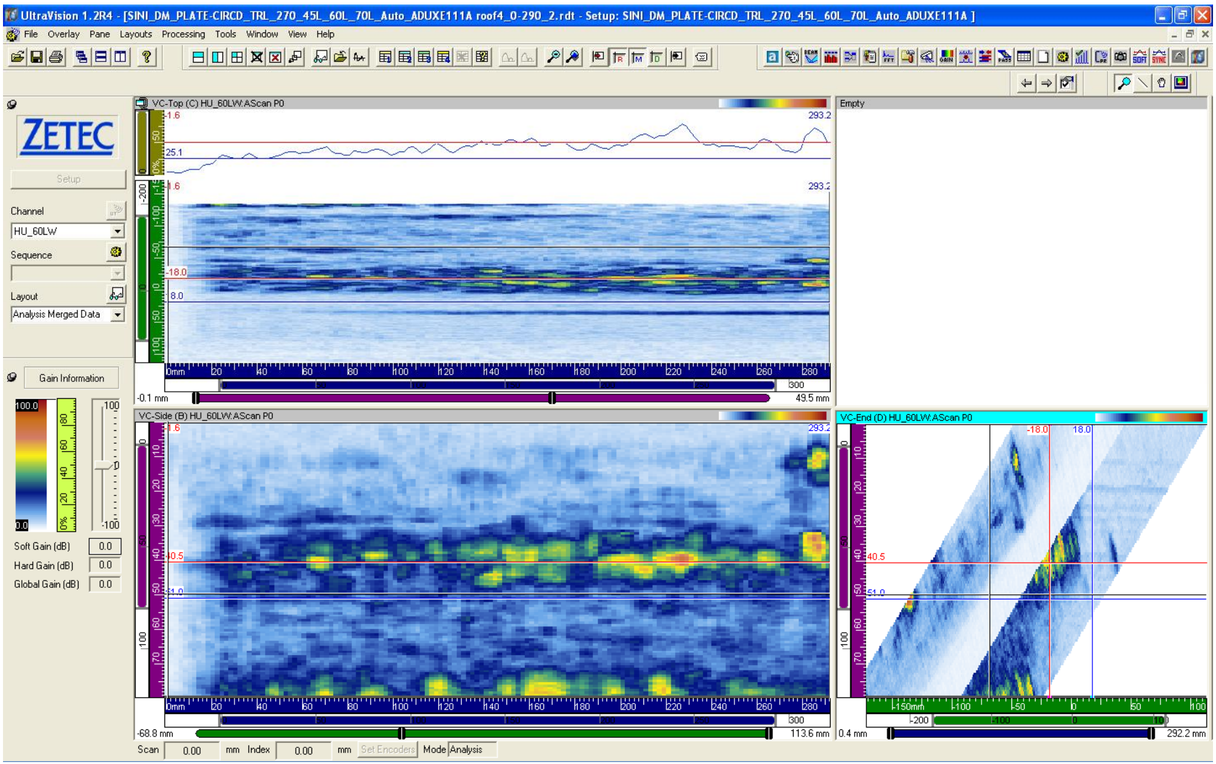

Figure 1.25. BWR mock-up data at 60° longitudinal wave from SS side. Indications from the weld joint/parent material boundary at varying amplitudes along the scan length.

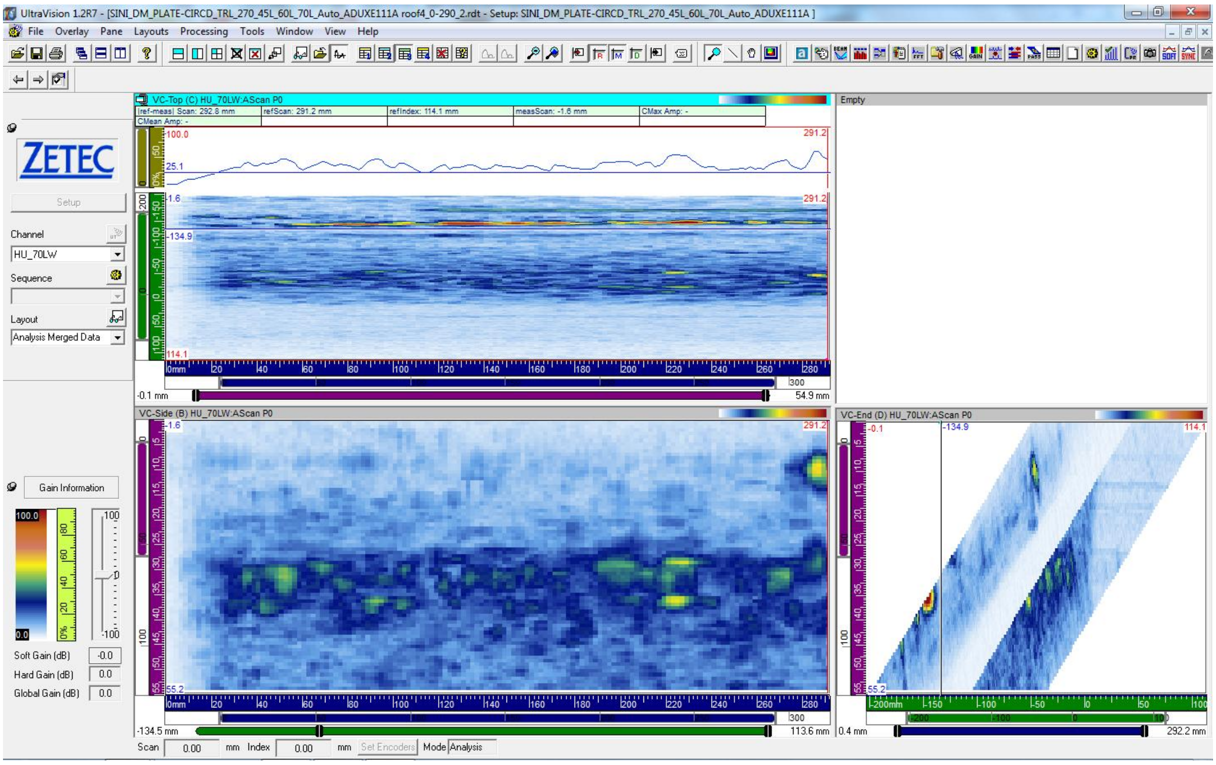

Figure 1.26. BWR mock-up data at 70° longitudinal wave from SS side. Strong noise from the weld material.

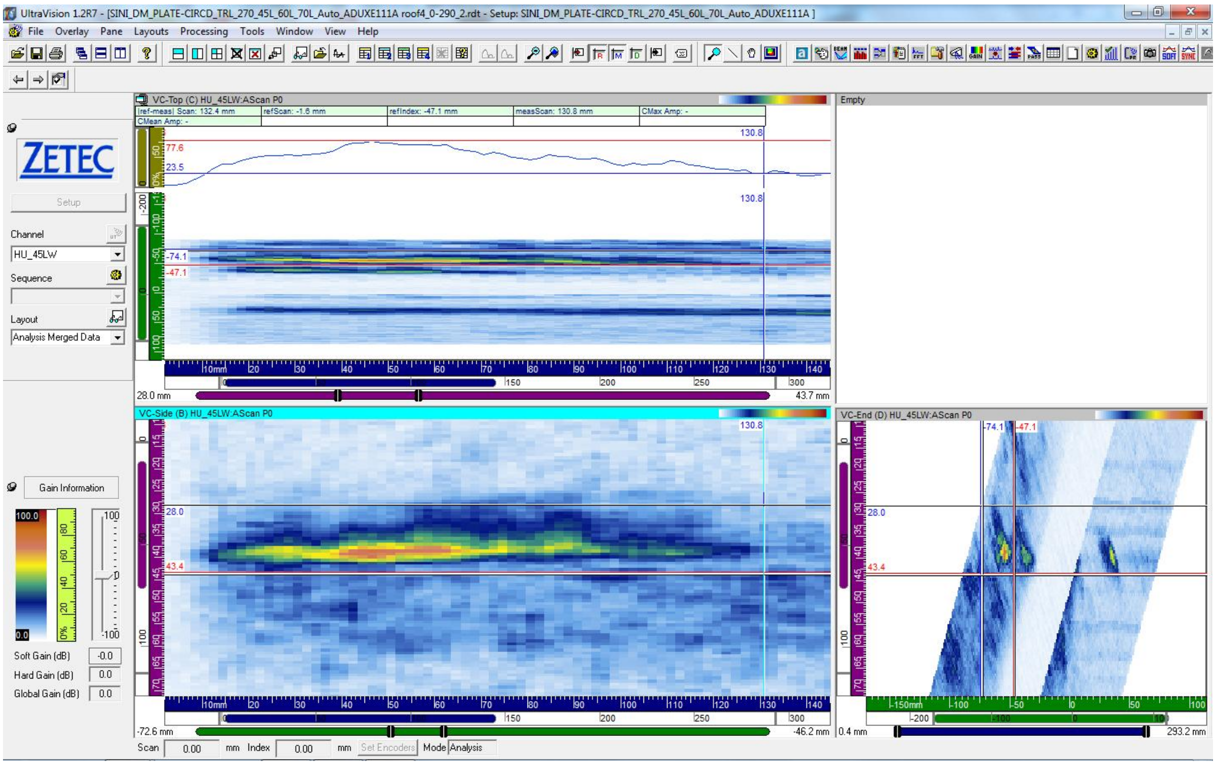

Figure 1.27. Flaw 1 at 45° longitudinal wave from SS side. Good SNR with clear start and end points.

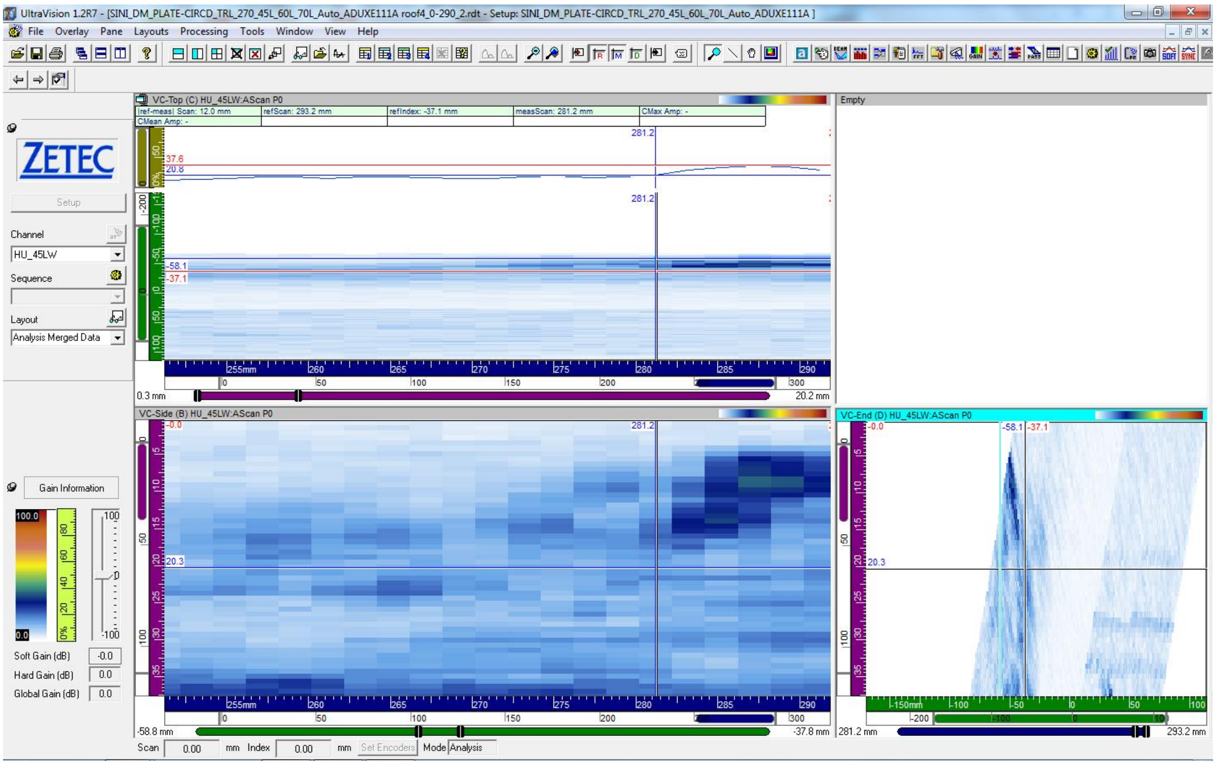

Figure 1.28. Flaw 5 at 45° longitudinal wave from SS side.

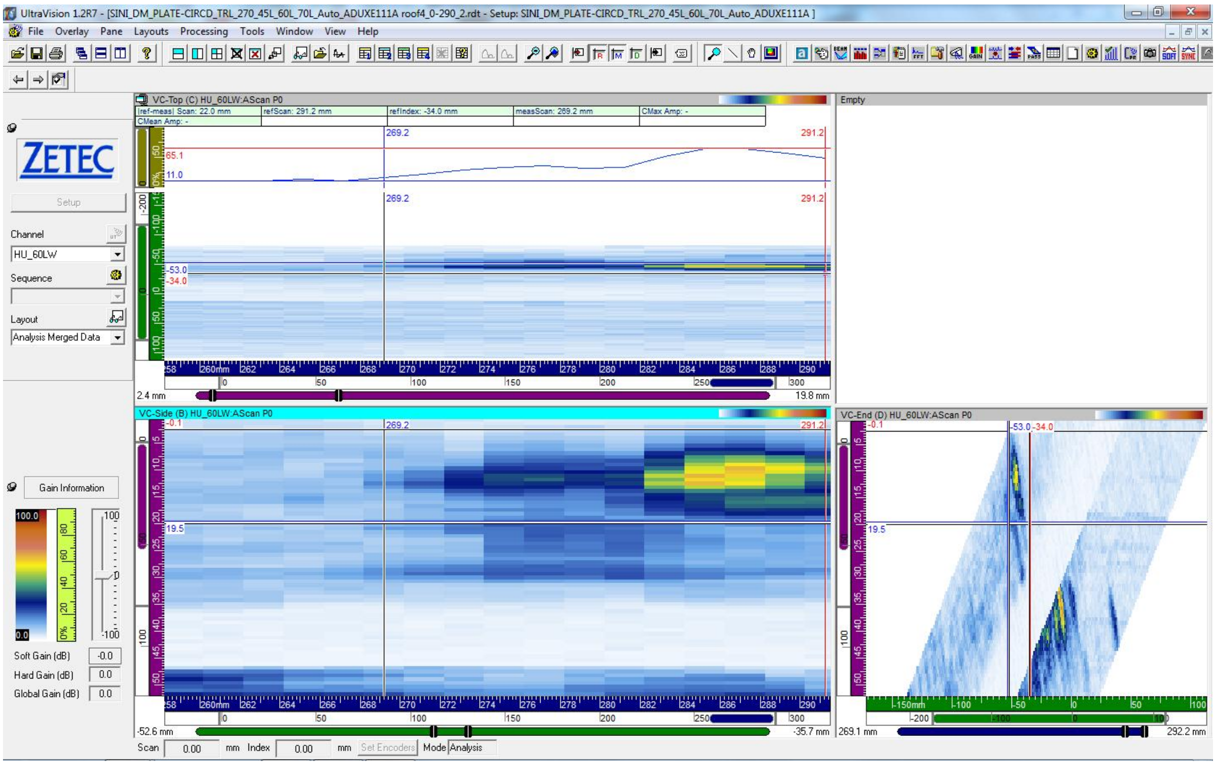

Figure 1.29. Flaw 5 at 60° longitudinal wave from SS side. Good SNR.

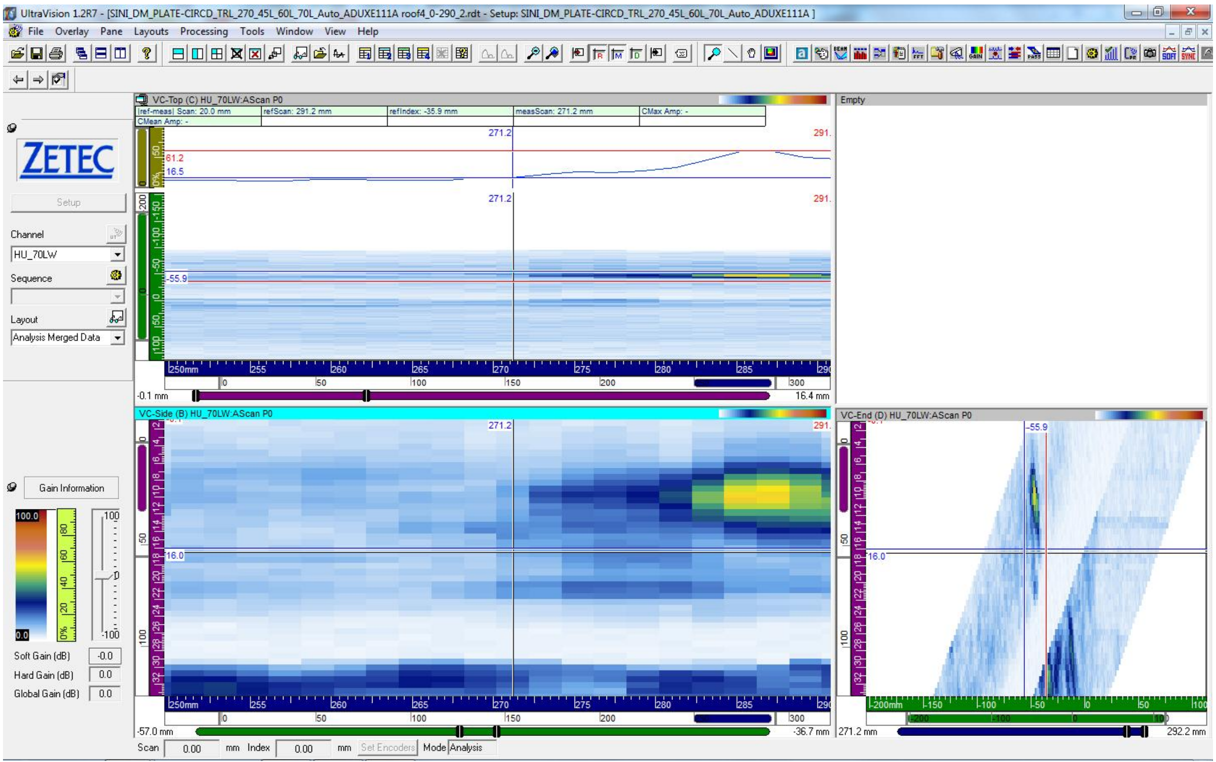

Figure 1.30. Flaw 5 at 70° longitudinal wave from SS side. Good SNR.

1.6 CIRCU TRL 270 scan 265–355 mm

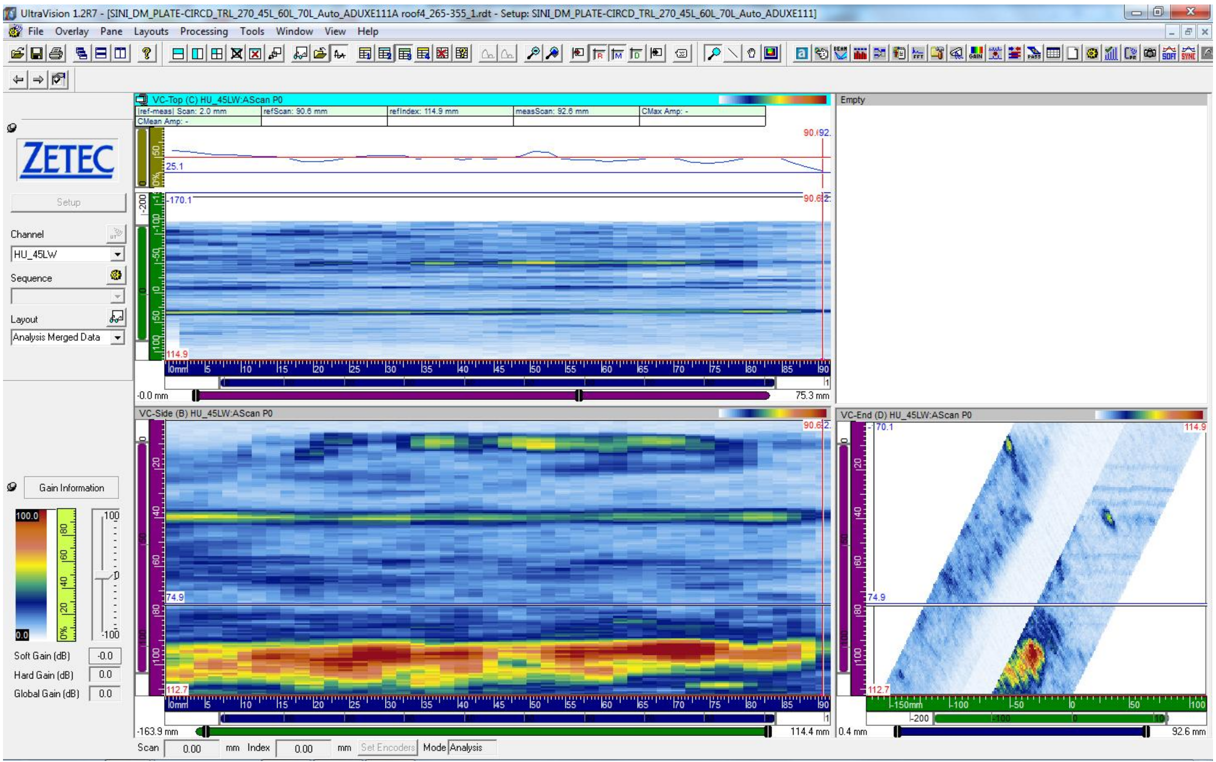

Figure 1.31. BWR mock-up data at 45° longitudinal wave from SS side.

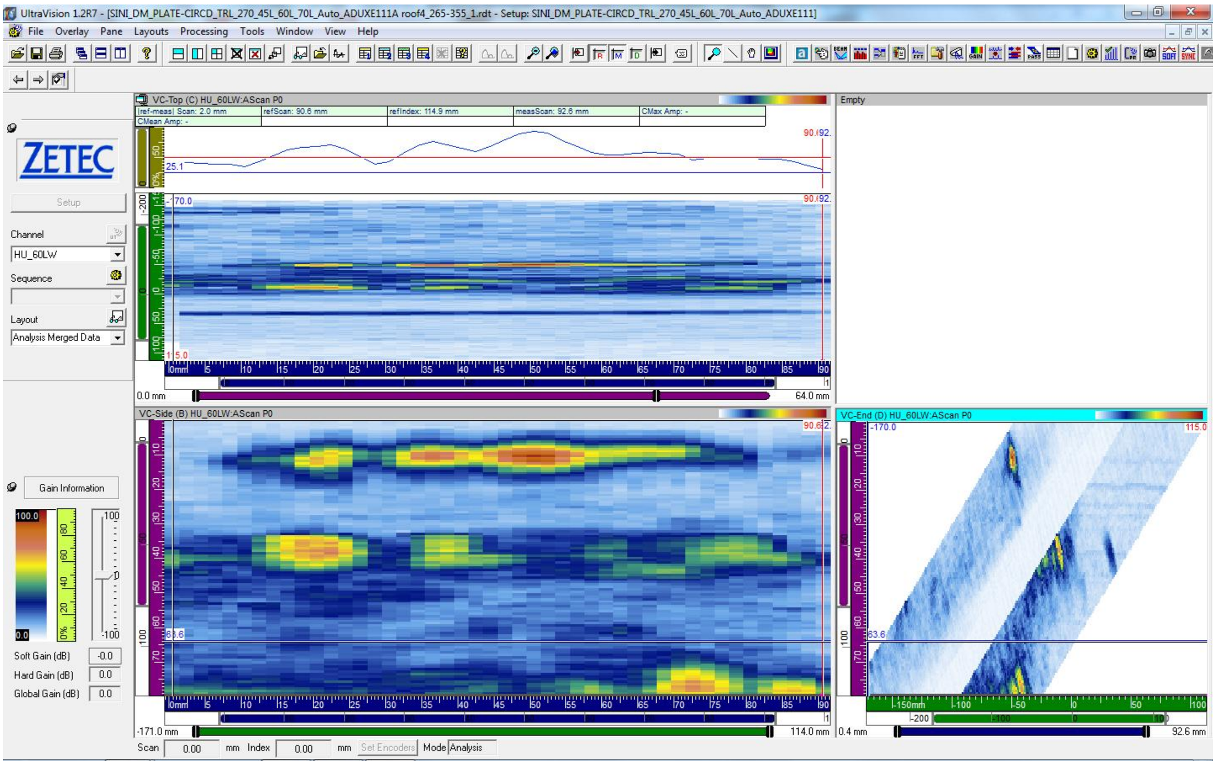

Figure 1.32. BWR mock-up data at 60° longitudinal wave from SS side.

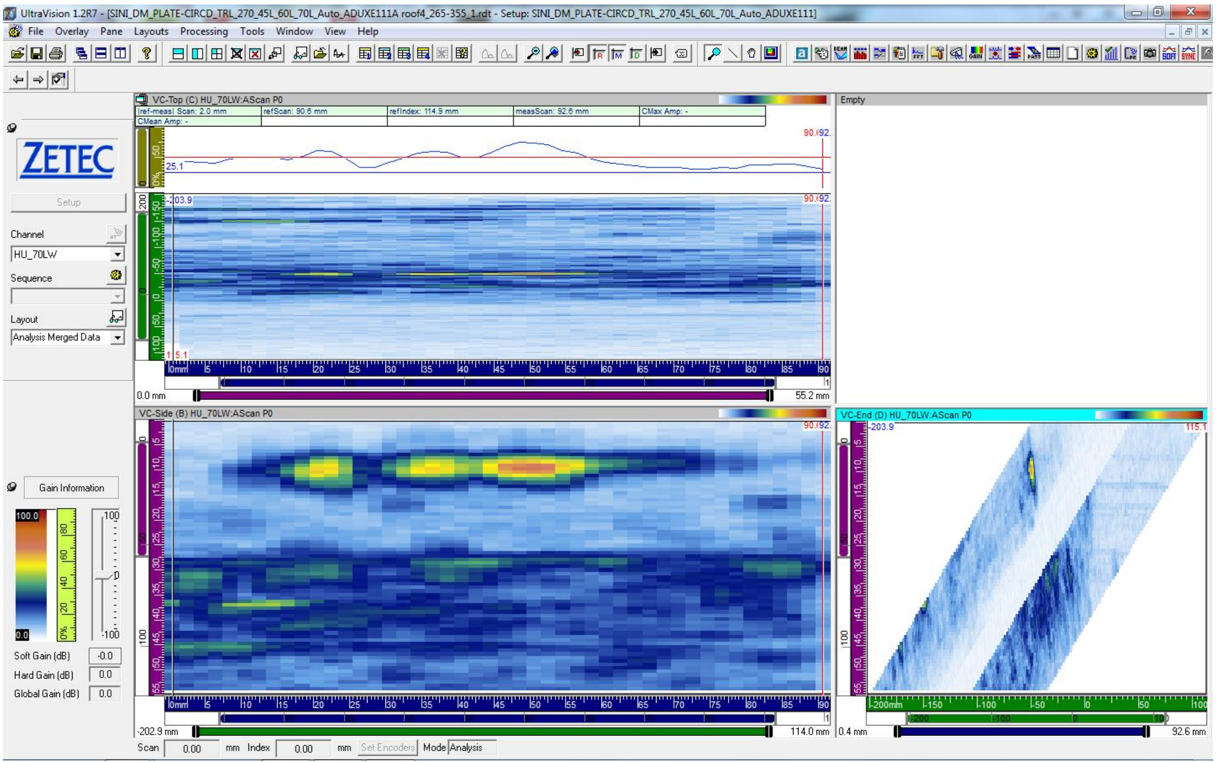

Figure 1.33. BWR mock-up data at 70° longitudinal wave from SS side.

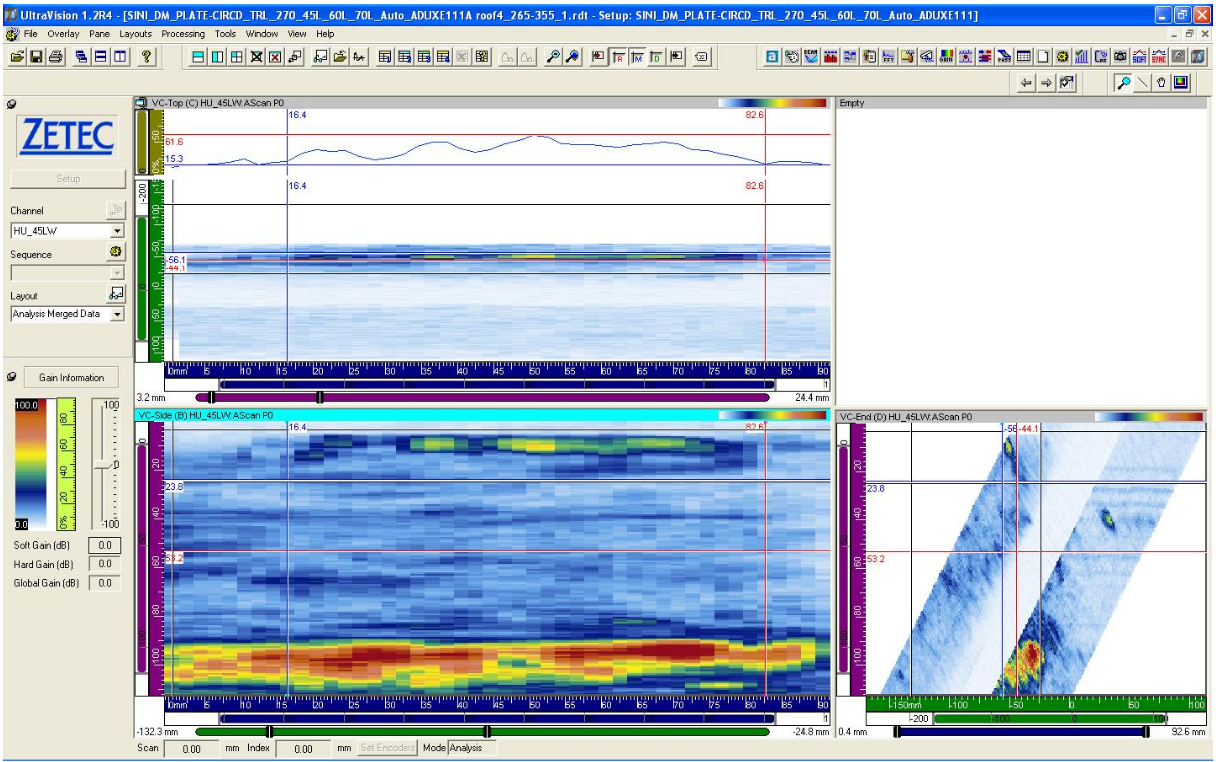

Figure 1.34. Flaw 5 at 45° longitudinal wave from SS side. Good SNR with clear start and end points.

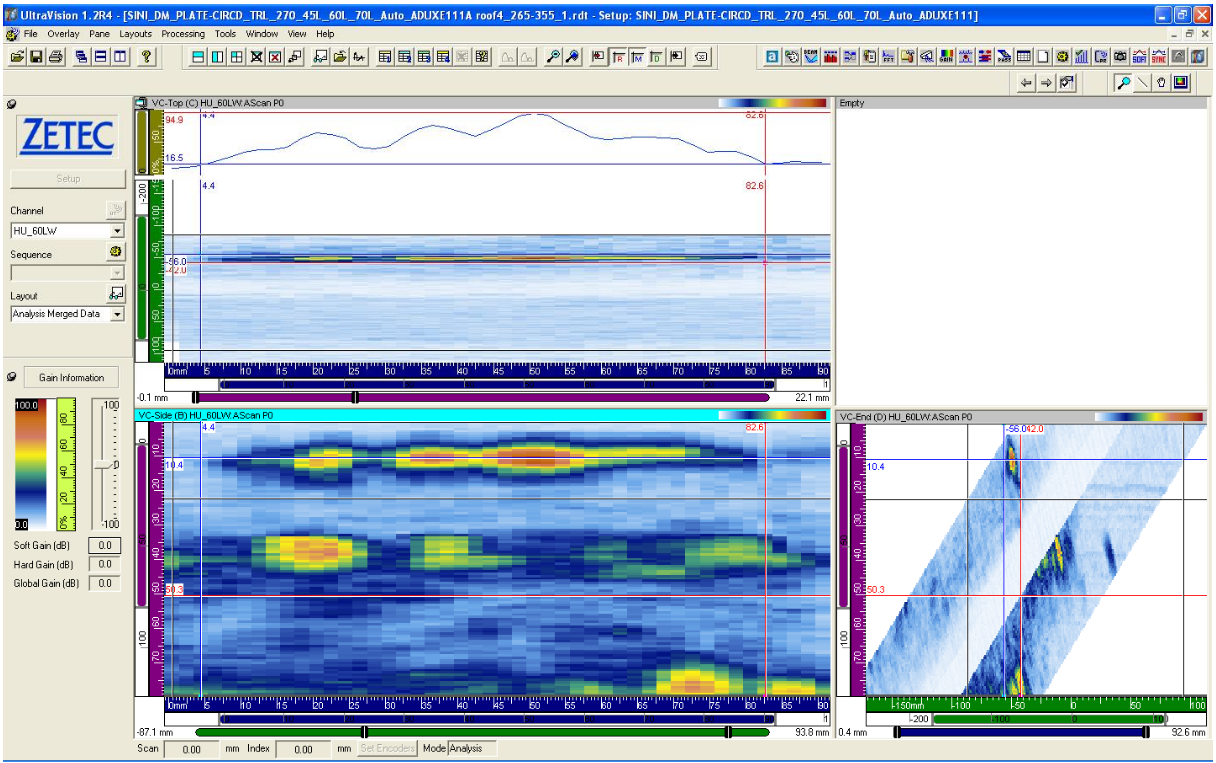

Figure 1.35. Flaw 5 at 60° longitudinal wave from SS side.

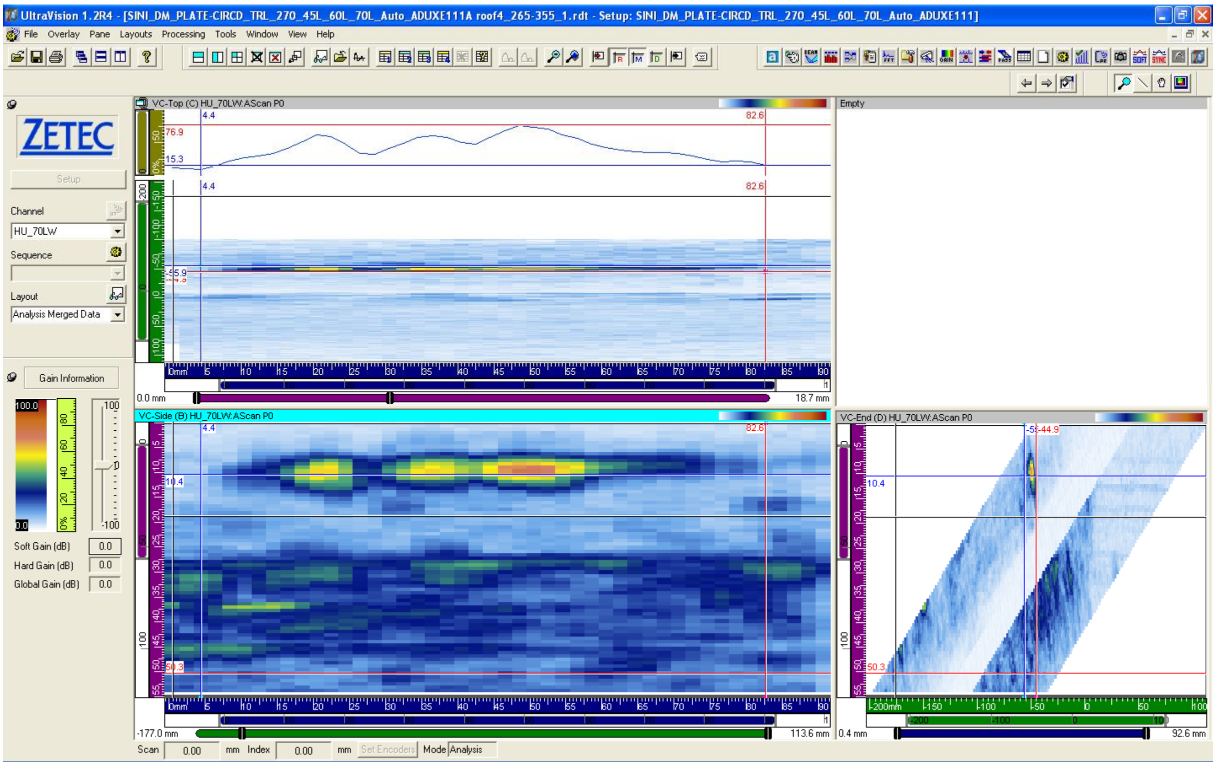

Figure 1.36. Flaw 5 at 70° longitudinal wave from SS side.

1.7 CIRCU TRS 270 scan 0–290 mm

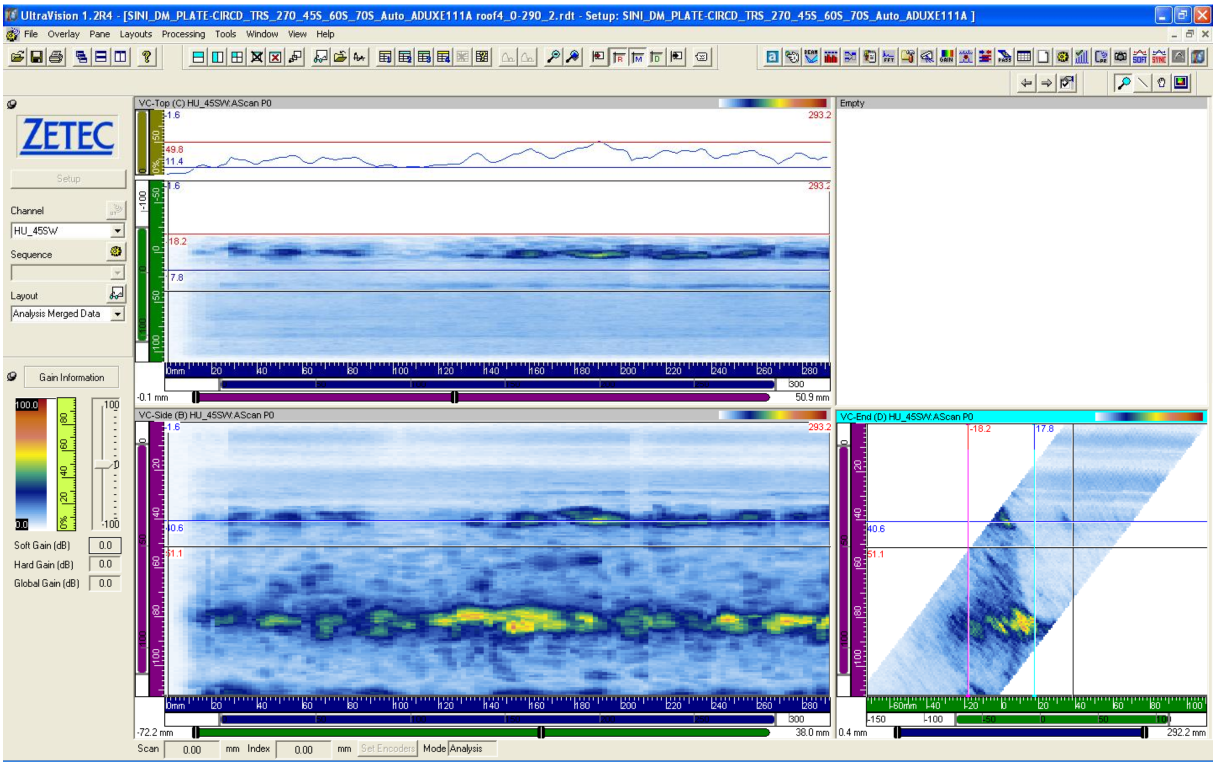

Figure 1.37. BWR mock-up data at 45° shear wave from SS side.

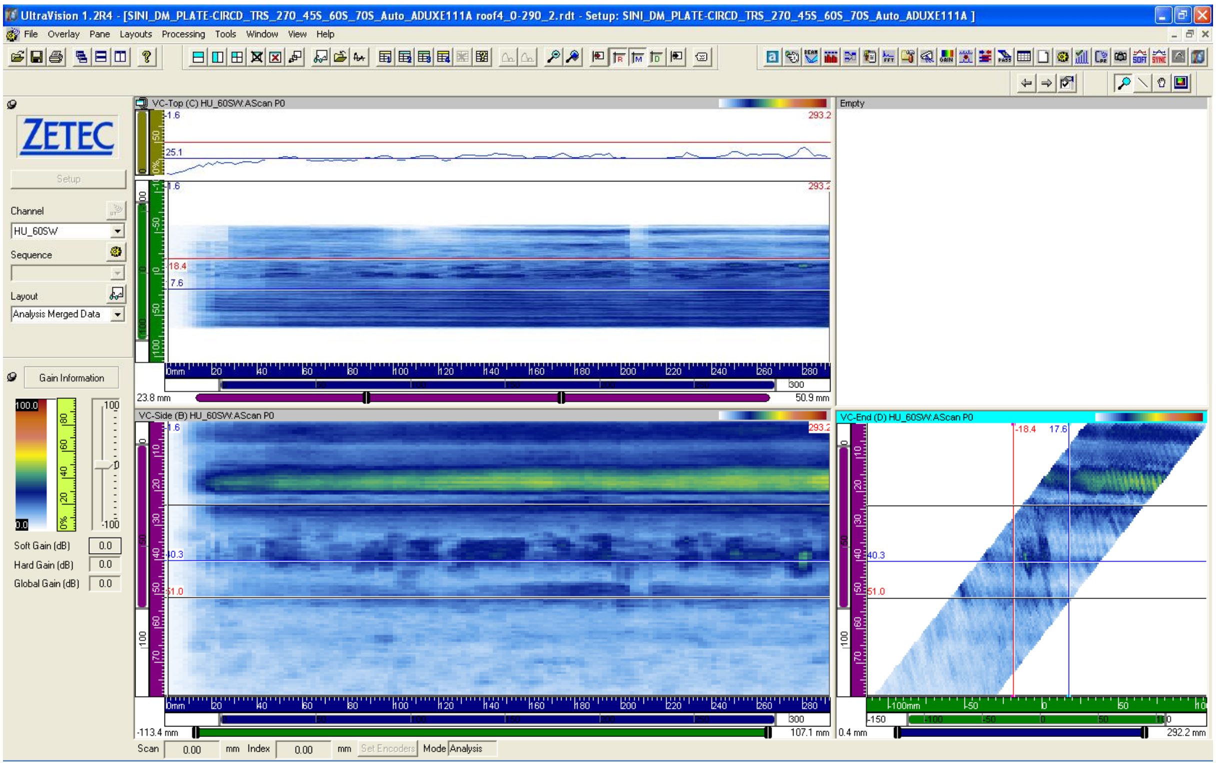

Figure 1.38. BWR mock-up data at 60° shear wave from SS side.

1.8 CIRCU TRS 270 scan 265–355 mm

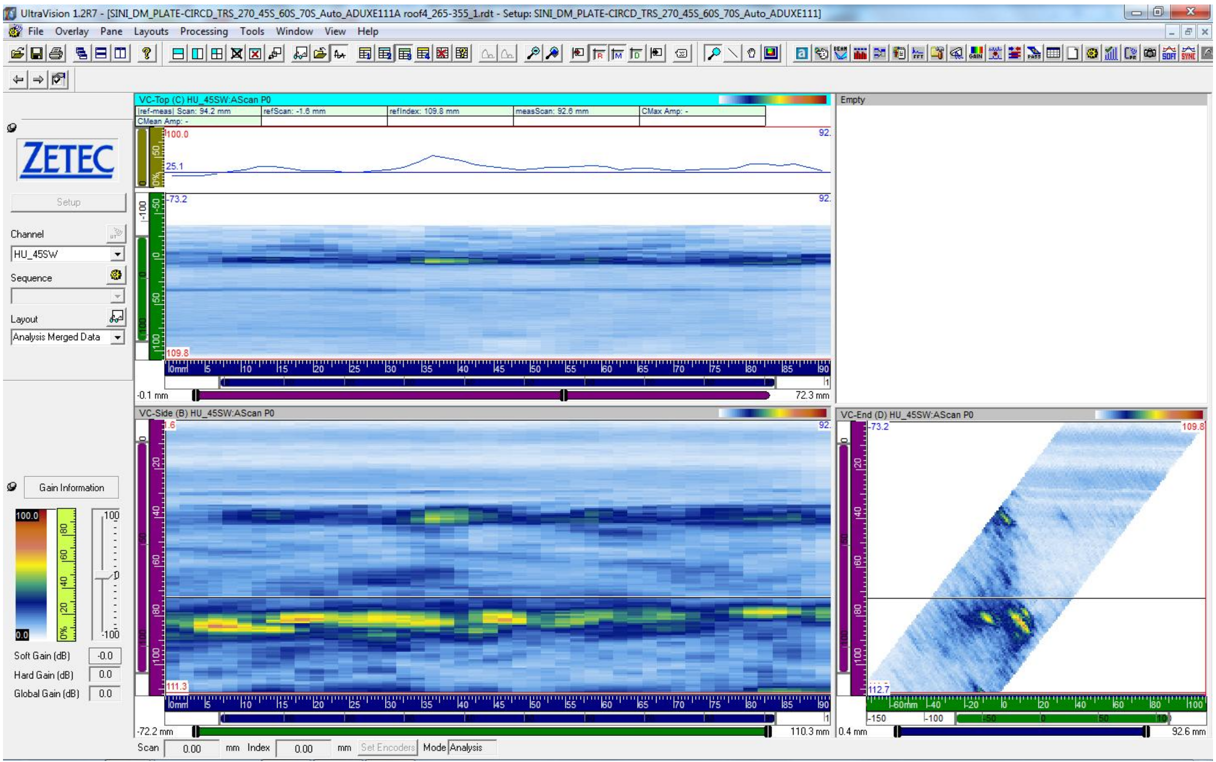

Figure 1.39. BWR mock-up data at 45° shear wave from SS side.

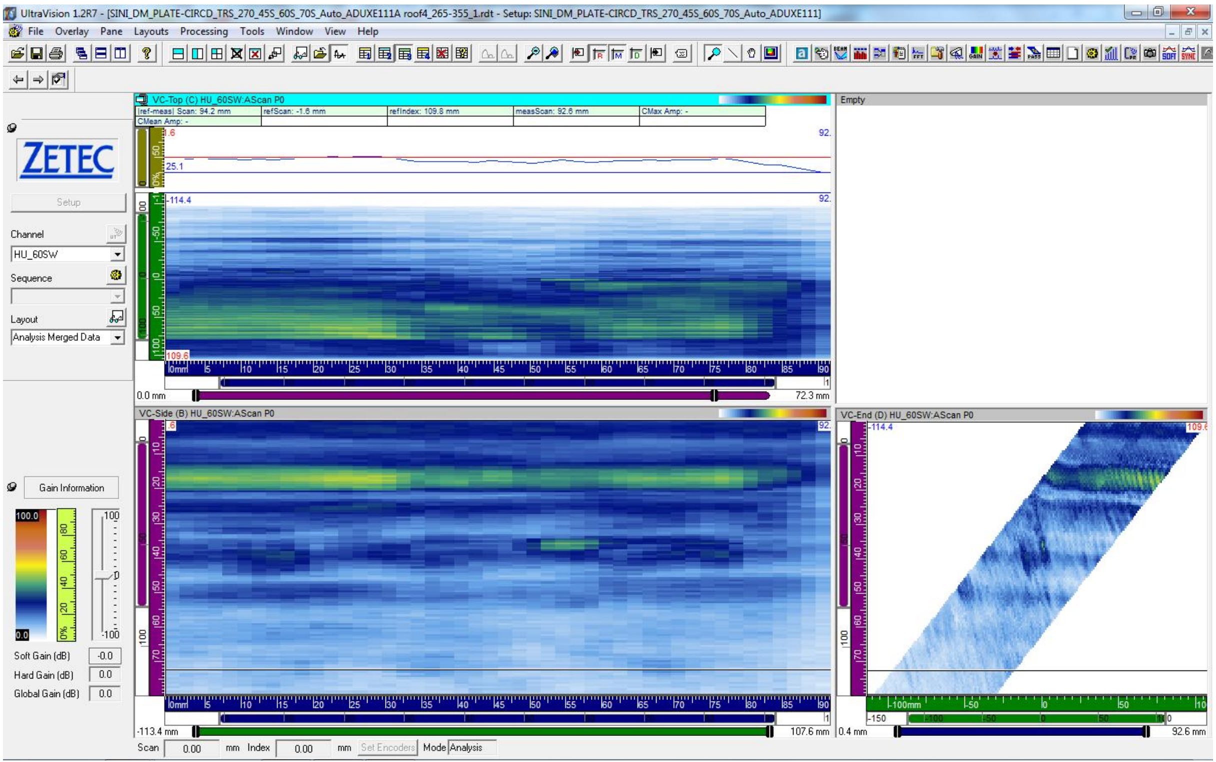

Figure 1.40. BWR mock-up data at 60° shear wave from SS side.

APPENDIX 2. The Alloy 52 NGW mock-up phased array testing data

2.1 CIRCD TRL 90 scan 0–280 mm

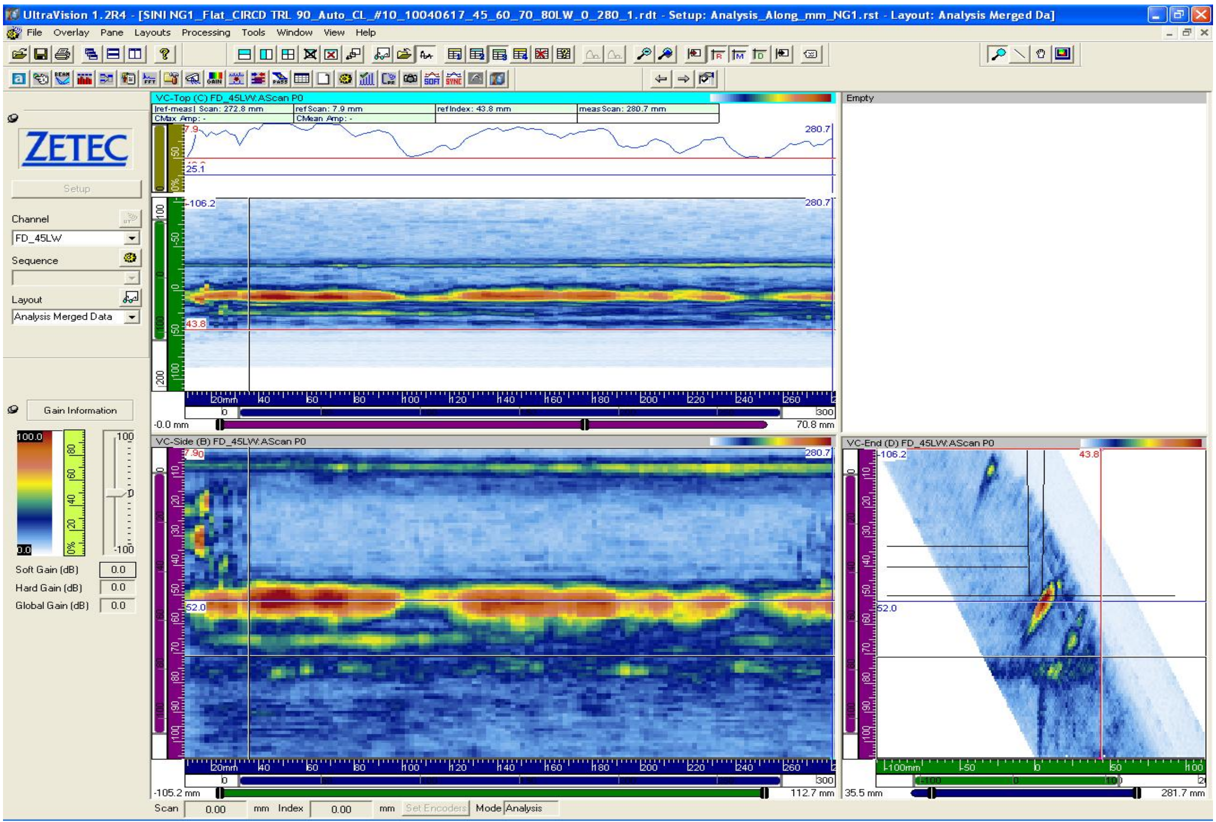

Figure 2.1. Alloy 52 NGW mock-up data at 45° longitudinal wave from CS side with continuous indication from the counter bore on the test block surface and from the weld root reinforcement. Also flaw 1 visible.

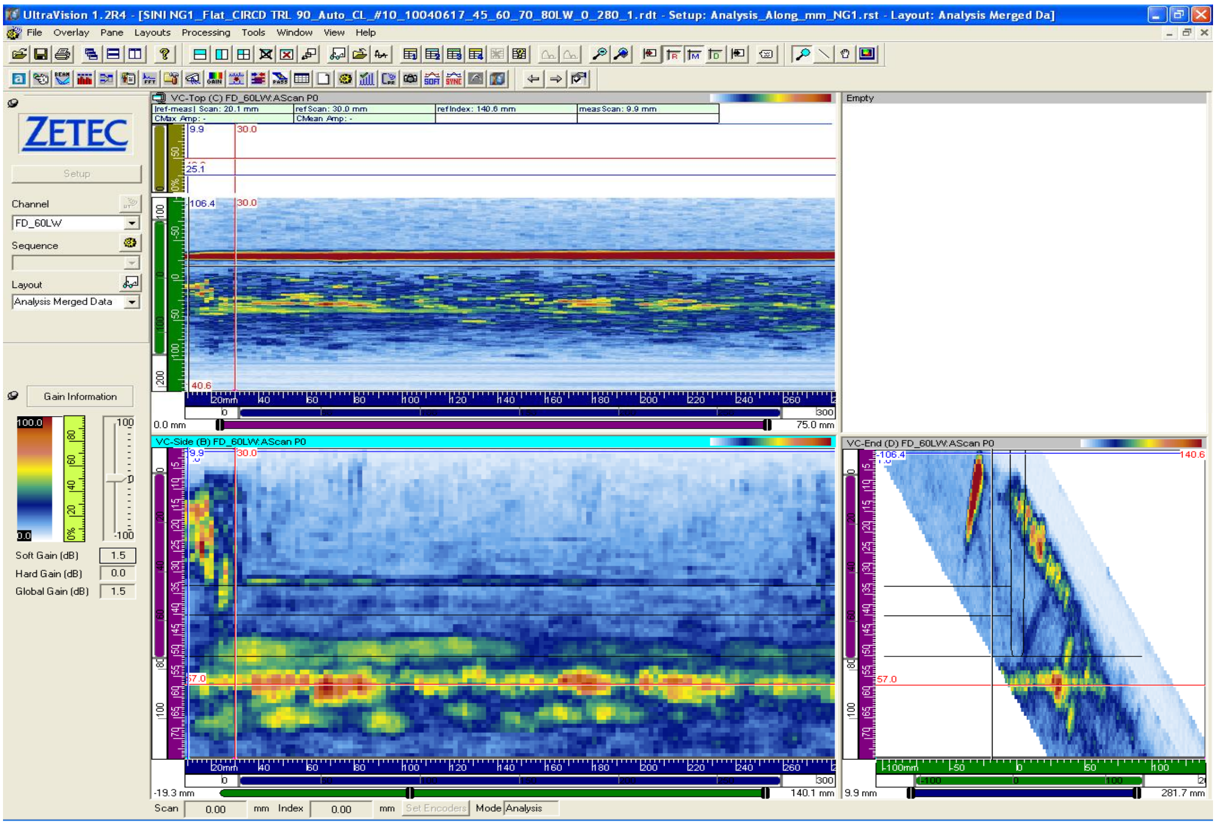

Figure 2.2. Alloy 52 NGW mock-up data at 60° longitudinal wave from CS side with continuous indication from the counter bore on the test block surface and mode converted continuous indication from the parent material/cladding boundary. Also flaw 1 visible.

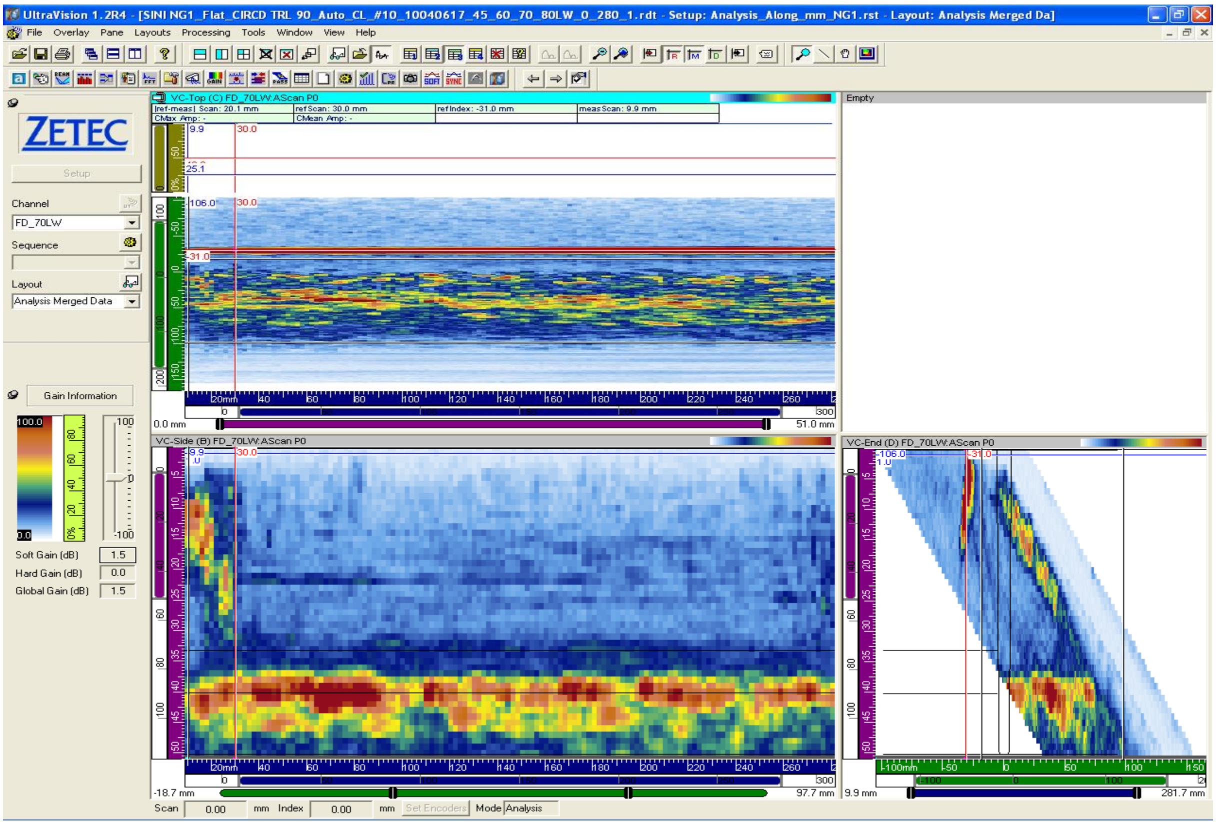

Figure 2.3. Alloy 52 NGW mock-up data at 70° longitudinal wave from CS side with continuous indication from the counter bore on the test block surface and mode converted continuous indication from the parent material /cladding boundary. Also flaw 1 visible.

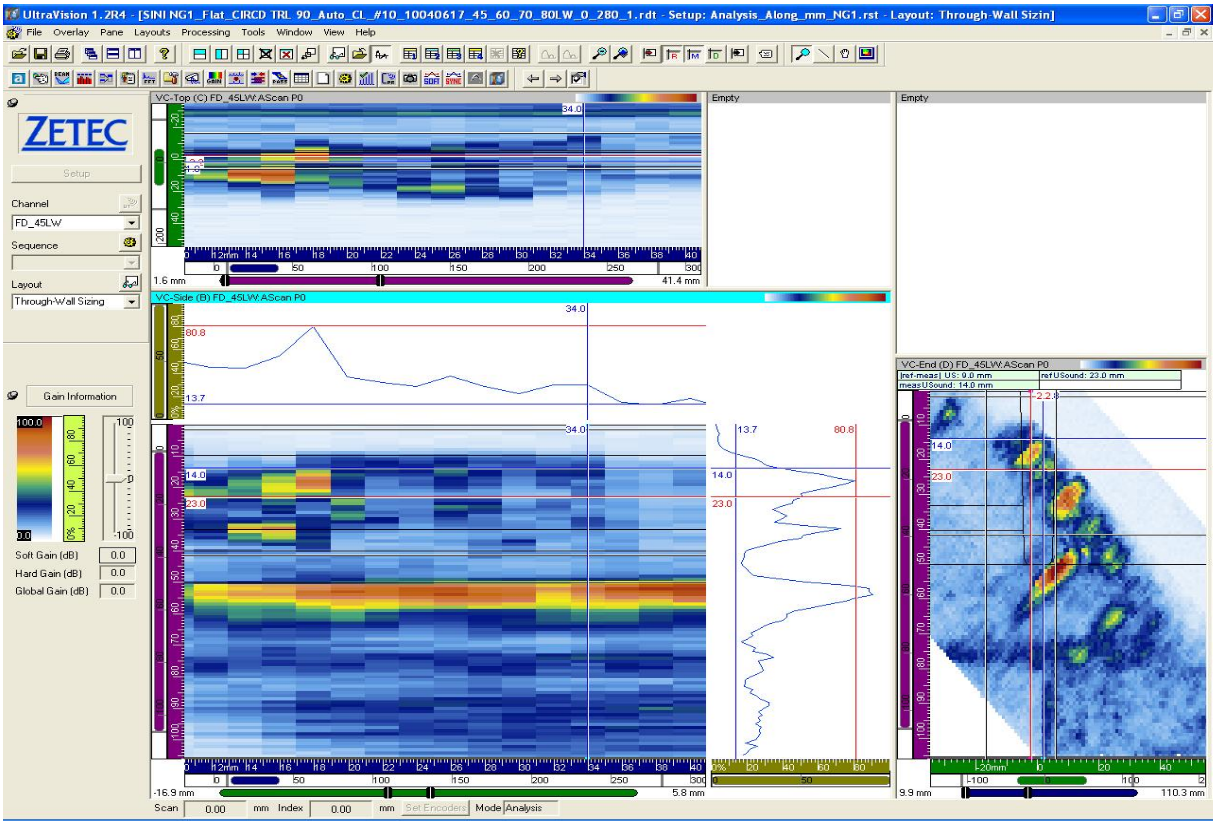

Figure A2.4. Flaw 1 at 45° longitudinal wave from CS side.

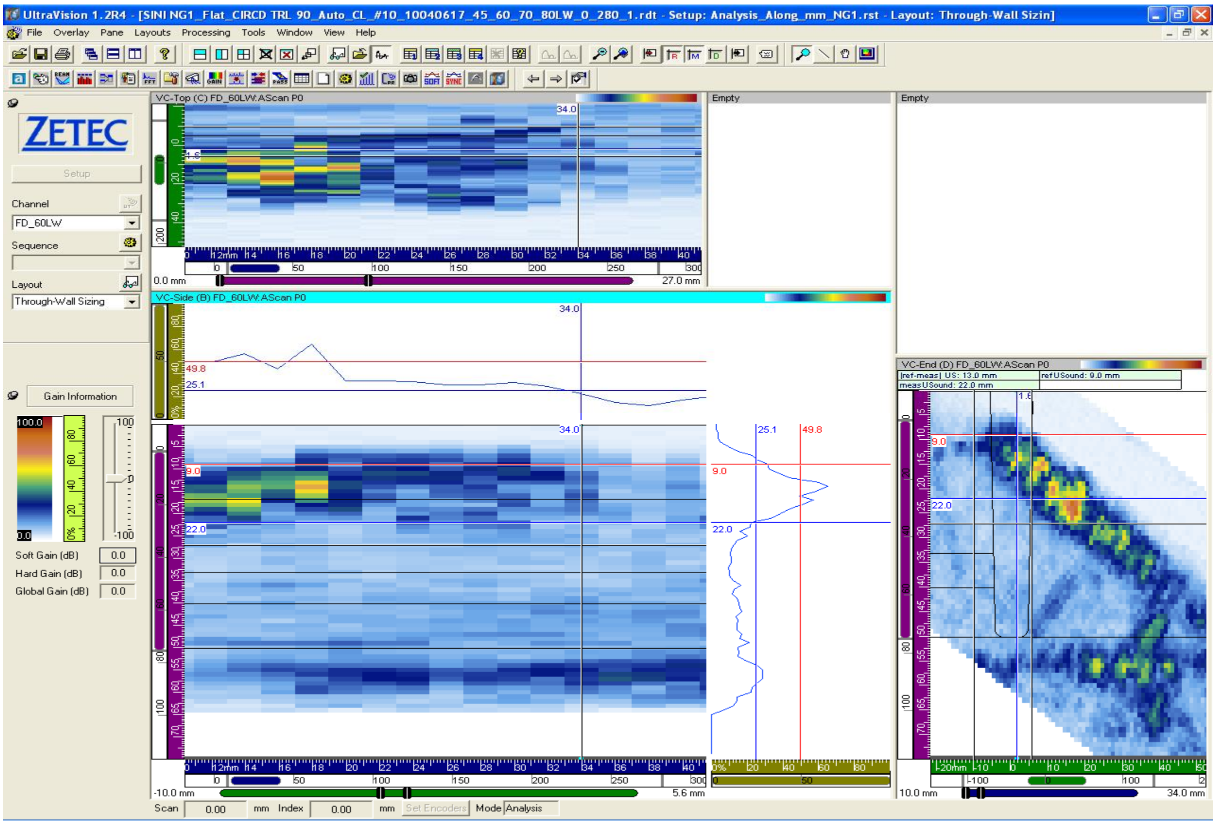

Figure A2.5. Flaw 1 at 60° longitudinal wave from CS side.

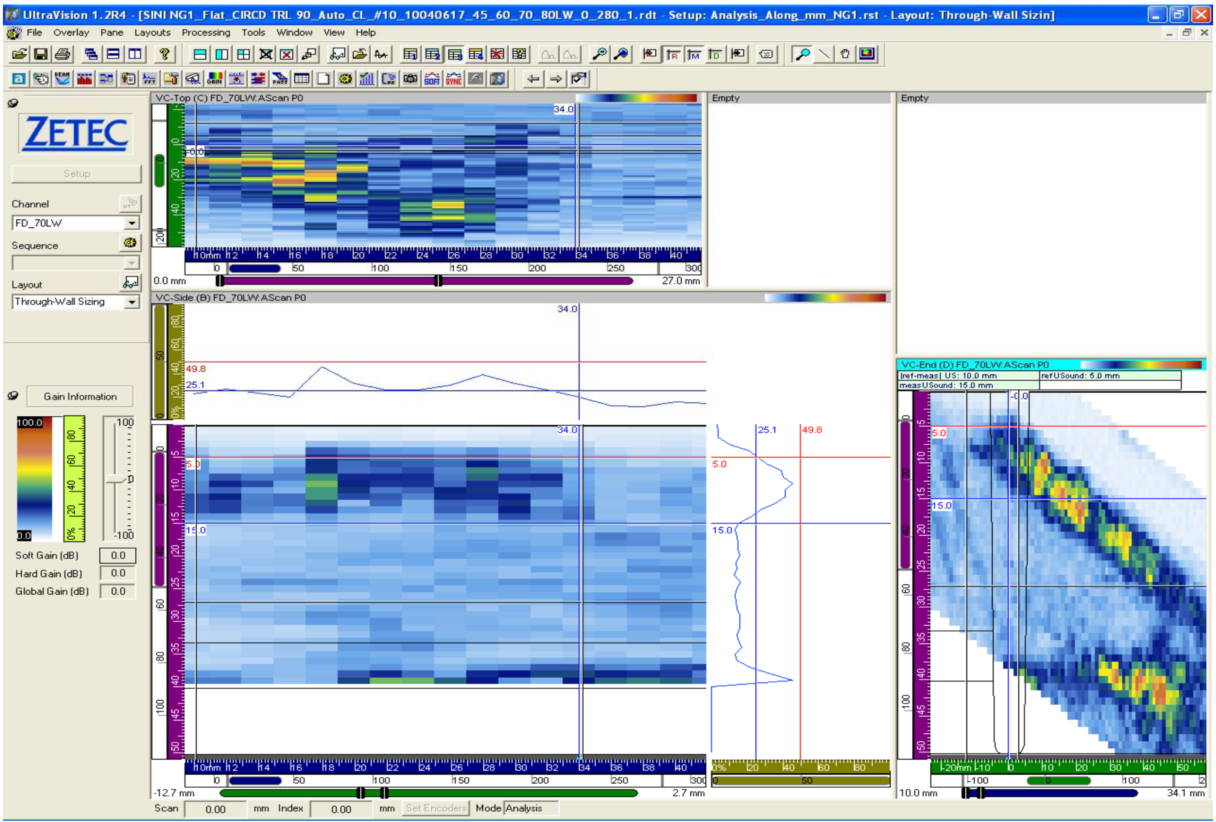

Figure A2.6. Flaw 1 at 70° longitudinal wave from CS side.

2.2 CIRCD TRL 90 scan 255–330 mm

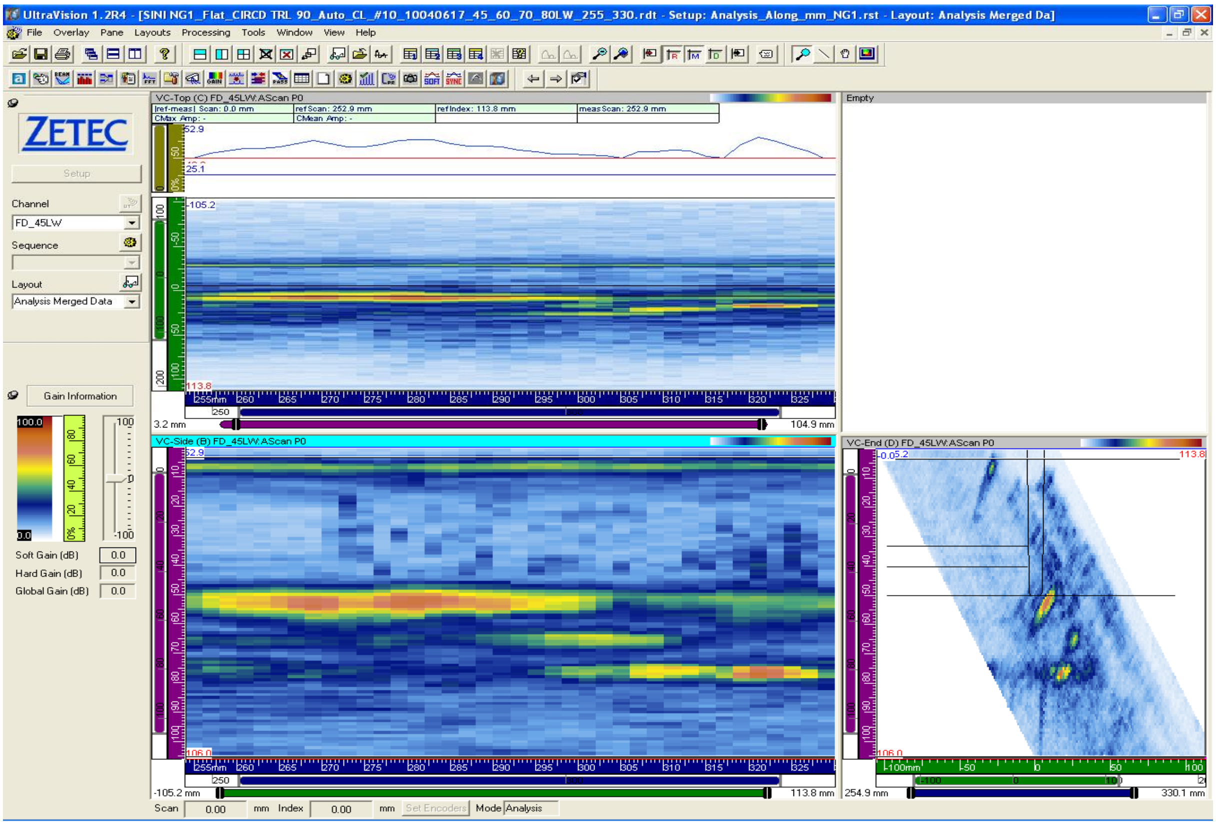

Figure 2.7. Alloy 52 NGW mock-up data at 45° longitudinal wave from CS side with continuous indication from the counter bore on the test block surface and from the weld root reinforcement.

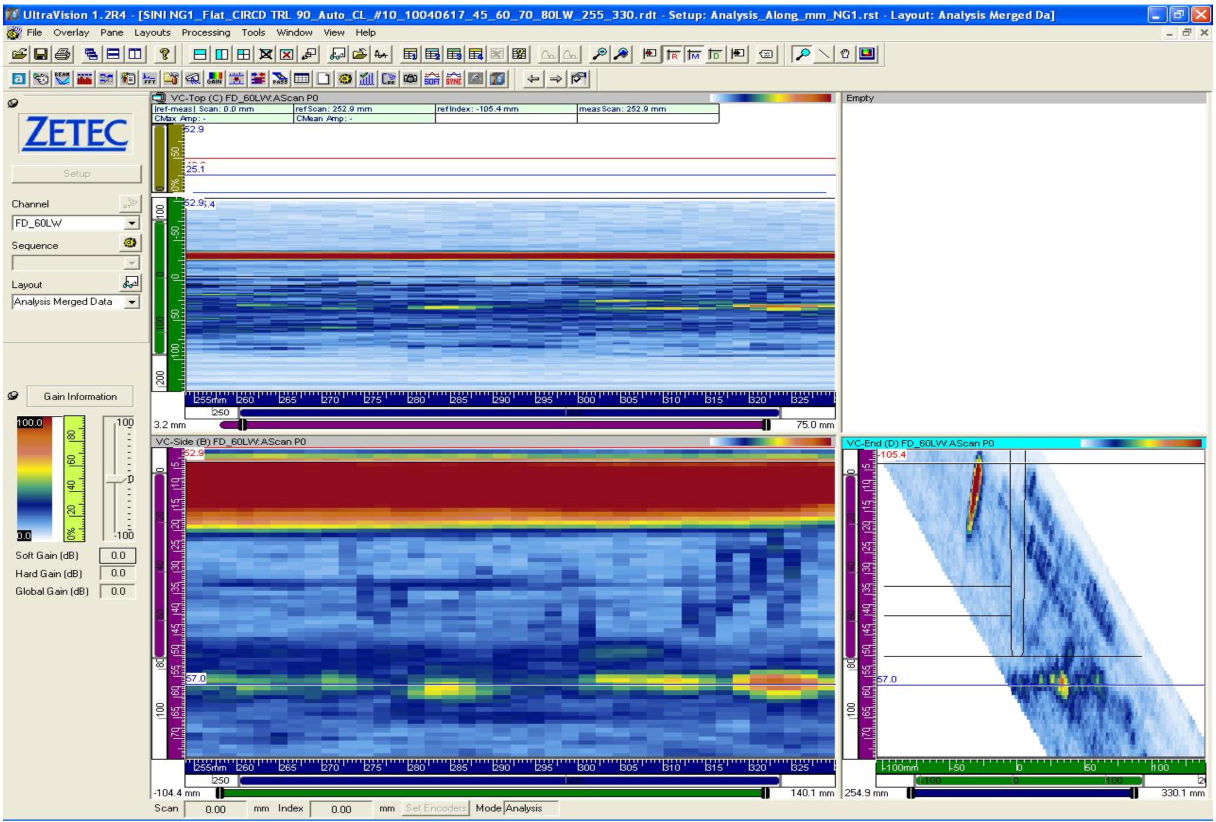

Figure 2.8. Alloy 52 NGW mock-up data at 60° longitudinal wave from CS side with continuous indication from the counter bore on the test block surface and mode converted continuous indication from the parent material/cladding boundary.

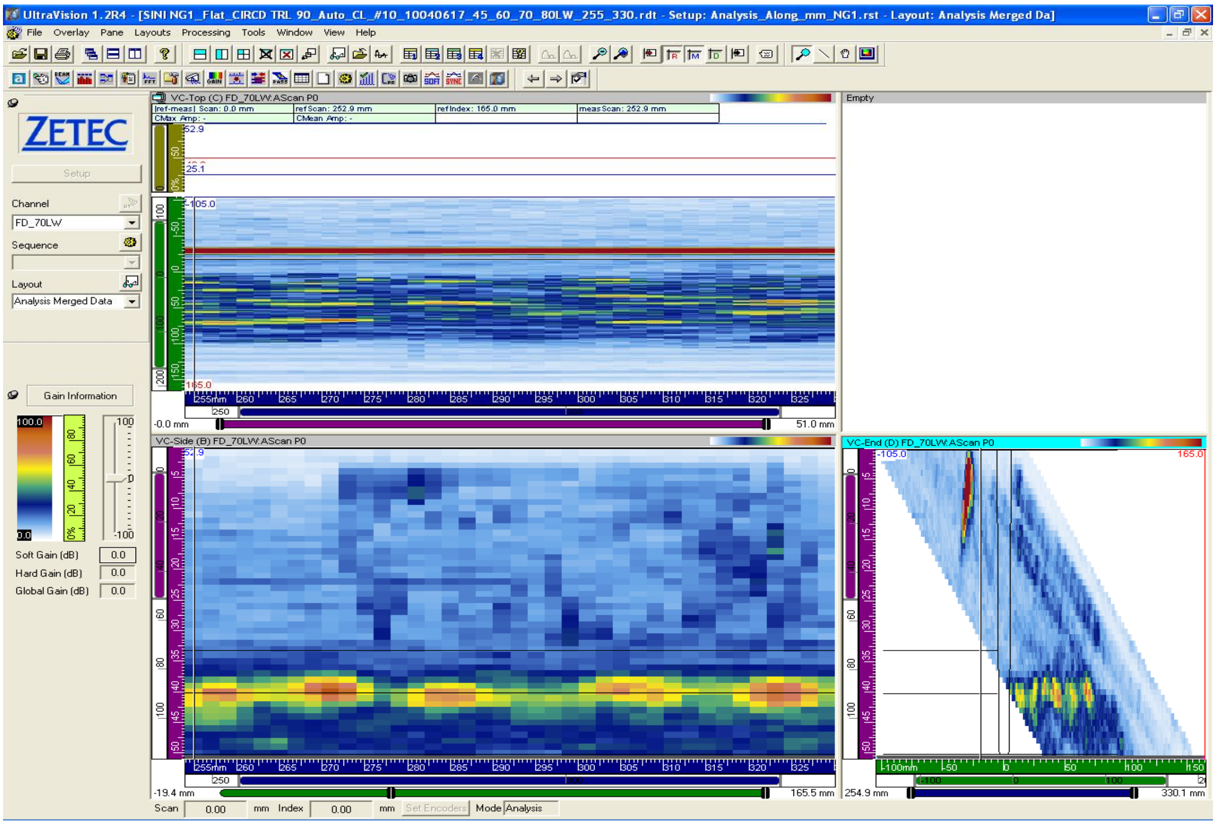

Figure 2.9. Alloy 52 NGW mock-up data at 70° longitudinal wave from CS side with continuous indication from the counter bore on the test block surface and mode converted continuous indication from the parent material/cladding boundary.

2.3 CIRCD TRS 90 scan 0–280 mm

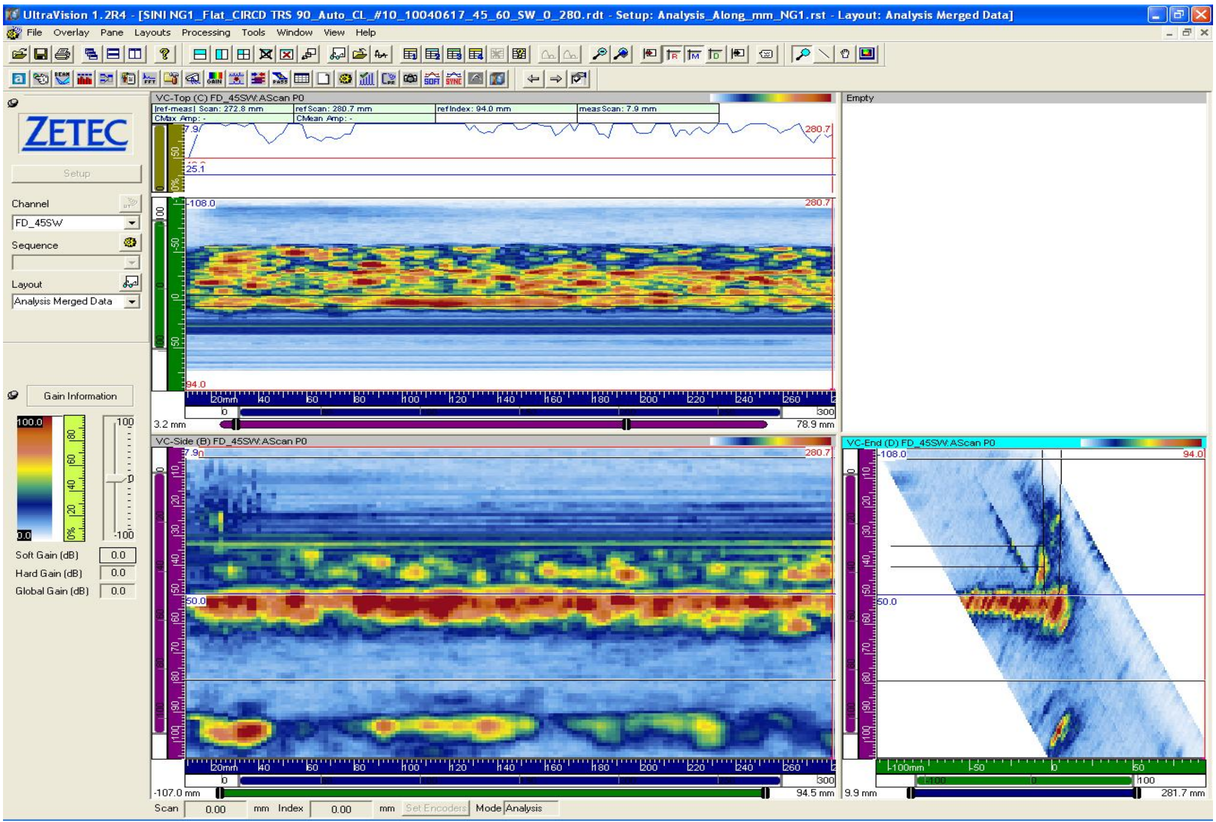

Figure 2.10. Alloy 52 NGW mock-up data at 45° shear wave from CS side with continuous indication the weld root reinforcement and back wall indication from the cladding. Also flaw 1 visible.

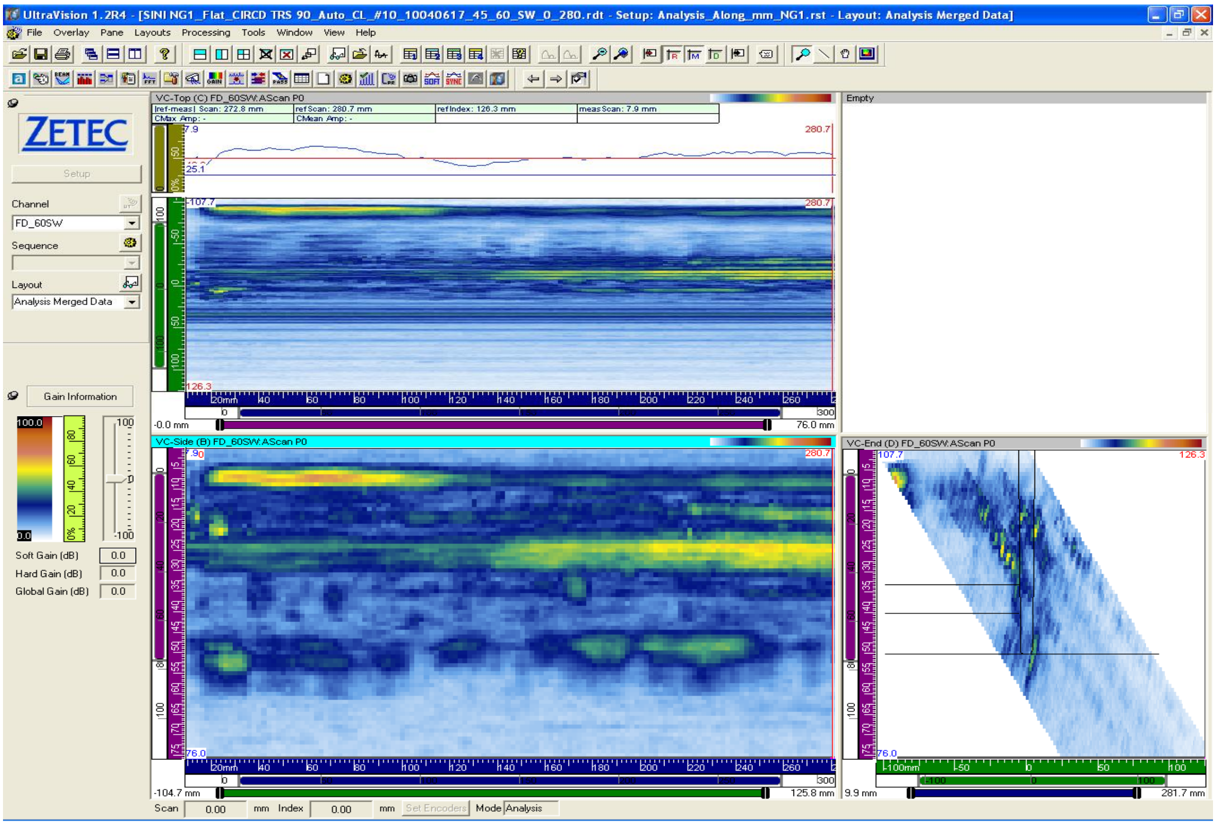

Figure 2.11. Alloy 52 NGW mock-up data at 60° shear wave from CS side with continuous indication from the counter bore on the test block surface and concave weld reinforcement. Also flaw 1 visible.

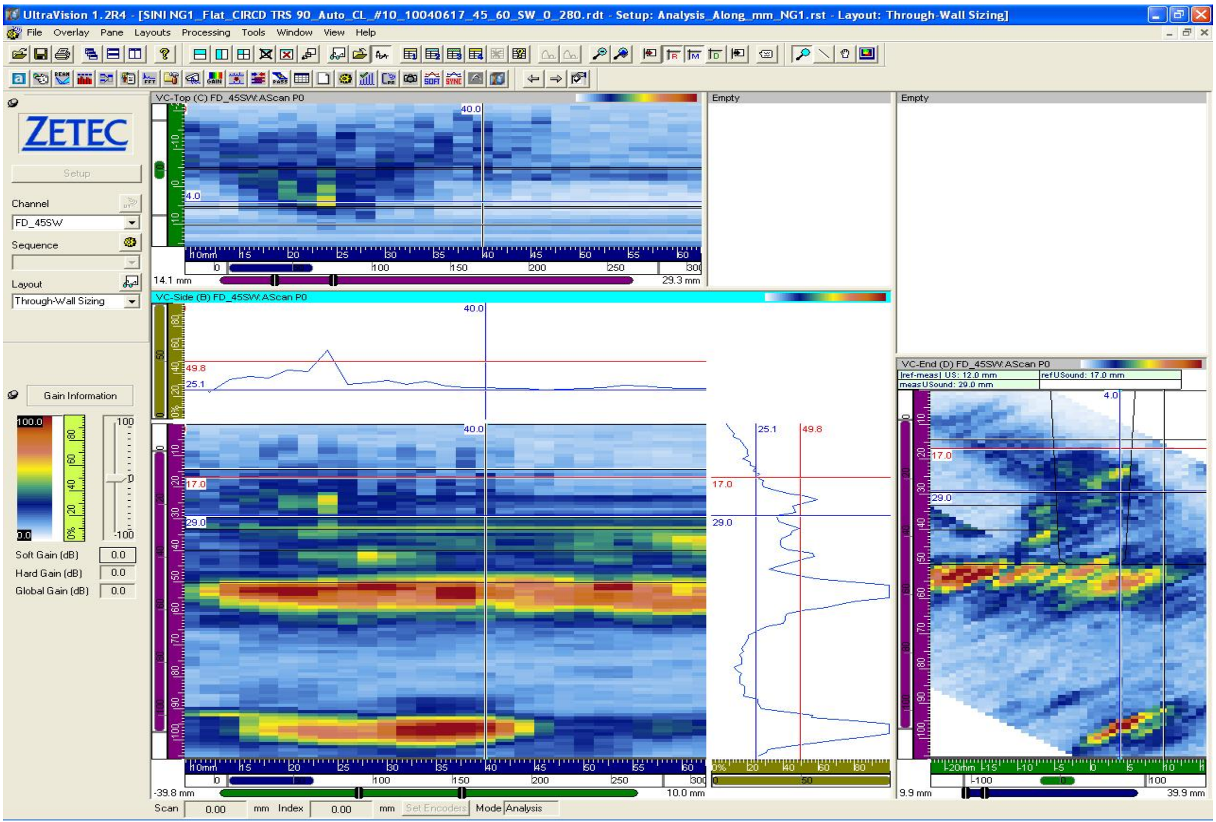

Figure 2.12. Flaw 1 at 45° shear wave from CS side.

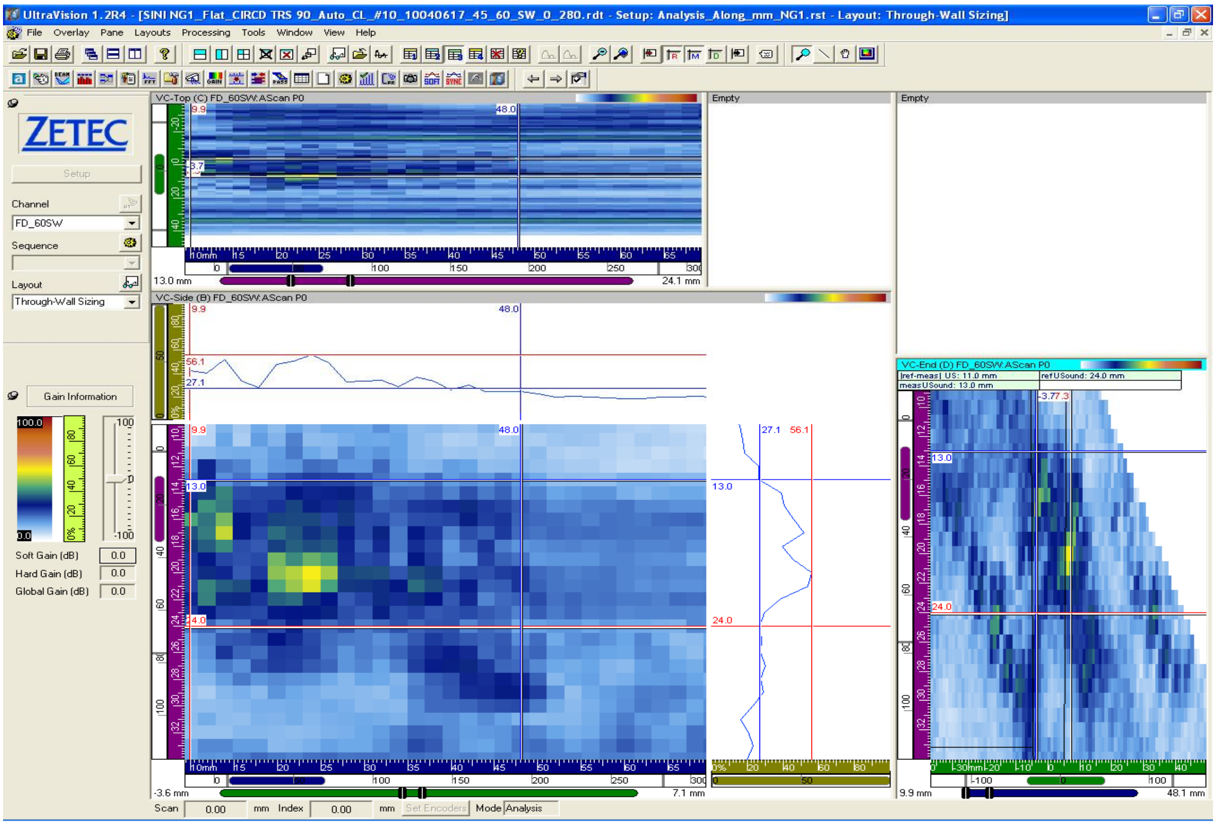

Figure 2.13. Flaw 1 at 60° shear wave from CS side.

2.4 CIRCD TRS 90 scan 255–330 mm

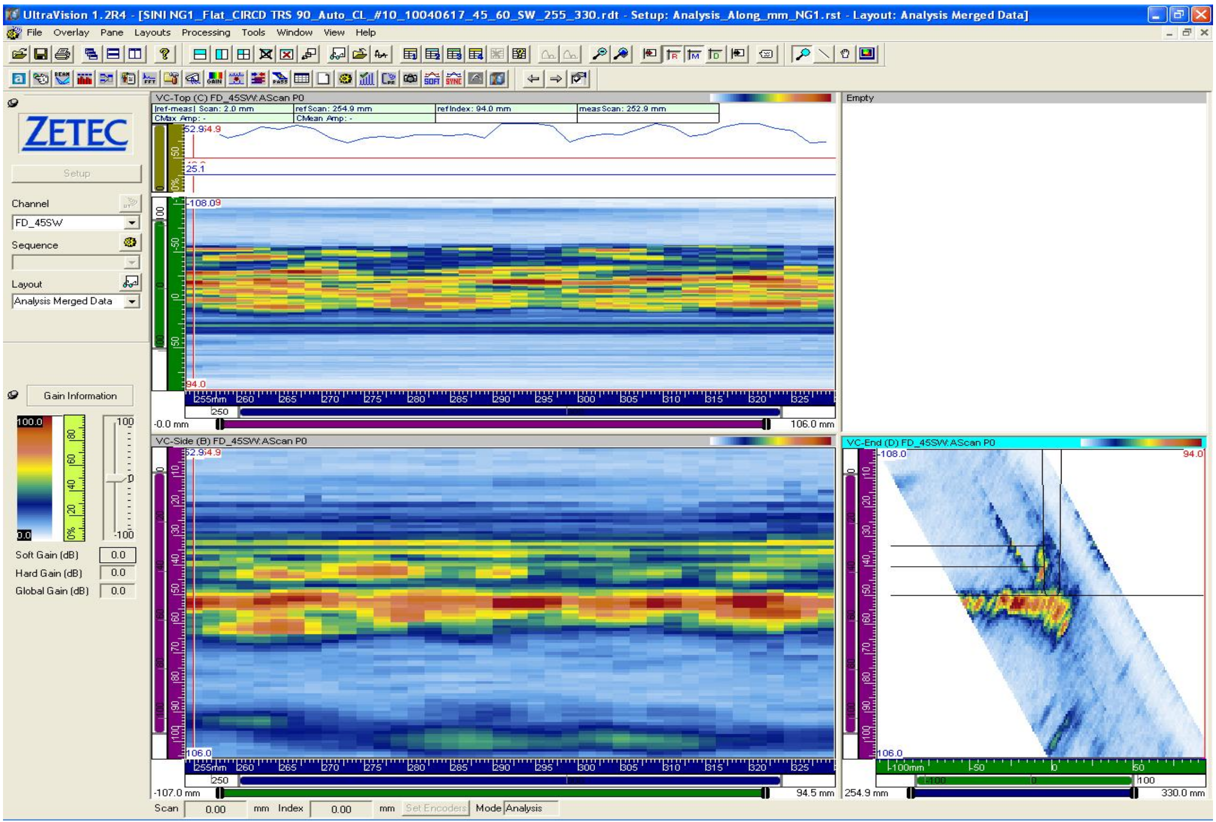

Figure 2.14. Alloy 52 NGW mock-up data at 45° shear wave from CS side with continuous indication the weld root reinforcement and back wall indication from the cladding.

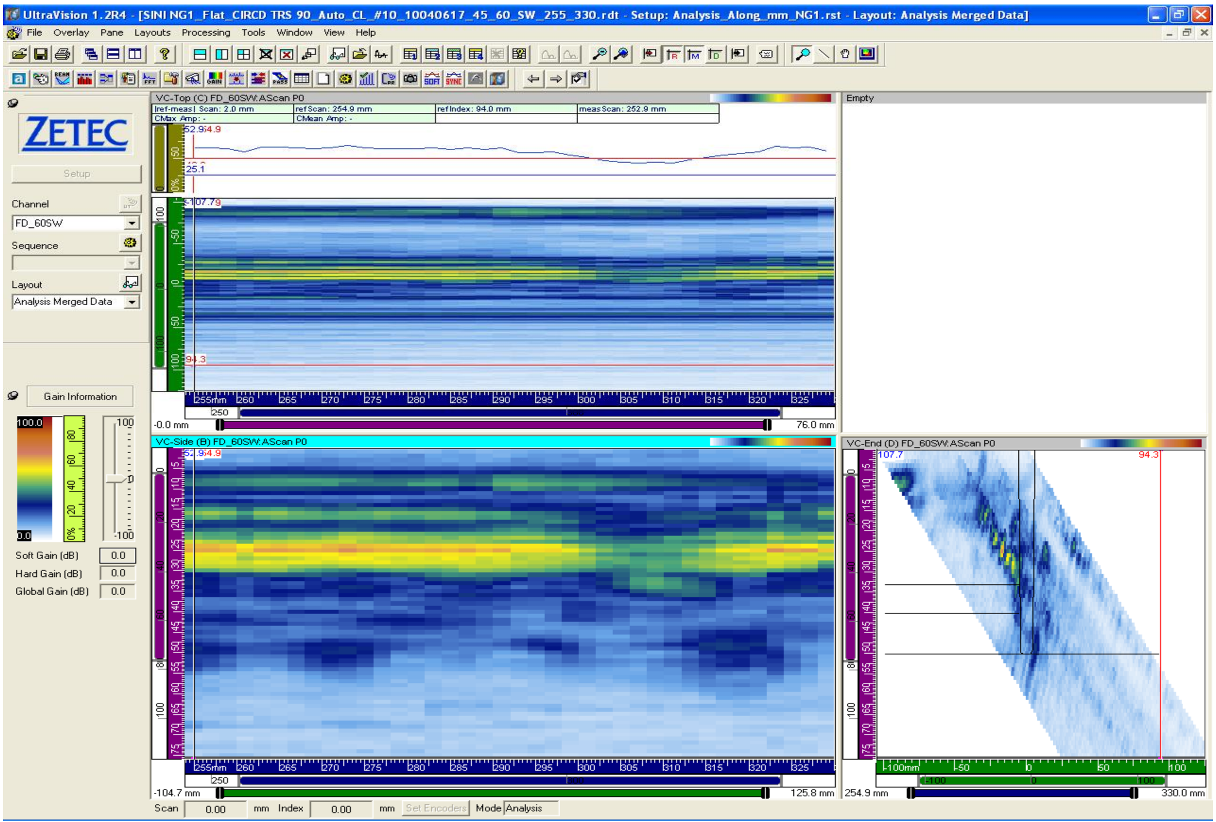

Figure 2.15. Alloy 52 NGW mock-up data at 60° shear wave from CS side with continuous indication the counter bore on the test block surface and concave weld reinforcement.

2.5 CIRCU TRL 270 scan 0–280 mm

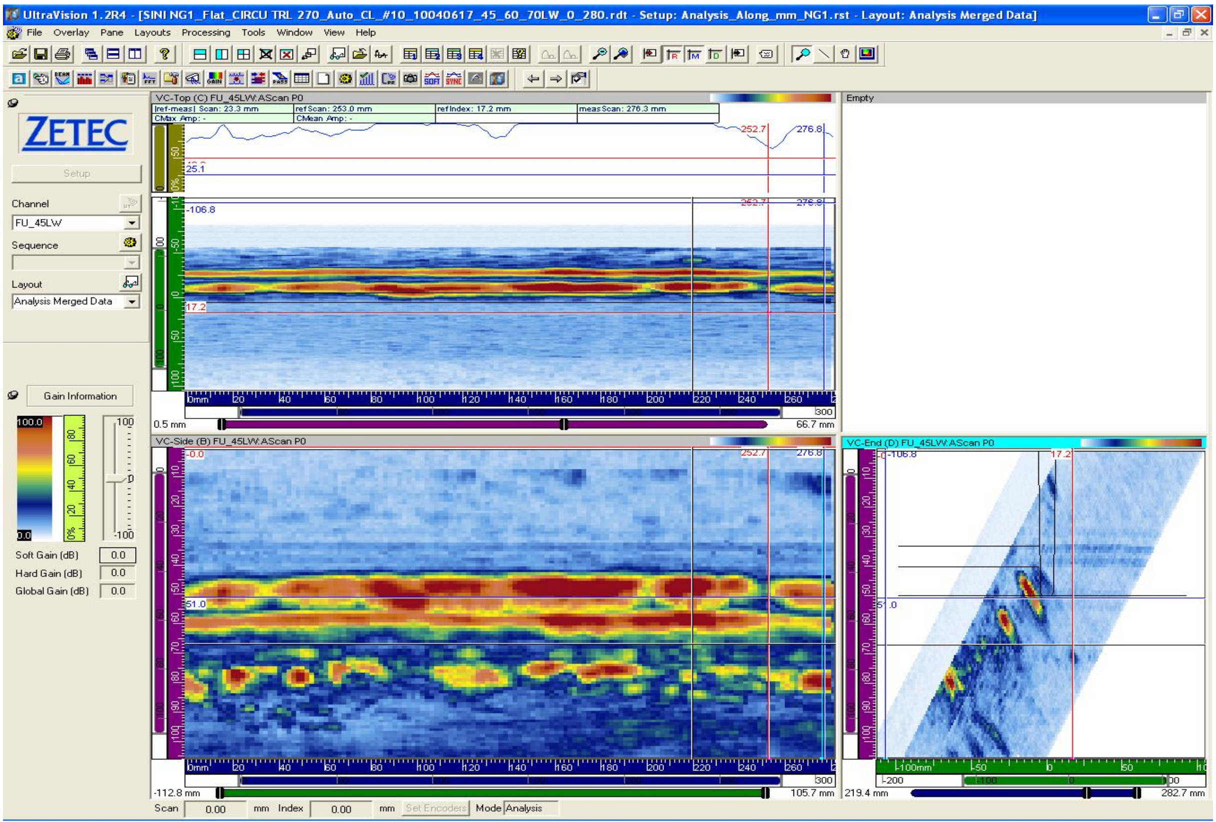

Figure 2.16. Alloy 52 NGW mock-up data at 45° longitudinal wave from SS side with continuous indication from the weld root reinforcement and mode converted indications at deeper location.

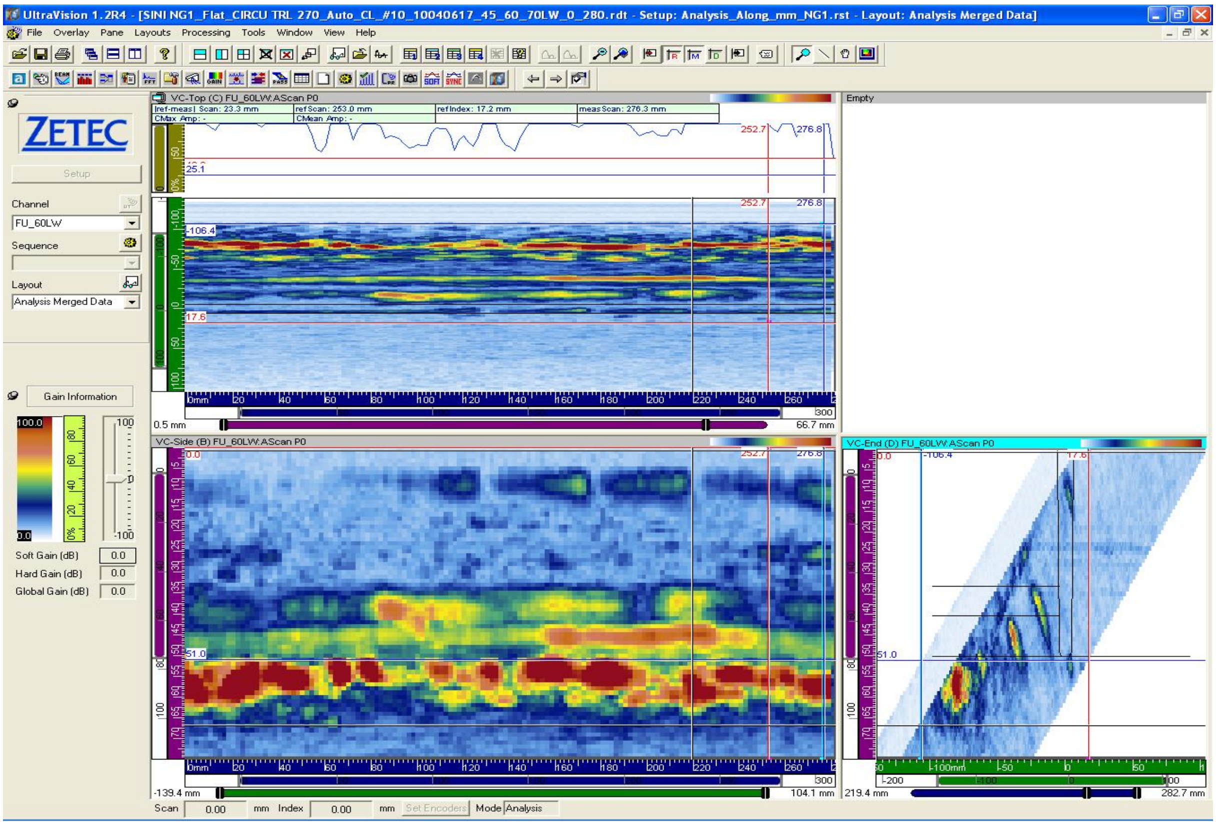

Figure 2.17. Alloy 52 NGW mock-up data at 60° longitudinal wave from SS side with geometrical and metallurgical indications.

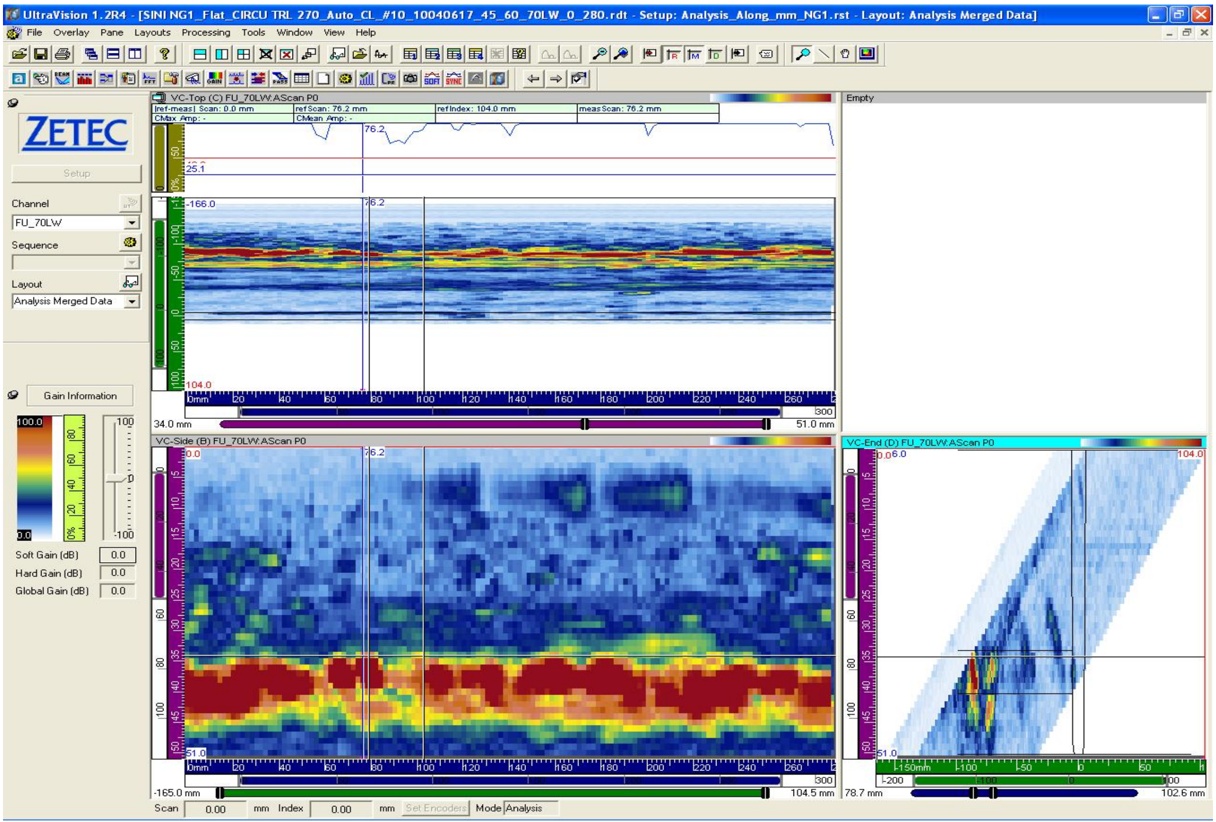

Figure 2.18. Alloy 52 NGW mock-up data at 70° longitudinal wave from SS side with strong geometrical and metallurgical indications.

2.6 CIRCU TRL 270 scan 255–330 mm

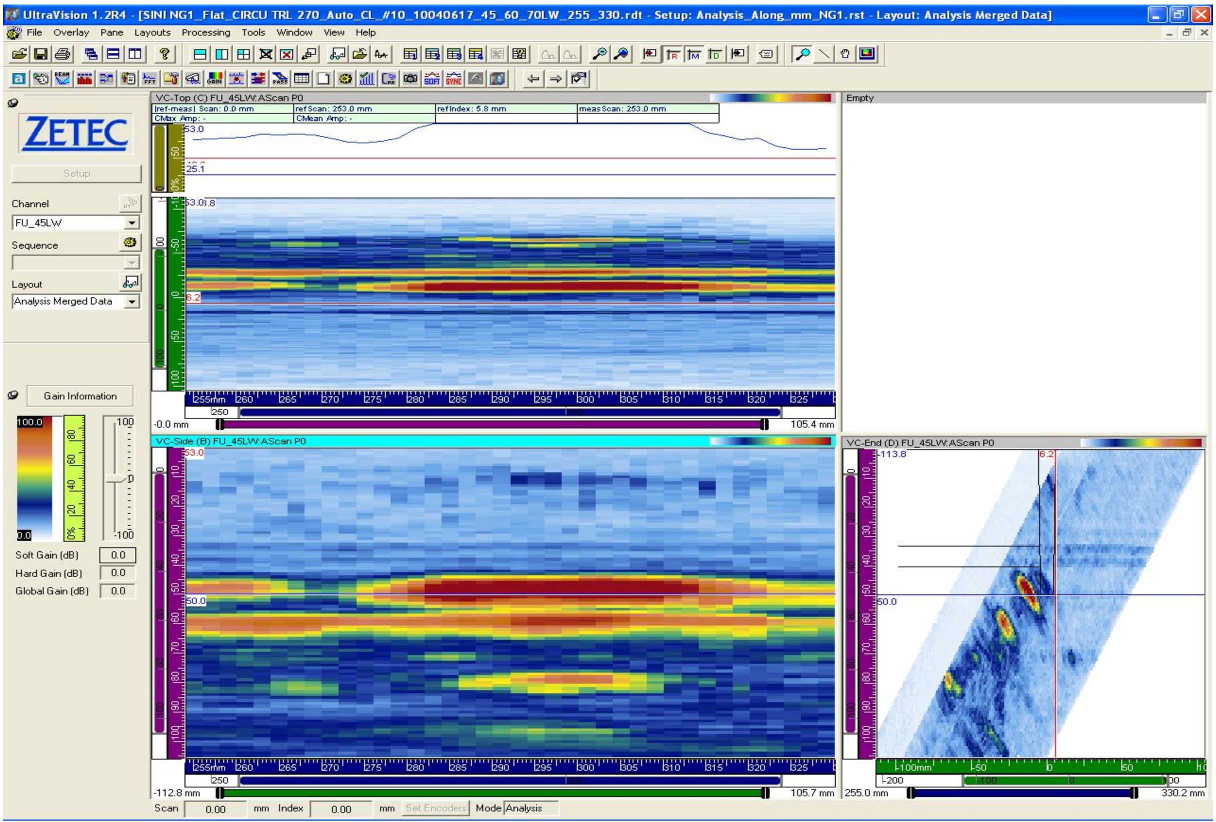

Figure 2.19. Alloy 52 NGW mock-up data at 45° longitudinal wave from SS side with continuous indication from the weld root reinforcement and mode converted indications at deeper location.

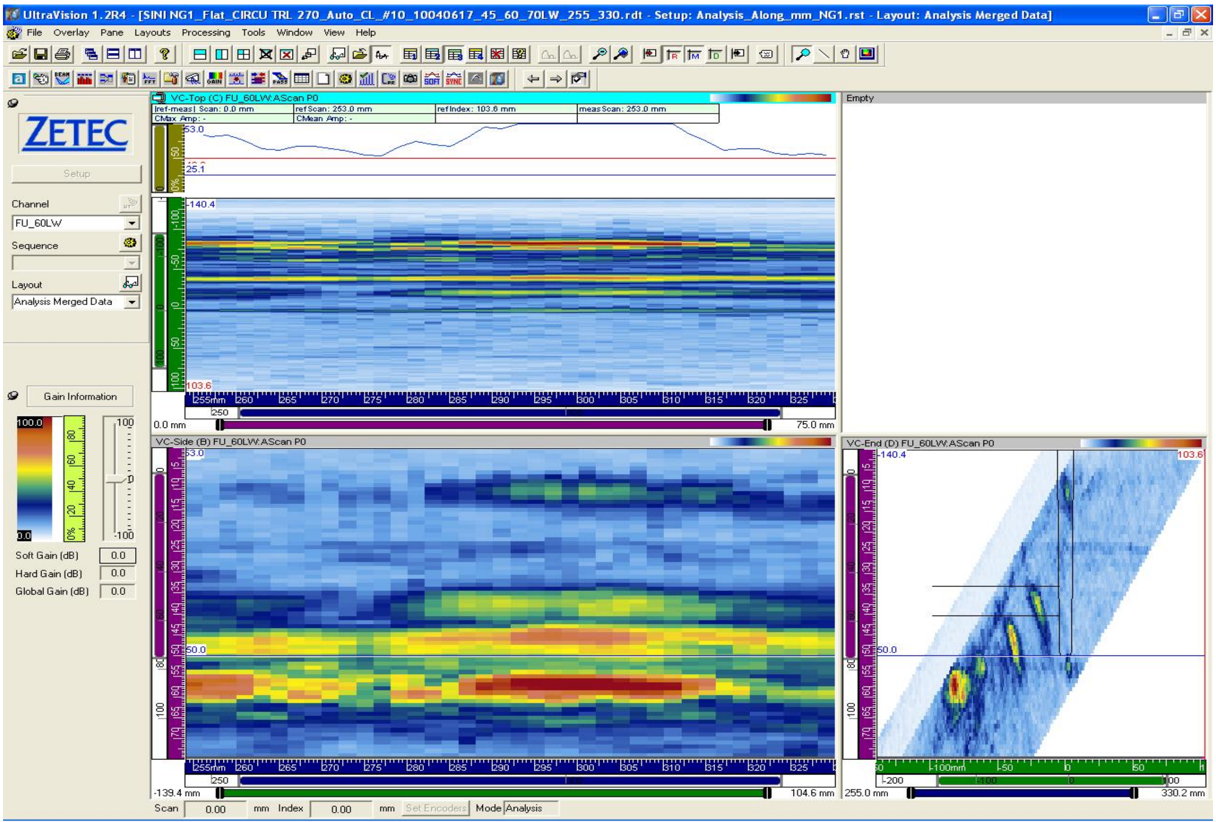

Figure 2.20. Alloy 52 NGW mock-up data at 60° longitudinal wave from SS side with geometrical and metallurgical indications.

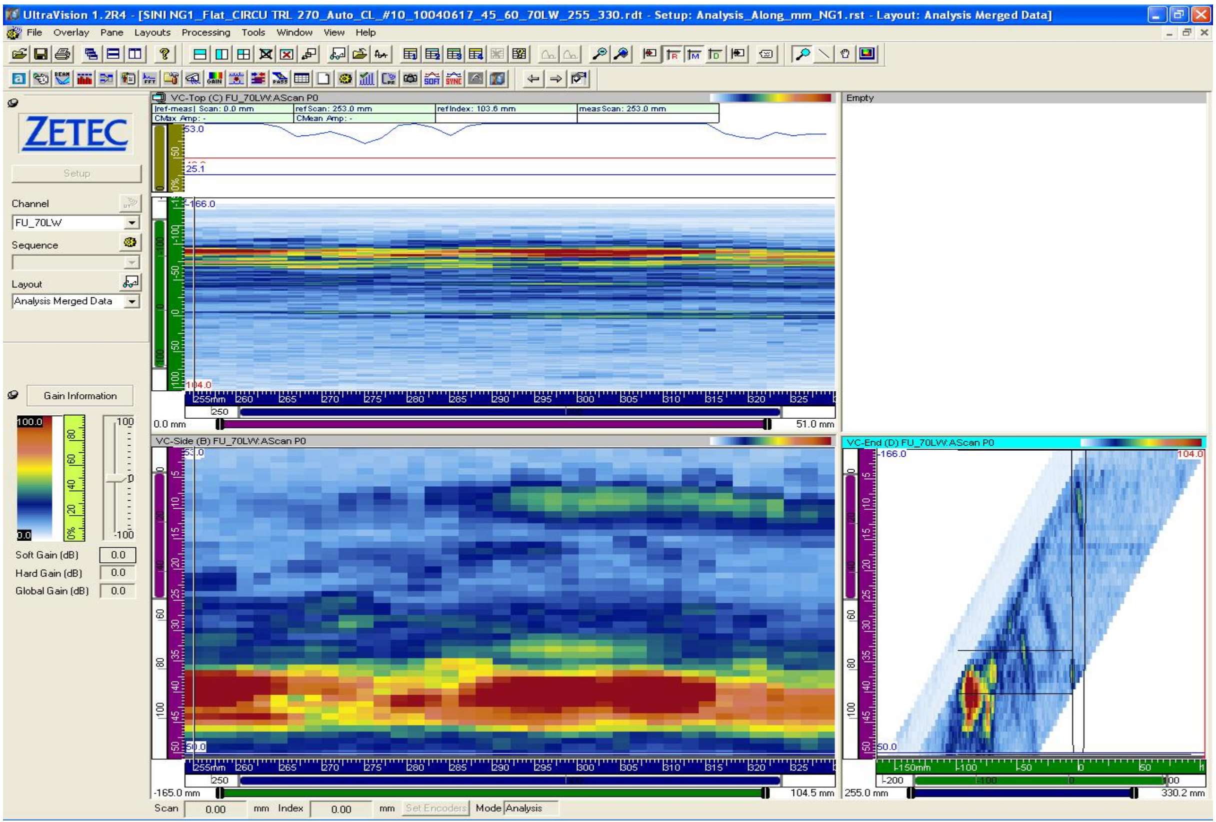

Figure 2.21. Alloy 52 NGW mock-up data at 70° longitudinal wave from SS side with geometrical and metallurgical indications.

2.7 CIRCU TRS 270 scan 0–280 mm

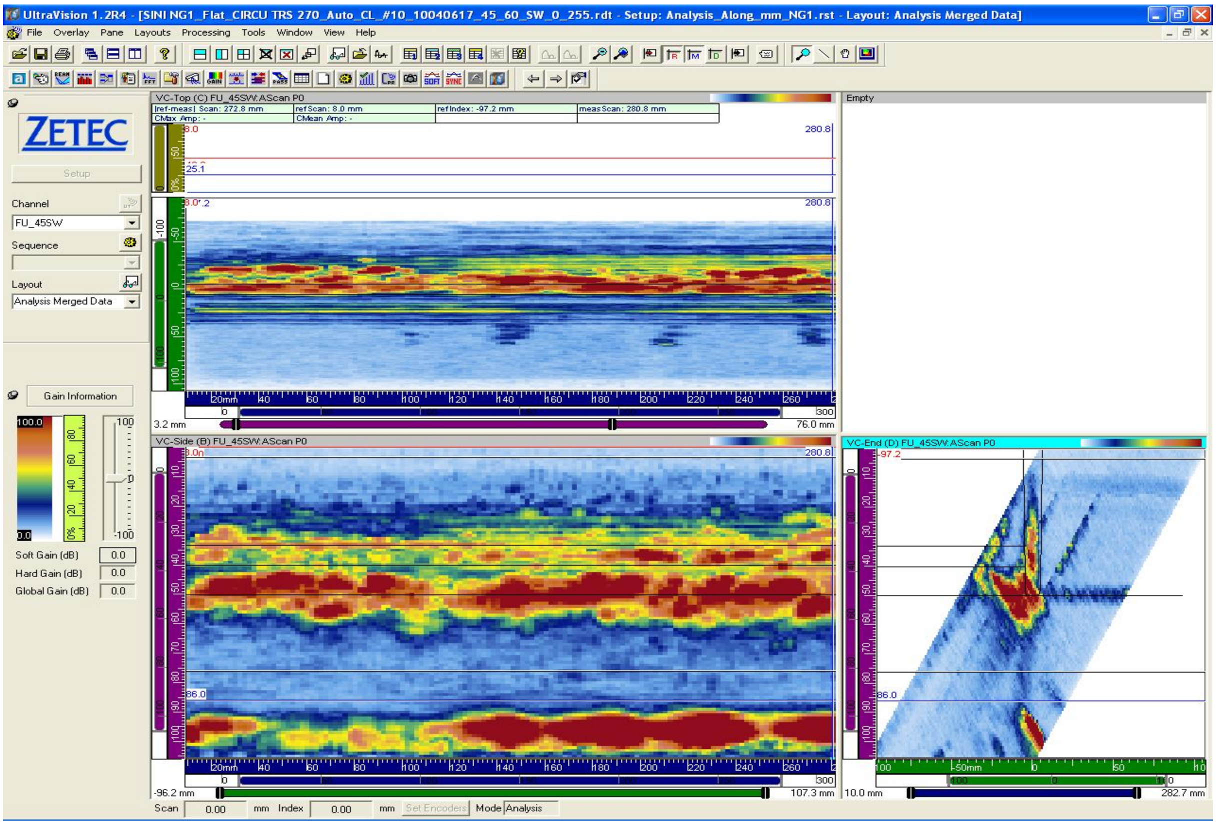

Figure 2.22. Alloy 52 NGW mock-up data at 45° shear wave from SS side with strong continuous indication from the weld as well as from the weld root reinforcement.

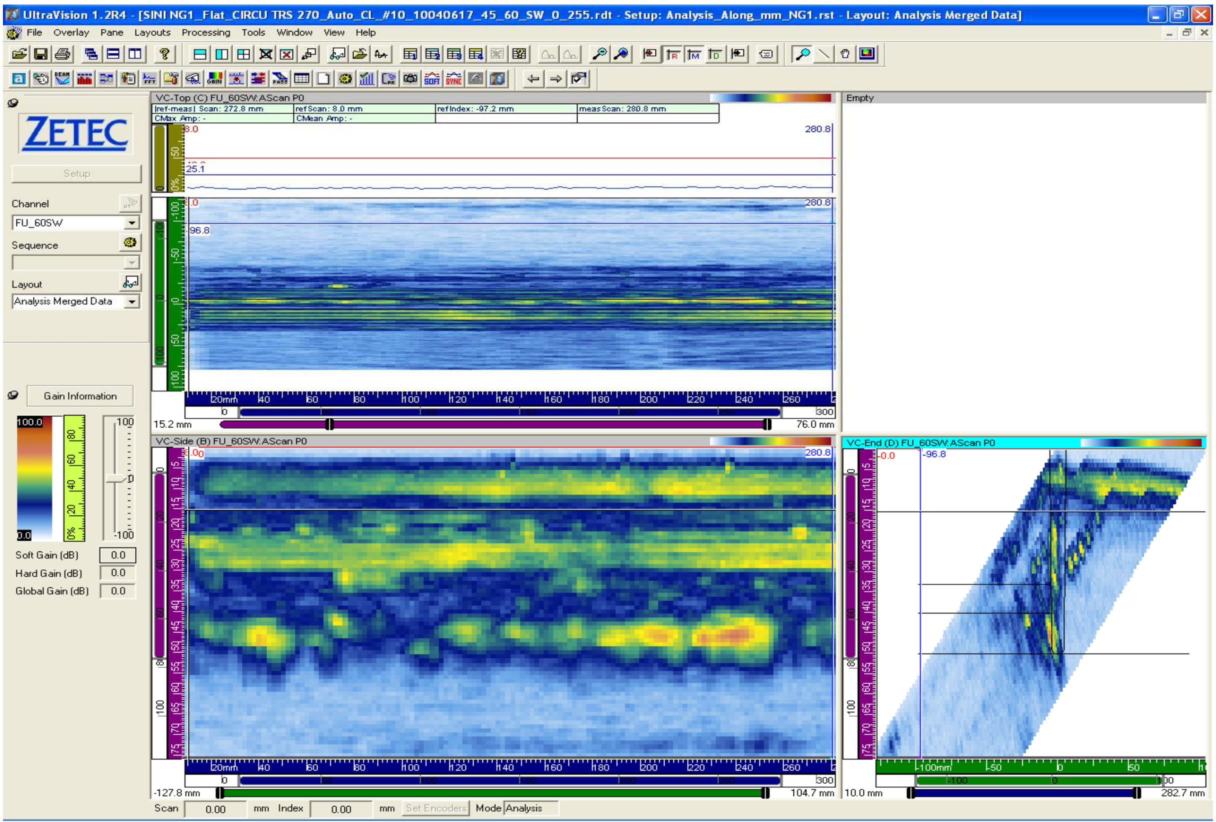

Figure 2.23. Alloy 52 NGW mock-up data at 60° shear wave from SS side with continuous indication from the weld as well as from the weld root reinforcement.

2.8 CIRCU TRS 270 SCAN 255–330 mm

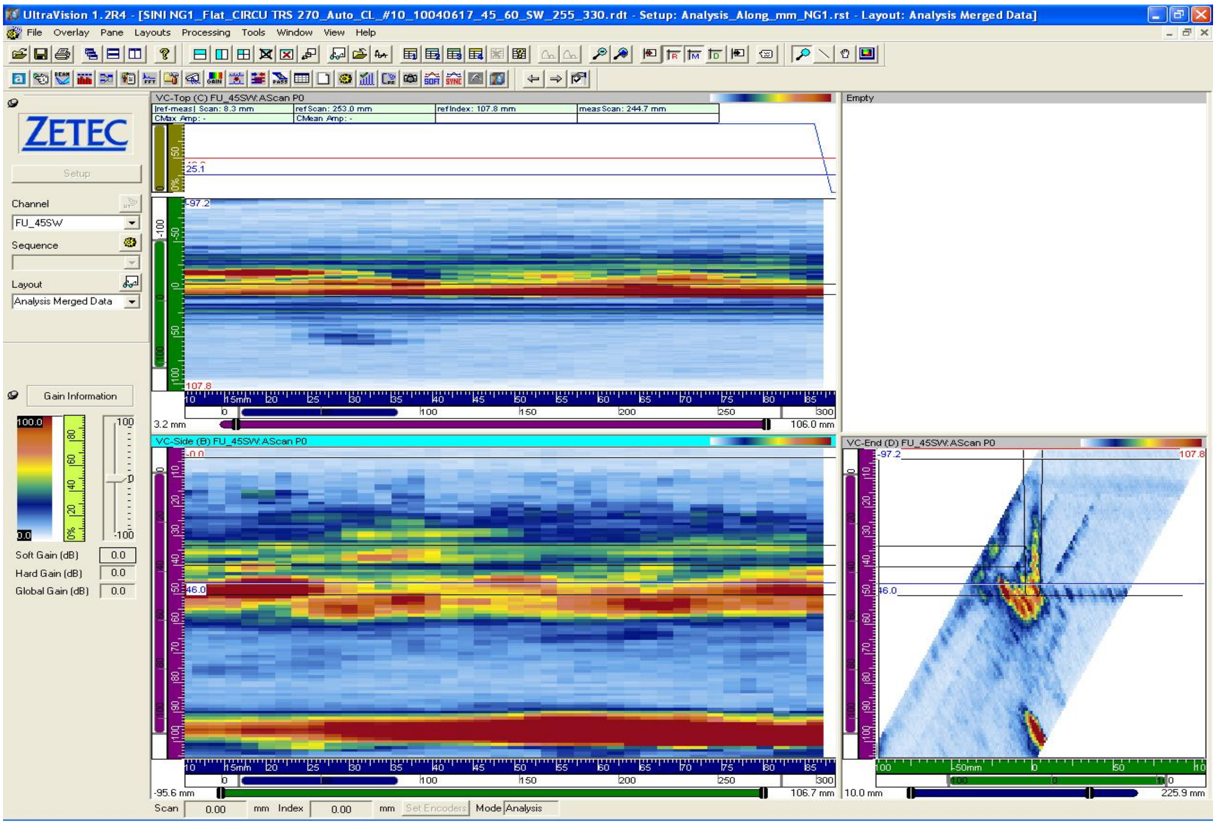

Figure 2.24. Alloy 52 NGW mock-up data at 45° shear wave from SS side with strong continuous indication from the weld as well as from the weld root reinforcement.

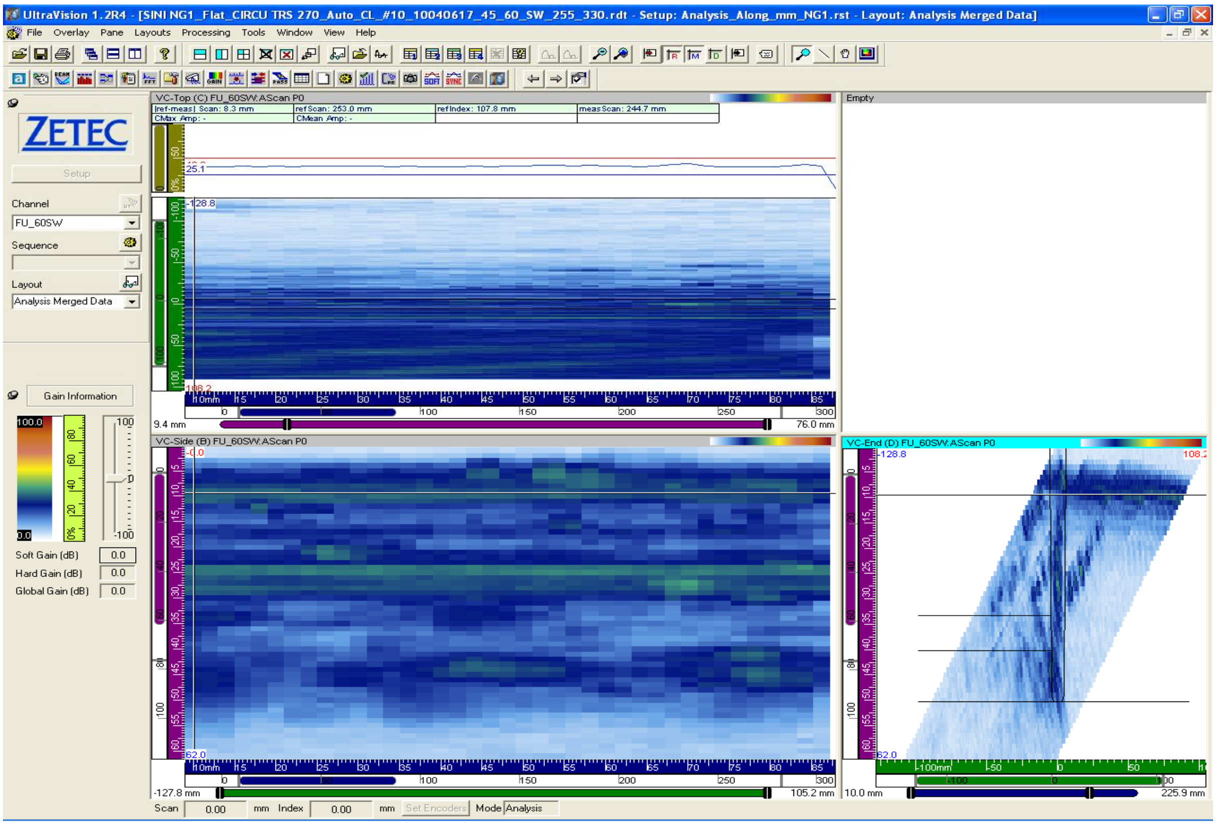

Figure 2.25. Alloy 52 NGW mock-up data at 60° shear wave from SS side with continuous indication from the weld as well as from the weld root reinforcement.

2.9 AXIAL TRL 0 data

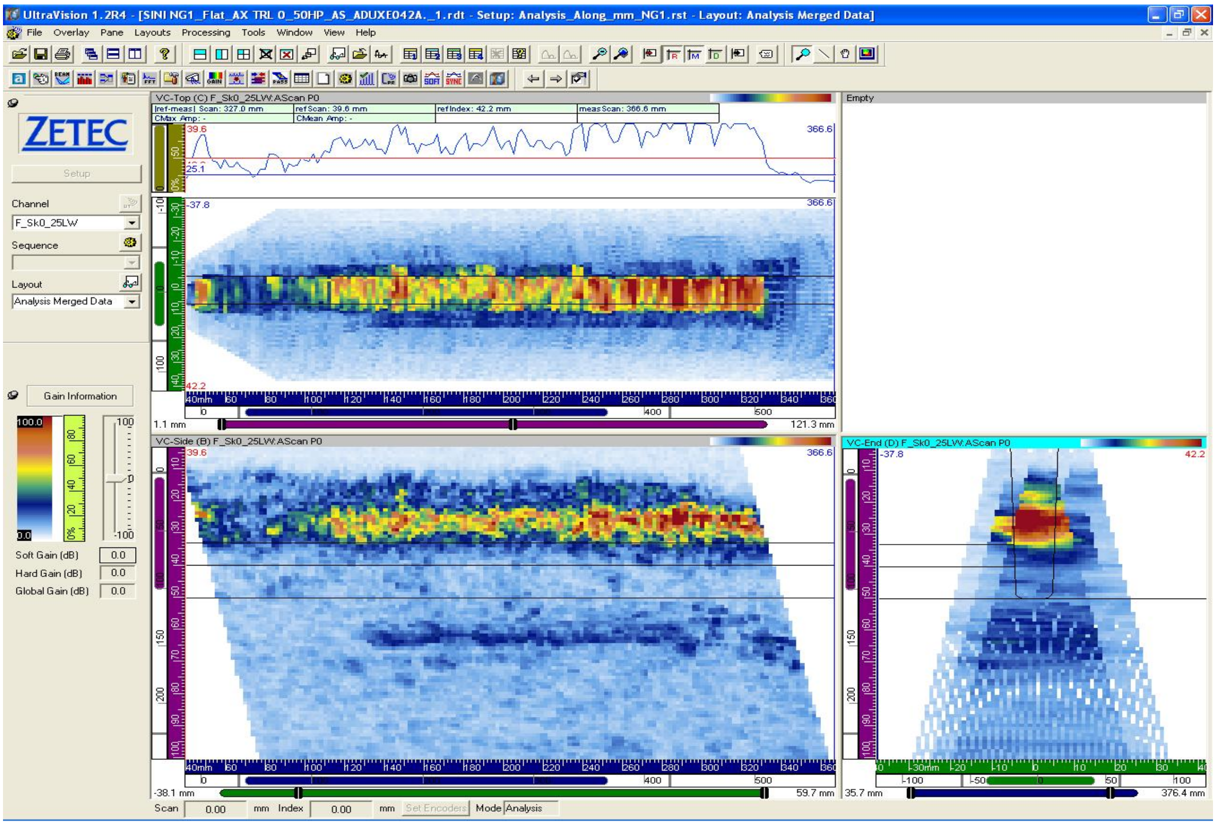

Figure 2.26. Alloy 52 NGW mock-up data at 25° longitudinal wave axial scan with sounding to the positive direction.

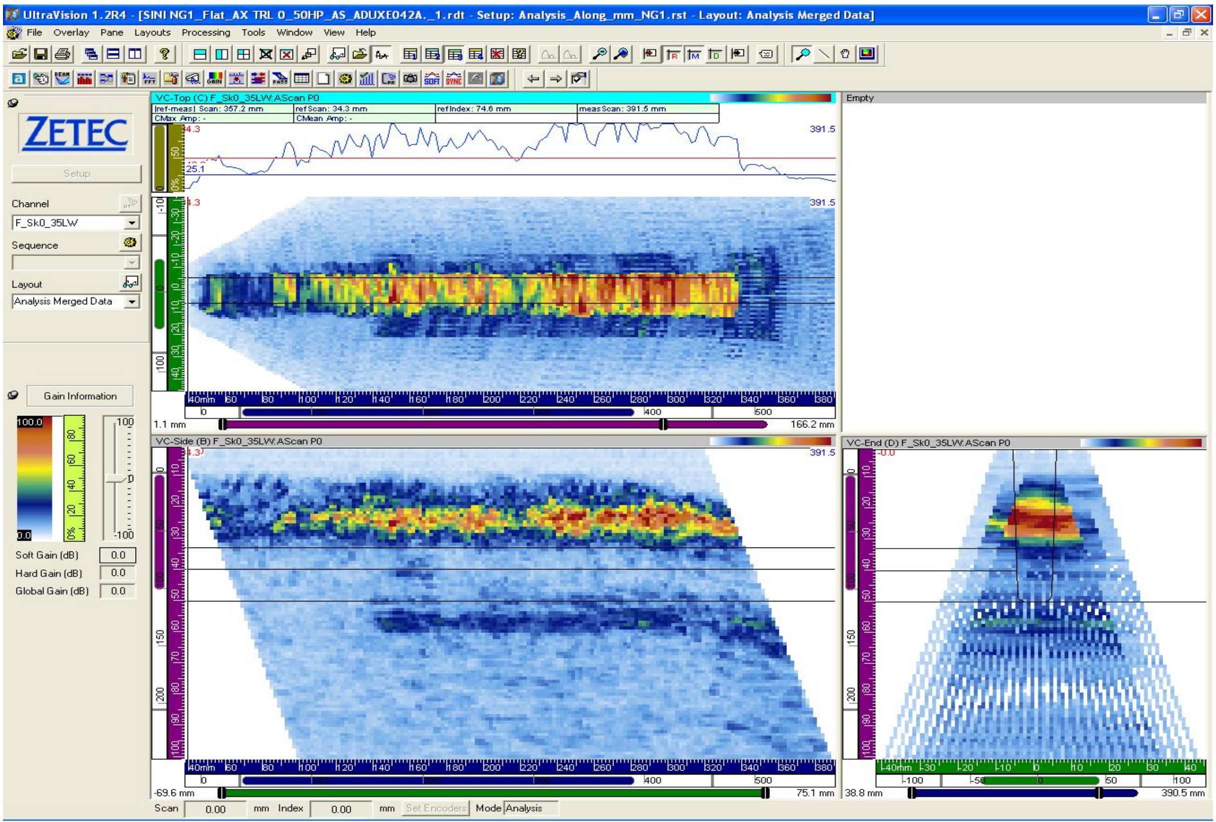

Figure 2.27. Alloy 52 NGW mock-up data at 35° longitudinal wave axial scan with sounding to the positive direction.

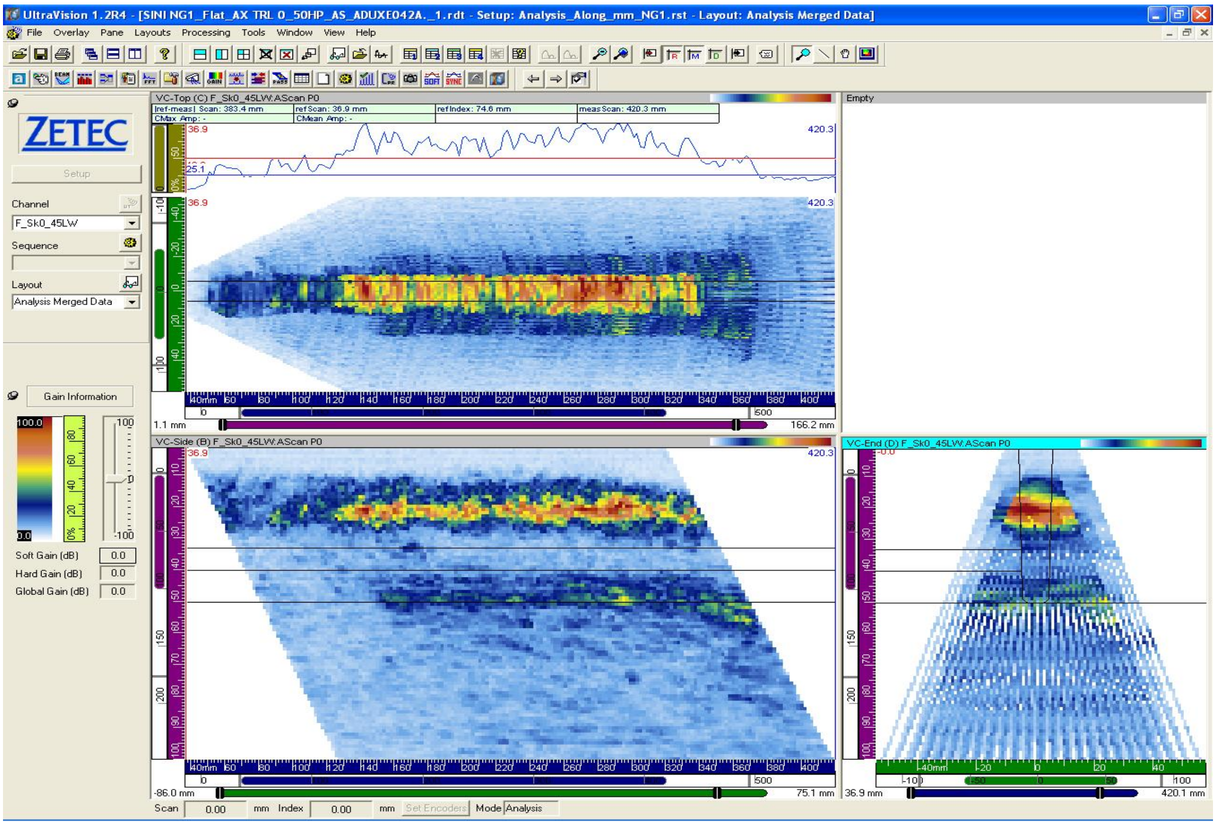

Figure 2.28. Alloy 52 NGW mock-up data at 45° longitudinal wave axial scan with sounding to the positive direction.

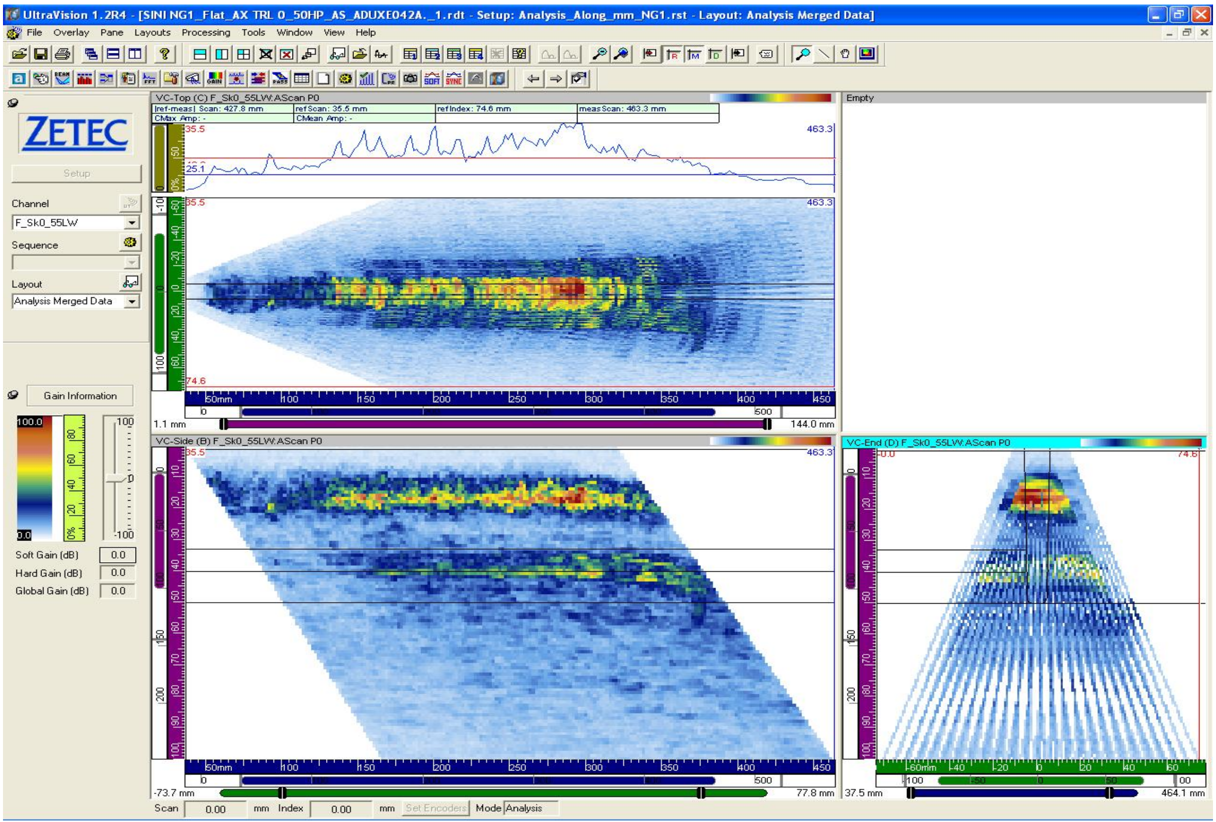

Figure 2.29. Alloy 52 NGW mock-up data at 55° longitudinal wave axial scan with sounding to the positive direction.

2.10 AXIAL TRL 180 data

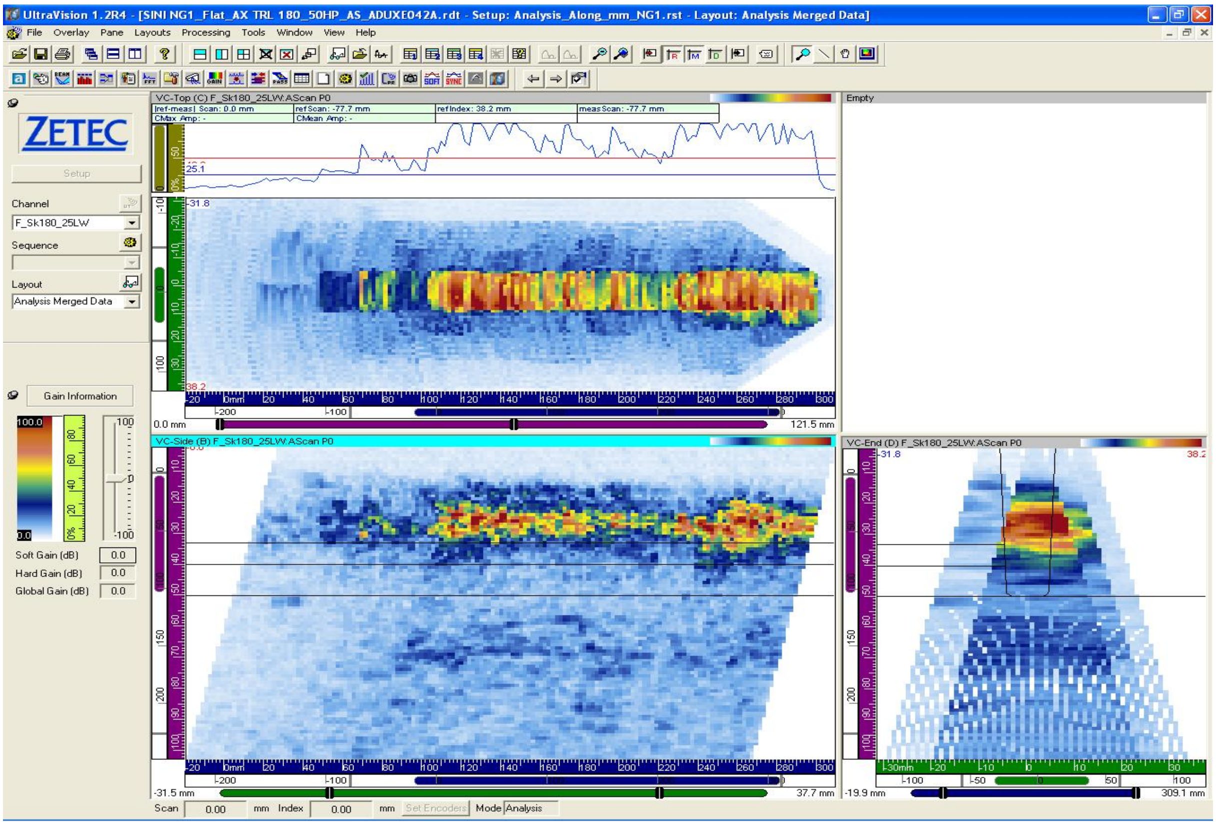

Figure 2.30. Alloy 52 NGW mock-up data at 25° longitudinal wave axial scan with sounding to the negative direction.

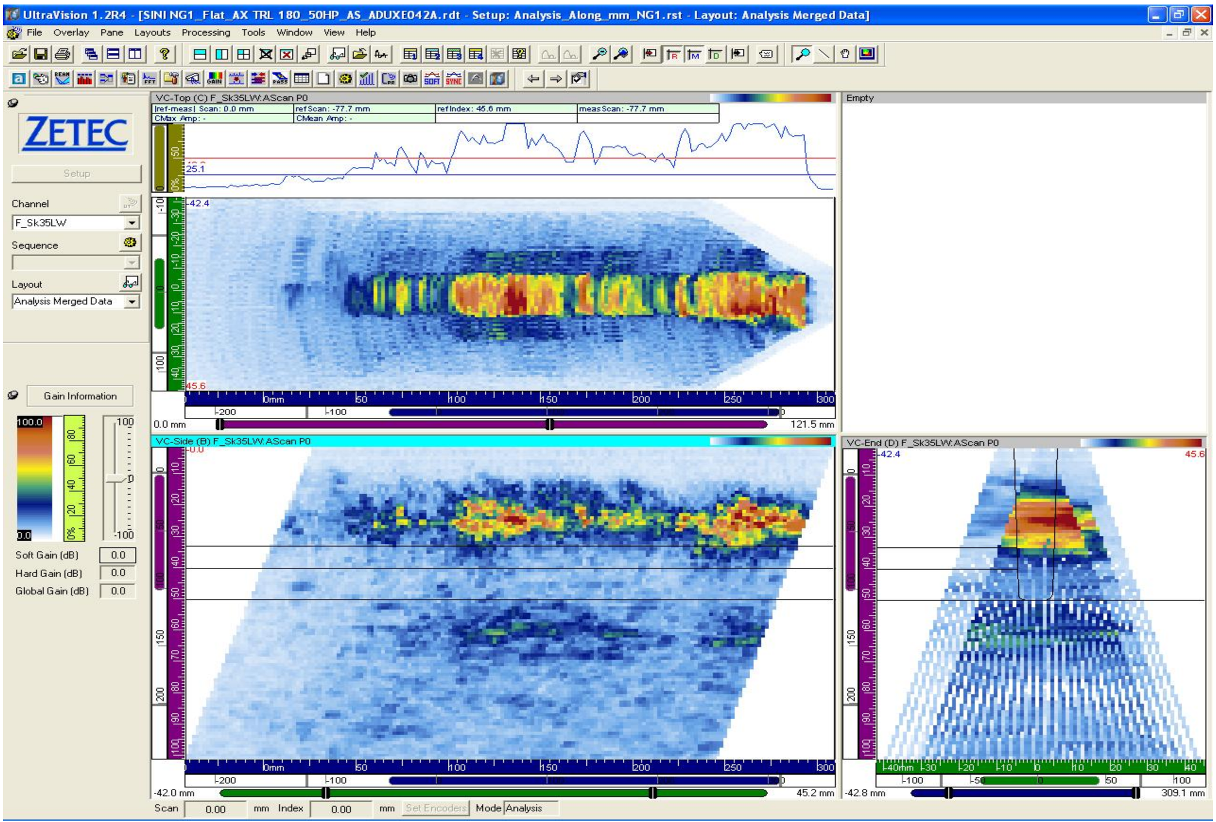

Figure 2.31. Alloy 52 NGW mock-up data at 35° longitudinal wave axial scan with sounding to the negative direction.

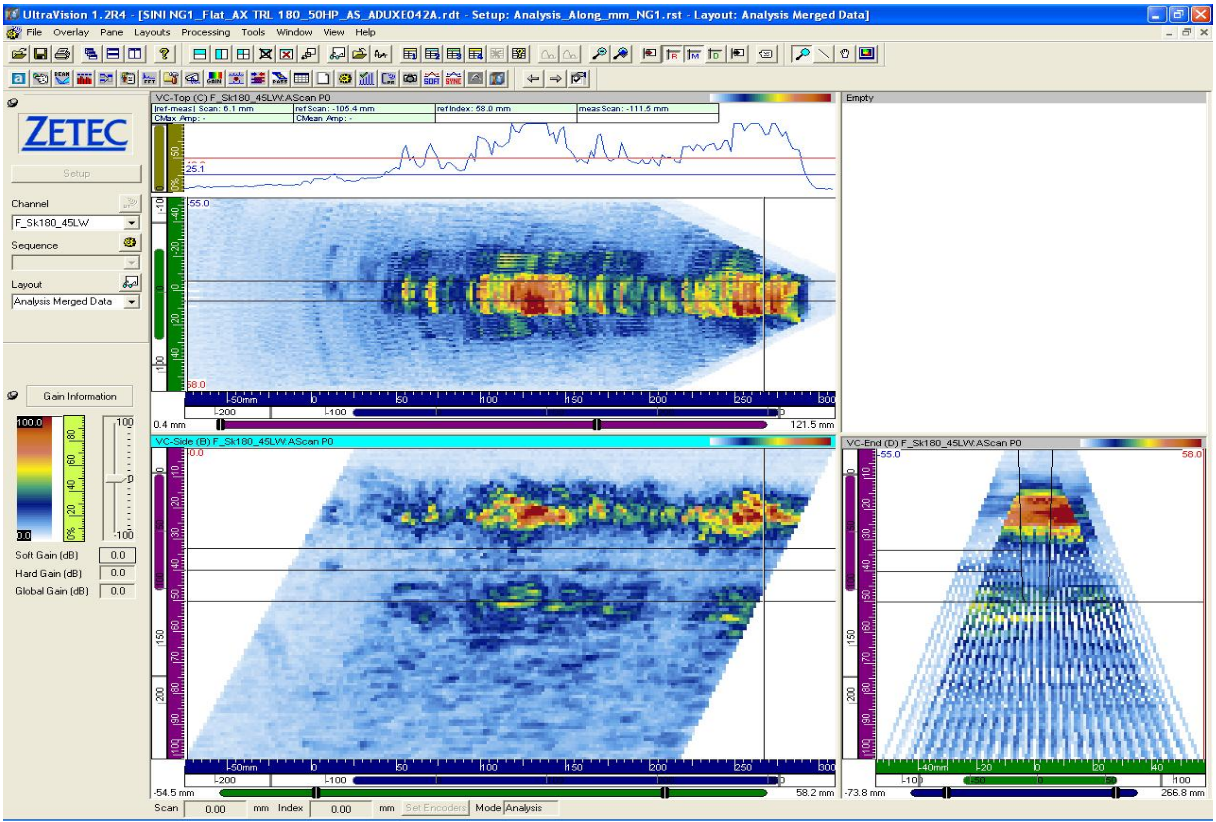

Figure 2.32. Alloy 52 NGW mock-up data at 45° longitudinal wave axial scan with sounding to the negative direction.

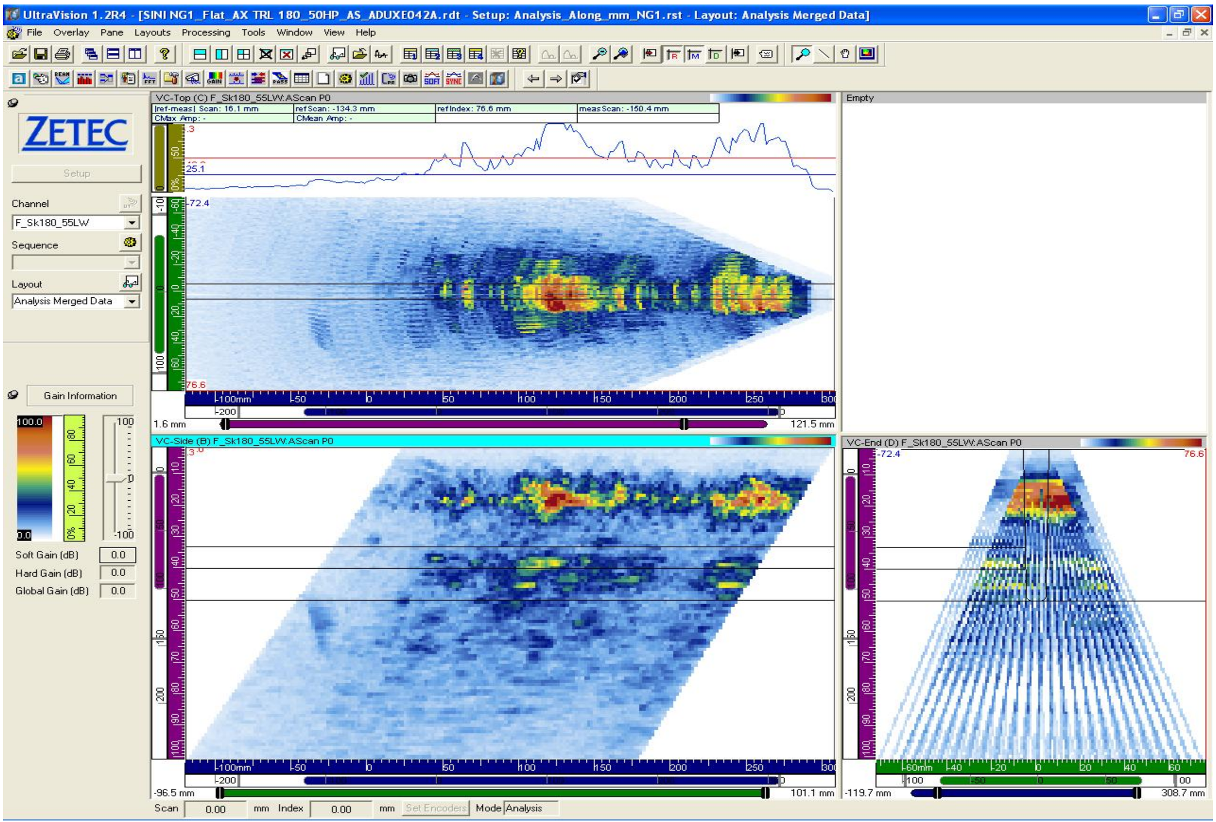

Figure 2.33. Alloy 52 NGW mock-up data at 55° longitudinal wave axial scan with sounding to the negative direction.